

# Protein engineering approaches for direct antigen targeting in CD8<sup>+</sup> T cell inducing vaccines

THÈSE N° 6864 (2016)

PRÉSENTÉE LE 14 MARS 2016

À LA FACULTÉ DES SCIENCES DE LA VIE

CHAIRE MERCK-SERONO EN TECHNOLOGIES D'ADMINISTRATION DE MÉDICAMENTS  
PROGRAMME DOCTORAL EN BIOTECHNOLOGIE ET GÉNIE BIOLOGIQUE

ÉCOLE POLYTECHNIQUE FÉDÉRALE DE LAUSANNE

POUR L'OBTENTION DU GRADE DE DOCTEUR ÈS SCIENCES

PAR

Vasiliki PANAGIOTOU

acceptée sur proposition du jury:

Prof. M. Dal Peraro, président du jury  
Prof. J. A. Hubbell, directeur de thèse  
Prof. P. Romero, rapporteur  
Prof. G. Georgiou, rapporteur  
Prof. B. Correia, rapporteur



ÉCOLE POLYTECHNIQUE  
FÉDÉRALE DE LAUSANNE

Suisse  
2016



# Acknowledgements

I would like to express my deepest gratitude to the following people for making this doctoral thesis possible:

First I would like to thank Professor Jeffrey A. Hubbell for directing my thesis, advising me and creating an inspiring environment for me to grow scientifically over that past 5 years.

Professor Vassily Hatzimanikatis for being a great mentor and for guiding me in difficult moments, but also for being a great friend to me outside the lab.

Professor Bruno Correia, Professor George Georgiou and Professor Pedro Romero for being members of my thesis committee and for sharing their knowledge and expertise with me. Professor Matteo Dal Peraro for being the president of my thesis jury.

Dr. Eleonora Simeoni for providing helpful scientific contributions and technical support with all my projects, and especially for her guidance at the beginning of my graduate thesis.

Xavier Quaglia, Giacomo Diaceri and Jean-Philippe Gaudry for their valuable technical contributions to all my projects. Without them, many of my experiments would have been impossible to complete. I would also like to thank Carol Bonzon and Ingrid Margot for providing administrative support.

I would especially like to thank Annie Gai, Adebola Ogunniyi, Scott Wilson and Carrie Brubaker for always being willing to review and edit my thesis. With Dr. Carrie Brubaker, I worked on evaluating the micelle platform presented in this thesis, and would like to express my gratitude to her for all the great and fun work we did together.

I would also like to thank Natalia Botelho for the valuable scientific discussions we had, and for being willing to share aliquots of XCL1 with me in emergency moments.

Priscilla Briquez who was kind enough to help me with the production of OVA-PIGF proteins and also translated the abstract of this thesis into French; I am very, very grateful to her for all of her help. And of course for the all the pizza she brought in the lab, late in the night!

All LMRP and LLCB people for being great colleagues and friends, and for making our lab environment a fun place to be every day, especially my office mates: Mattias, Annie, Jun, Ziad, Priscilla and Elif. Most of all, I would also like to thank Scott for always being there as a colleague, and as a friend to support me in bad moments and cheer with me in the happy ones. My deepest gratitude goes to Effie who has been more than I could ask for as a friend and colleague inside and outside the lab.

I would also like to thank my flatmate Chrysa for bearing with me all these years and for making home away from home a lovely place to go back every day after work.

Finally, I would like to thank my parents for inspiring me to pursue a PhD, and for their love and support all through to its completion. My thesis is dedicated to you. I left my siblings till the end, to thank them for their unconditional love and for never making me feel that we have

not been leaving together for the past 8 years. They are the most precious thing I will ever have.

## Abstract

Effective vaccine design and public vaccination programs have led to the eradication of several diseases and protected millions of people from deadly infections. However, neutralizing antibodies induced by most vaccine technologies cannot address intracellular infections, which require the activation of cytolytic mechanisms. CD8<sup>+</sup> T cells promote effector mechanisms for infected cell killing subsequent to their priming by antigen-presenting cells. Their activation occurs upon detection of intracellular antigen presented in the context of major histocompatibility complex (MHC) class I, a pathway that many current subunit vaccine technologies are trying to approach by cross-presentation. Advances in CD8<sup>+</sup> T cell-inducing subunit vaccines include direct targeting of antigens to cross-presenting cells and are studied in this thesis.

Antigen delivery to the appropriate cell type for cross-presentation to CD8<sup>+</sup> T cells can occur with fusion antibodies. Our laboratory has previously demonstrated that intravenously injected antigens bearing an erythrocyte-binding antibody domain (TER119) target the liver and are cross-presented to CD8<sup>+</sup> T cells. We used this technology to fuse TER119 and ovalbumin (OVA) antigen with the BBOX domain of the high mobility group box 1 (HMGB1) danger signal and co-administer it with CpG-B adjuvant in a hepatic vaccine context. In liver vaccines, activation of local cytotoxic responses with long-lasting memory represents an important challenge. Erythrocyte-mediated OVA delivery with adjuvants resulted in cytotoxic CD8<sup>+</sup> T lymphocyte (CTL) activation with memory formation in the liver. Furthermore, protection was provided after infection with *Listeria monocytogenes* in mice immunized with immunogenic TER119 constructs.

An alternative method for antigen targeting is through a dendritic cell (DC) subset known to cross-prime CD8<sup>+</sup> T cells, called CD8<sup>+</sup> DCs. Recent studies in mice showed successful vaccination against OVA fused to XCL1 ligand, which uniquely binds CD8<sup>+</sup> DCs. In order to attract CD8<sup>+</sup> DCs to the site of injection for increased antigen uptake, we co-injected XCL1-OVA with a fusion protein consisting of XCL1 and the extracellular matrix (ECM) binding domain of placenta growth factor-2 (PIGF-2<sub>123-144</sub>), called XCL1-PIGF. XCL1-PIGF binds extracellular matrix at the injection site and attracts CD8<sup>+</sup> DCs locally. In the context of prophylactic and therapeutic

vaccination, the combination of two fusion proteins (XCL1-OVA and XCL1-PlGF) enhanced cytotoxicity and prolonged survival against B16-OVA melanoma.

In a similar context, PlGF-2<sub>123-144</sub> was fused to OVA as a method to trap antigen at the injection site and form a depot effect that would promote slow antigen release and result in enhanced uptake by DCs. OVA-PlGF was evaluated in a prime-boost vaccine both for humoral and cellular responses and was compared to the free OVA vaccine formulation. Contrary to the hypothesis of our design, no striking differences were observed between fused OVA-PlGF and free OVA groups when cellular activation and antibody production were considered.

Finally, antigen transport via biomaterial delivery platforms was evaluated as an alternative method to deliver antigens to immunologically relevant sites. Our laboratory and others have shown that nanoscale carriers promote CTL responses in vaccination. However, the fabrication of polymer-based nanoparticle vaccines commonly requires relatively complicated procedures for covalent attachment of components to the carrier surface. Here we present a cationic micelle vaccination platform in which OVA and adjuvant (CpG-B and/or MPLA) loading is mediated by non-covalent molecular encapsulation and adsorption. Following a prime and double boost vaccination, CTL responses were raised in the spleen and lymph nodes of vaccinated mice, along with antigen-specific antibody production. These findings highlight the advantages of the micelle carrier platform in vaccine applications.

Overall, this thesis presents novel techniques to target antigens to the appropriate cell compartments, facilitating CTL activation in vaccination either by direct targeting of antigen fused to antibodies and chemokines, or antigen delivery with polymeric vehicles. These platforms for optimized delivery seek to improve current approaches and impact the design of new strategies in CD8<sup>+</sup> T cell inductive vaccination.

**Keywords:** subunit vaccine, CD8<sup>+</sup> T cells, CTL, cross-presentation, hepatic targeting, TER119, XCL1, PlGF-2, micelles, *Listeria monocytogenes*, B16-OVA, tumor vaccine

## Résumé

Le design de vaccins efficaces a permis d'éradiquer de nombreuses maladies et de protéger des millions de personnes contre des infections mortelles. Les anticorps neutralisant induits par la plupart des vaccins ne peuvent pas lutter contre des infections intracellulaires, qui requièrent une action cytolytique des lymphocytes T (LT) CD8<sup>+</sup>. Ceux-ci possèdent des mécanismes effecteurs permettant de tuer les cellules infectées suite à la reconnaissance d'un antigène intracellulaire, présenté par le Complexe Majeur d'Histocompatibilité I des cellules présentatrices d'antigènes (CPA). La voie de « présentation croisée » de l'antigène par les CPA est actuellement la cible de nombreux vaccins sous-unités. Cette thèse se focalise sur le développement de plateformes de vaccination CD8 et sur l'étude du ciblage spécifique des antigènes sur les CPA utilisant la présentation croisée.

Notre laboratoire a précédemment démontré que des antigènes fusionnés à un domaine d'anticorps liant les globules rouges (TER119) sont efficacement présentés aux LT CD8<sup>+</sup> dans le foie. Nous utilisons ici cette technologie pour le développement de vaccins hépatiques, et avons créé une protéine de fusion contenant TER119, l'antigène ovalbumine (OVA) et le domaine BBOX d'HMGB1 servant d'adjuvant. La co-administration de cette protéine tripartite avec du CpG-B induit l'activation des LT CD8<sup>+</sup> cytotoxiques (LTc) et la formation d'une mémoire immunitaire à long-terme dans le foie, résolvant ainsi une limitation importante des vaccins hépatiques actuels. De plus, cette technologie a engendré une protection immunitaire efficace dans un modèle murin d'infection par la *Listeria monocytogenes*.

Les cellules dendritiques (CD) CD8<sup>+</sup> sont connues pour leur capacité à présenter efficacement de façon croisée les antigènes aux LT CD8<sup>+</sup>. De récentes études ont montré que la fusion entre OVA et la chimiokine XCL1 permettait d'attirer et de lier les CD CD8<sup>+</sup>, fournissant ainsi une vaccination adéquate contre OVA. Afin de promouvoir un effet localisé de XCL1, nous l'avons fusionné à un domaine (PIGF) ayant une forte affinité pour les matrices extracellulaires. Nous avons ensuite co-injecté XCL1-OVA et XCL1-PIGF dans le but de recruter les CD CD8<sup>+</sup> au site d'injection et d'accroître l'internalisation de l'antigène. La combinaison de ces deux protéines de fusion a augmenté la cytotoxicité de la réponse immunitaire contre OVA et a prolongé la survie de souris ayant un mélanome B16F10-OVA.

Dans un contexte similaire, la protéine de fusion OVA-PIGF a été développée afin de séquestrer l'antigène au site d'injection et de former un dépôt qui permettrait la libération ralentie de l'antigène et une meilleure assimilation par les CD. Les groupes OVA-PIGF et OVA ont été comparés dans un modèle de vaccination à un rappel. Contre toute attente, aucune différence n'a pu être observée entre les deux groupes au niveau de l'activation des cellules immunitaires et de la production d'anticorps.

Finalement, l'utilisation de biomatériaux peut également permettre de libérer des antigènes dans les compartiments appropriés des cellules immunitaires. Il a été montré que des vaccins basés sur des nanoparticules de polymères améliorent les réponses des LTc. Cependant, la fabrication de ces vaccins requiert une conjugaison covalente de l'antigène au nanoparticules, une procédure relativement complexe. Nous avons donc développé des micelles cationiques dans lesquelles l'antigène OVA et l'adjuvant (CpG-B et/ou MPLA) peuvent être encapsulés de façon non-covalente et complexés par des interactions électrostatiques. Dans un modèle de vaccination à deux rappels, cette plateforme micellaire entraîne une augmentation de la réponse des LTc dans la rate et les ganglions lymphatiques, ainsi que la production d'anticorps spécifiques contre OVA. Ces résultats mettent en évidence les avantages de ce nanomatériau pour la formulation de vaccins.

Ainsi, cette thèse présente de nouvelles technologies de vaccination permettant l'administration des antigènes à des compartiments cellulaires spécifiques afin de faciliter l'activation des LTc, soit 1) par le ciblage spécifique de l'antigène sur les CPAs, grâce à sa fusion avec des anticorps ou des chimiokines, ou 2) par une administration médiée par des nanomatériaux polymériques. Ces technologies démontrent le potentiel de stratégies d'optimisation d'administration des antigènes pour le développement de nouveaux vaccins CD8 plus performants.

**Mots clés :** Vaccins sous-unités, cellules T CD8<sup>+</sup>, présentation croisée, ciblage hépatique, TER119, XCL1, PIGF-2, micelles, *Listeria monocytogenes*, B16F10-OVA, tumeur



## Table of Contents

<b>CHAPTER 1 :</b>	<b>1</b>
<b>OVERVIEW OF THE THESIS</b>	<b>1</b>
<b>1.1 MOTIVATION</b>	<b>2</b>
<b>1.2 BACKGROUND</b>	<b>4</b>
1.2.1 THE INNATE AND ADAPTIVE IMMUNE RESPONSES	4
1.2.2. IMMUNE RESPONSES IN VACCINATION	9
1.2.3. CD8 <sup>+</sup> T CELL-INDUCING VACCINES	11
1.2.4. RATIONAL VACCINE DESIGN	12
<b>1.3. ACCOMPLISHMENTS</b>	<b>16</b>
<b>REFERENCES</b>	<b>17</b>
<b>CHAPTER 2:</b>	<b>23</b>
<b>HEPATIC TARGETING OF VACCINAL ANTIGENS</b>	<b>23</b>
<b>2.1 ABSTRACT</b>	<b>24</b>
<b>2.2. INTRODUCTION</b>	<b>25</b>
<b>2.3. MATERIALS AND METHODS</b>	<b>27</b>
<b>2.4. RESULTS AND FIGURES</b>	<b>31</b>
2.4.1. PRODUCTION AND CHARACTERIZATION OF ERYTHROCYTE-BINDING ANTIGENS.	31
2.4.2. TER119-BBOX-OVA BEARS A DANGER SIGNAL.	33
2.4.3. UPTAKE OF TER119-BBOX-OVA BY HEPATIC CELLS AND UPREGULATION OF ANTIGEN PRESENTING CELLS IN THE LIVER.	34
2.4.4. EFFICIENT CROSSPRESENTATION OF TER119-BBOX-OVA + CpG IMPROVES THE PROLIFERATION OF OVA-SPECIFIC CD8 <sup>+</sup> T CELLS.	36
2.4.5. IMMUNIZATION WITH TER119-BBOX-OVA MIXED WITH CpG LEADS TO ENHANCED CYTOTOXICITY OF CD8 <sup>+</sup> T CELLS MAINLY IN THE LIVER OF VACCINATED MICE.	39
2.4.6. IMMUNIZATION WITH TER119-BBOX-OVA MIXED WITH CpG CREATES MEMORY CD8 <sup>+</sup> T CELLS THAT CAN BE ACTIVATED UPON RECALL IN THE LIVER.	40
2.4.7. EFFECTOR CD8 <sup>+</sup> T CELLS INDUCED AFTER TER119-BBOX-OVA + CpG IMMUNIZATION KILL LISTERIA MONOCYTOGENES-INFECTED CELLS.	43
<b>2.5. DISCUSSION</b>	<b>44</b>
<b>REFERENCES</b>	<b>48</b>
<b>CHAPTER 3:</b>	<b>53</b>
<b>ENHANCED CD8<sup>+</sup> T CELL-TARGETING VACCINATION BY PROLONGED BINDING OF XCL1 FUSION PROTEINS AT THE INJECTION SITE</b>	<b>53</b>
<b>3.1. INTRODUCTION</b>	<b>54</b>
<b>3.2. MATERIALS AND METHODS</b>	<b>57</b>
<b>3.3 RESULTS AND FIGURES</b>	<b>61</b>
3.3.1. PLGF-2 <sub>123-144</sub> FUSION PROLONGS XCL1 RETENTION AT INJECTION SITE THROUGH ECM BINDING.	61
3.3.2. XCL1-PLGF RECRUITS CROSS-PRESENTING DCs TO THE SITE OF INJECTION.	62
3.3.3. XCL1-PLGF MIXED WITH XCL1-OVA ENHANCES ANTIGEN UPTAKE BY CROSS-PRESENTING DCs AND PROMOTES CROSS-PRIMING OF CD8 <sup>+</sup> T CELLS.	63
3.3.4. ENHANCED CYTOLYTIC ACTIVITY OF CD8 <sup>+</sup> T CELLS IN THE LNS OF MICE VACCINATED WITH XCL1-OVA + XCL1-PLGF.	64
3.3.5. XCL1-PLGF ENHANCES THE EFFICACY OF XCL1-OVA TUMOR VACCINES IN BOTH A PROPHYLACTIC AND A THERAPEUTIC MANNER.	66

<b>3.4. DISCUSSION</b>	<b>69</b>
<b>REFERENCES</b>	<b>72</b>
<b>CHAPTER 4:</b>	<b>75</b>
<u>DEPOT EFFECT INVESTIGATION OF ANTIGEN AFFINITY WITH THE INJECTION SITE IN VACCINATION</u>	<u><b>75</b></u>
<b>4.1. INTRODUCTION</b>	<b>76</b>
<b>4.2. MATERIALS AND METHODS</b>	<b>78</b>
<b>4.3. RESULTS AND FIGURES</b>	<b>81</b>
<b>4.4. DISCUSSION</b>	<b>86</b>
<b>REFERENCES</b>	<b>88</b>
<b>CHAPTER 5:</b>	<b>91</b>
<u>A CATIONIC MICELLE COMPLEX IMPROVES CD8<sup>+</sup> T CELL RESPONSES IN VACCINATION AGAINST UNMODIFIED PROTEIN ANTIGEN</u>	<u><b>91</b></u>
<b>5.1. ABSTRACT</b>	<b>92</b>
<b>5.2. INTRODUCTION</b>	<b>93</b>
<b>5.3 MATERIALS AND METHODS</b>	<b>95</b>
<b>5.4. RESULTS AND DISCUSSION</b>	<b>99</b>
5.4.1. PREPARATION AND CHARACTERIZATION OF CATIONIC MICELLES AND MICELLAR AGGREGATES.	99
5.4.2. SINGLY-ADJUVANTED VACCINATION UTILIZING CATIONIC MICELLES ENHANCES CYTOTOXIC RESPONSES IN SPLEEN- AND LYMPH NODE-RESIDENT CD8 <sup>+</sup> T CELLS.	102
5.4.3. SINGLY-ADJUVANTED VACCINATION WITH CATIONIC MICELLES INDUCES HUMORAL RESPONSES.	106
5.4.4. DOUBLY-ADJUVANTED VACCINATION DOES NOT PROVIDE ADDITIVE EFFECT OF THE TWO ADJUVANTS.	107
<b>5.6. CONCLUSIONS</b>	<b>111</b>
<b>REFERENCES</b>	<b>111</b>
<b>SUPPORTING INFORMATION</b>	<b>115</b>
<b>CHAPTER 6:</b>	<b>117</b>
<u>CONCLUSIONS AND FUTURE DIRECTIONS</u>	<u><b>117</b></u>
<b>6.1 CONCLUSIONS</b>	<b>118</b>
<b>REFERENCES</b>	<b>121</b>
<b>CURRICULUM VITAE</b>	<b>123</b>

## **Chapter 1 :**

### Overview of the Thesis

## 1.1 Motivation

Vaccination is the most cost effective medical intervention to prevent infectious diseases. The first documented observation of immunological memory was made by Thucydides in 430 B.C., during the Peloponnesian War, when he reported that the deadly plaque of Athens never attacked the same man twice [1]. Many years later, the first vaccine was developed by Edward Jenner, against smallpox, and this was considered the foundation of immunology and the origin of the vaccination era [2]. Since then, profound reduction or elimination of many diseases has been achieved through vaccination and life expectancy in the developed world has increased [3-5]. The first vaccines, and the most successful to date, were live attenuated vaccines consisting of viable pathogens that have been altered to reduce their virulence. Although live vaccines have been very efficient in protecting against several diseases and have been used for many years, concerns about the safety of these complex mixtures have motivated the development of a new generation of vaccines called subunit vaccines.

This new generation of vaccines is based on proteins/peptides or carbohydrate antigens purified from a pathogen or produced by recombinant techniques. Subunit vaccines are safer than live attenuated vaccines, but they are not as immunogenic. Nowadays, a new field in immunology has emerged for technologies that focus on enhancing the immunogenicity of subunit vaccines and supporting a more efficient administration of the antigen. Immunostimulatory compounds, called adjuvants, are incorporated into subunit vaccine formulations to boost their immunogenicity. Moreover, novel delivery systems facilitate the targeting of the antigen to the proper cell types and trigger potent immune responses. Various adjuvants have been developed for subunit vaccination [6], with the most commonly used being alum [7]. Vaccines incorporating this adjuvant are very efficient in the induction of humoral responses and can, in particular, trigger the production of neutralizing antibodies. However, they generally fail to stimulate the T cell compartments of the immune system that are mandatory for dealing with chronic infectious agents, viruses and tumors.

The eradication of tumors and intracellular pathogens like human papillomavirus (HPV), human immunodeficiency virus (HIV), *Mycobacterium*

*tuberculosis*, hepatitis B and C and malaria requires robust cytotoxic T lymphocyte responses, which makes development of effective subunit vaccines for these diseases challenging. For some challenging pathogens, cellular vaccines have been developed, but their efficacy is sub-optimal and/or short-lived. Examples include the Bacillus Calmette-Guérin (BCG) vaccine against tuberculosis, which is effective in preventing severe tuberculosis in children but does not prevent infection or re-activation of latent disease [8] and hepatitis B, where patients with chronic situations fail to initiate responses against the virus [9]. Moreover, prophylactic subunit vaccines for HPV, which can prevent the development of cervical cancer (Gardasil), and therapeutic vaccines against prostate cancer (Sipuleucel-T (Provenge®)) and melanoma [10, 11] are available on the market. However, subunit vaccines against many chronic infections, such as HIV, malaria and hepatitis C, as well as tumors caused by viral infections, like liver cancers, remain unmet needs. Effective vaccines for these diseases must activate CD8<sup>+</sup> T cells to exert cytotoxic effects against the infected or mutant cells. Activation of this cell type can occur by presenting the antigen to the MHC class I molecule that will facilitate the engagement to CD8<sup>+</sup> T cells. Enhancing the response of these cells and eliciting long-lasting cytotoxic immune responses against specific pathogens is the task of current CD8<sup>+</sup> T cell-inducing vaccine design efforts.

Among the strategies pursued to enhance the efficacy of CD8<sup>+</sup> T cell subunit vaccines in recent years, direct targeting of the antigen to the appropriate cell type with the use of surface ligands or delivery vehicles has been explored. The most widely studied approach involves delivery of molecules to dendritic cells (DCs), which are the most potent antigen presenting cells (APCs) and the most common targets in T cell vaccines [12]. Examples of DC surface molecule linkers include antibodies towards specific markers or chemokine ligands that bind to receptors on DCs, reviewed later in this Introduction. Moreover, among many other delivery systems developed, a novel nanoparticle-antigen carrier was established in our laboratory that elicited potent T cell responses in vaccinations [13]. The aim of this thesis is to explore alternative ways for efficient delivery of antigens in immune cell compartments or organs where previous vaccination has failed, such as the liver. Moreover, we also aimed to provide new platforms for targeting antigens to DCs in a chemokine-ligand fusion manner and a delivery vehicle with the overall goal to enhance long-lasting cytotoxic CD8<sup>+</sup> T cell responses.

## 1.2 Background

### 1.2.1 The innate and adaptive immune responses

During the course of evolution, living organisms developed an immune system designed to protect them from invasion by pathogenic species. Immune systems vary in complexity from bacteria to vertebrates, but in essence, these systems have evolved to enable the detection and elimination of opportunistic microbes and other pathogens, by eliciting immune responses to protect the host. An immune response refers to the sequence of the reactions orchestrated by the different components of the immune system – which includes nucleic acids, proteins and cells – working in concert to clear an infection from within the host. The immune system is composed by two arms, the innate and adaptive. The innate immune system is the most prevalent form of immunity in living organisms, as it exists in both vertebrate and invertebrate species, while only vertebrates possess an adaptive immune system. Even though each immune system has its distinct role and function, innate and adaptive immunity are tightly connected arms of the overall immune system that interact to provide robust responses against pathogens. In vertebrates, early mechanisms of innate immunity elicit appropriate signals that eventually activate the adaptive immune system, to provide target-specific immune responses.

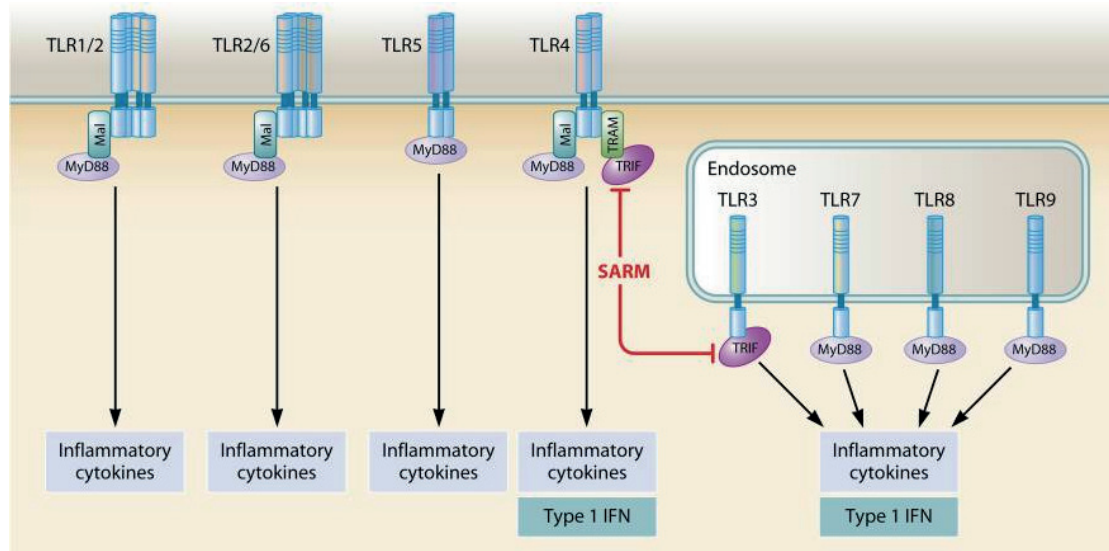
Innate immunity provides the first line of defense against pathogens. It is not antigen specific, but acts rapidly to recognize non-self species within the host, and this triggers pro-inflammatory responses against such species [14, 15]. The innate immune system in humans consists of the following types of cells:

- epithelial cells that form a physical barrier, such as the skin, to prevent the entry of pathogens,
- neutrophils, which are often the first to respond to an infection by releasing chemokines to attract more cells,
- macrophages. which are the most efficient migratory phagocytic cells, capable of engulfing microbes and inducing inflammation by secretion of chemokines,
- natural killer (NK) cells that recognize and kill virus-infected cells or tumor cells,
- mast cells that are associated with cytokine release in response to pathogens,

but are also responsible for responses in allergies and anaphylaxis,

- neutrophils, eosinophils and basophils known as granulocytes that upon activation they release a range of toxins to deal with bacteria and other infections, and finally,
- dendritic cells (DCs) that are phagocytic cells involved in the processing and presentation of antigen, and are the major link between the innate and adaptive immune systems.

The innate immune system functions by recognizing and responding to highly conserved structures in microbes called pathogen-associated molecular patterns (PAMPs), using receptors present on the innate immune cells. These receptors are known as pattern recognition receptors (PRRs) [16]. The best-known examples of PAMPs are bacterial lipopolysaccharides, peptidoglycans, lipoteichoic acids, mannan, bacterial DNA, double-stranded RNA, and glucans. These PAMPs all share unique structural motifs, and are recognized by PRRs present on professional antigen-presenting cells (APCs) of the innate immune system (i.e. macrophages, dendritic cells and B cells). Binding of PAMPs by PRRs immediately activates intracellular signal transduction pathways, leading to the secretion of pro-inflammatory cytokines and the upregulation of costimulatory molecules on APCs [17]. The Toll-like receptor family (TLRs) is a very well-characterized class of PRRs. TLRs can be divided into 2 subfamilies: cell surface TLRs (TLR-1, -2, -4, -5, -6 and -10) that mainly recognize bacteria, and intracellular TLRs (TLR-3, -7, -8 and -9) specialized in the recognition of foreign nucleic acids, as seen in Fig. 1. Engagement of TLRs by microbial components leads to induction of genes responsible for antimicrobial host defense [18].



**Figure 1: TLR molecules and activation pathways** (adapted from Clinical Microbiology Reviews [17]). TLR-1,-2,-4,-5,-6, are displayed on the cell surface and TLR-3, -7, -8, -9 are located in the endosome. Most TLRs utilize MyD88 as the adaptor for signal transduction with the exception of TLR-3, which is dependent on TRIF for signaling, and TLR-4, where both are involved.

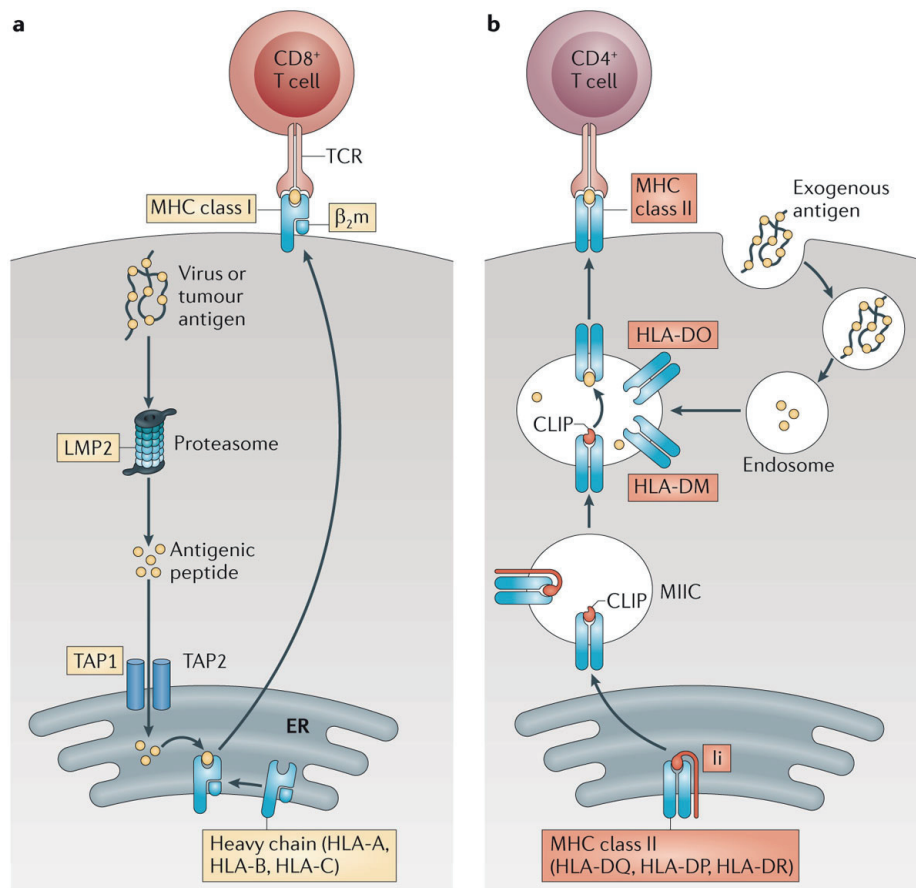
The two main molecules responsible for activation of distinct pathways for the production of inflammatory cytokines and type I interferon (IFN) are MyD88 and TRIF (Toll receptor-associated activator of interferon), respectively. These molecules bind to the cytoplasmic domain of TLRs [19, 20], as described in Fig. 1. Upon activation, a signal is transmitted through cytoplasmic molecules to the nucleus, where three signaling pathways are responsible for mediating TLR-induced responses, namely: the Nf- $\kappa$ B pathway, the mitogen-activated protein kinases (MAPKs) pathways and IFN regulatory factors (IRFs) pathway [21, 22]. The result is release of pro-inflammatory cytokines such as IL-1, IL-6, TNF $\alpha$  and IFN $\gamma$  production, which promotes the maturation of DCs.

As stated above, DCs are the bridge between innate and adaptive immunity. The adaptive immune system mounts more sophisticated immune responses than the innate system that are highly specific to a particular antigen. These responses are carried out by a subset of white blood cells called lymphocytes, divided in two main classes called B cells and T cells. B cells trigger antibody production whereas T cells role is to react against a foreign antigen either by cytokine release or direct killing of infected cells. There are two subclasses of T cells, CD4<sup>+</sup> and CD8<sup>+</sup> T cells, with distinct functions described below in details.



Following the uptake of antigen, DCs become activated and upregulate their costimulatory molecules (CD80, CD86, CD40) and antigen-presenting MHC molecules. Activation and maturation of DCs is a prerequisite for optimal interaction with CD4<sup>+</sup> and CD8<sup>+</sup> T cells of the adaptive immune system. In particular, after maturing, DCs migrate to the regional lymph nodes to present the antigenic peptides in the context of relevant MHC molecules. MHC class I molecules report intracellular events such as viral infection to CD8<sup>+</sup> T cells. Protein fragments of cytosolic and nuclear origin generated by proteolysis, are loaded on MHC class I molecules in the endoplasmic reticulum (ER) and the complex is transported to the APC surface (Fig. 2a). In contrast, endocytosed extracellular proteins generate peptides by lysosomal proteolysis of phagocytosed material, and these peptides are loaded on MHC class II molecules (Fig. 2b) [23, 24]. A representation of these two distinctive functions is seen in Fig. 2.

Presentation of peptide via the MHC class I pathway facilitates the engagement of cytotoxic CD8<sup>+</sup> T cells (CTLs), through a process called direct presentation. CTLs play a major role in the control of viral infection and killing of tumor cells. Upon activation, CTLs carry out the lysis of infected cells by the perforin granule exocytosis pathway or by the activation of the Fas ligand (FasL), which leads to programmed cell death [25]. Furthermore, CD8<sup>+</sup> T cells also secrete cytokines such as IFN $\gamma$  and TNF $\alpha$  to recruit and activate other effector cells [26]. CTL responses can also be elicited against antigens derived from an exogenous source. In this case, antigens are loaded onto the MHC class I molecule and the complex primes CD8<sup>+</sup> T cells in a process called ‘cross-presentation’, first described by Bevan et.al. [27]. On the other hand, presentation via the MHC class II pathway stimulates activation and differentiation of CD4<sup>+</sup> T lymphocytes into different T helper (Th) subsets, namely: Th1, Th2 and Th17 [24]. Th1 responses are mainly characterized by secretion of the IFN $\gamma$  cytokine, and are important for protection against viruses and intracellular bacteria. Th2 responses involve the secretion of IL-4, IL-5 and IL-13 cytokines against extracellular protozoa at mucosal surfaces, and are involved in allergic responses. Finally, Th17 is a recently discovered subset with important functions against certain bacterial infections, and a possible role in autoimmunity.



**Figure 2:** The MHC class I and MHC class II antigen-presentation pathways. (adopted from Nature immunology reviews [28]) **a.** Intracellular antigens such as viruses and tumor antigens are transported to the ER and loaded onto MHC class I molecules. MHC class I complexes traffic to the cell surface where they present the antigen to CD8<sup>+</sup> T cells. **b.** Antigens from extracellular sources are phagocytosed and processed by endolysosomal enzymes into peptide fragments. The peptides are then loaded onto the MHC class II groove and presented to CD4<sup>+</sup> T cells.

Another role of the adaptive immune system is the induction of humoral responses. Maturation of B cells into plasma cells, following help from CD4<sup>+</sup> T cells, results in the production of antibodies with high affinity through the induction of somatic hypermutation [29]. Antibodies are glycoproteins that belong to the immunoglobulin family and exist in five isotypes: IgG, IgM, IgA, IgD and IgE. The isotypes differ in the constant regions of the antibody protein sequence, conferring the different effector functions observed with each isotype. IgG immunoglobulins are the most abundant, and are further divided to IgG1, IgG2, IgG3 and IgG4 subclasses [30]. Antibodies protect the host by three main ways:

- binding to pathogens and inhibiting their toxic effects (neutralization),

- coating pathogens so that phagocytes can phagocytose or engulf and kill them (opsonization), and
- activating the complement cascade.

Responses mediated by antibody production (humoral responses) and CD4<sup>+</sup> and CD8<sup>+</sup> T lymphocytes (cellular responses) are both necessary for the clearance of pathogens, and thus are the targets of immune induction in vaccination.

### **1.2.2. Immune responses in vaccination**

Vaccines are designed to elicit strong and durable antigen-specific immune responses with long-lasting memory. Vaccination relies on the effective administration of non-pathogenic forms (i.e. live, attenuated or subunit forms) of an infectious agent to induce a sustained immune response. Various elements of the innate and the adaptive immune systems affect the efficacy with which antigen is processed and presented, and also the nature of the overall immune response. Early vaccination approaches with “B cell vaccines” triggered the development of long-lived plasma cells that induced antibody-mediated immunity to neutralize or block infection. More recent approaches are directed towards activation of the cellular compartment of the adaptive immune system, to enable recognition and killing of pathogen-infected cells, using “T cell vaccines”. The immunological foundations for B cell and T cell vaccines are not mutually exclusive, and novel vaccines ought to prime both humoral and cellular responses. The objective of this thesis is to establish new strategies for the design of T cell vaccines and, as such, the following paragraphs focus on describing the T cell activation events in vaccination.

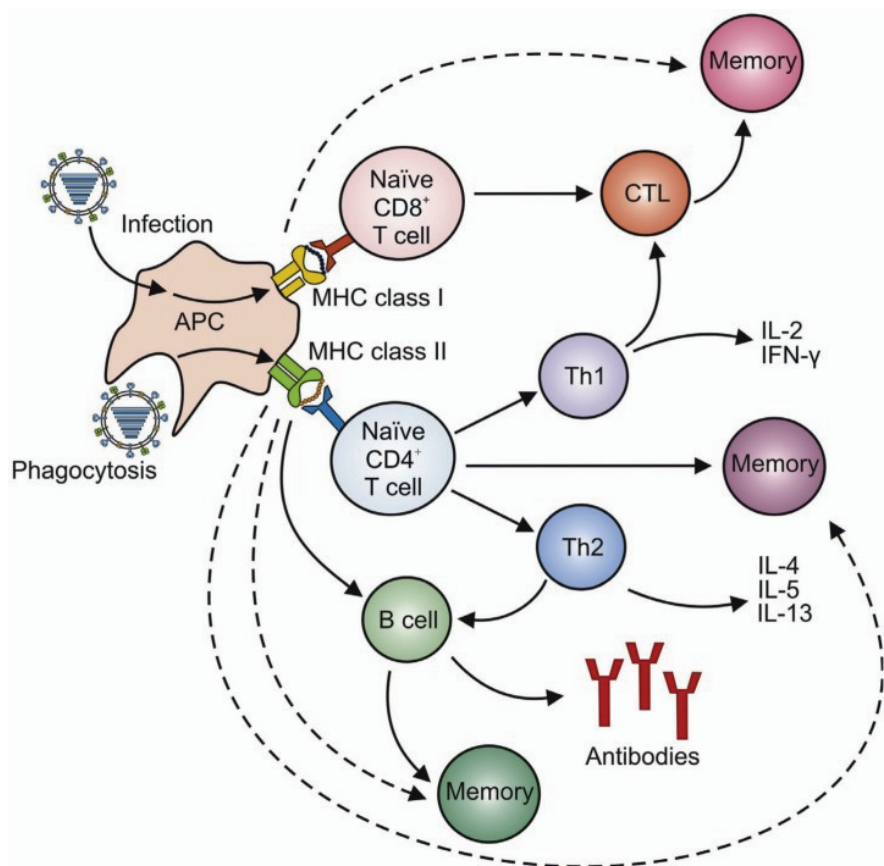
The kinetics of an immune response in vaccination can be divided into three different phases [31]. First, T lymphocytes must encounter the antigen presented by APCs within few hours after infection. Next, the CD4<sup>+</sup> and CD8<sup>+</sup> T cell compartments are activated and proliferation occurs rapidly, generating > 1000-fold increase in the number of clones, which are needed to elicit antigen-specific responses and to clear the infection from the host. This lasts for a few days, and when the infection is eradicated, > 90% of the newly generated T lymphocytes are cleared by apoptosis to return to homeostasis and prevent the development of autoimmunity. Eventually, memory T cells are raised from the once activated effector cells and these remain in circulation and/or in tissues ready to respond to re-infection. These memory cells express distinct

activation markers and intracellular proteins that distinguish them from naive and effector T cells, and they also express distinct chemokine and adhesion receptors that allow them to home to and to traffic through infected tissues and organs throughout the body [32].

Following a classical immunization pathway in vaccination, CD4<sup>+</sup> T cells, and in particular follicular helper (T<sub>FH</sub>) cells [33], provide help to B cells to promote isotype-switching and the generation of high affinity antigen-specific antibodies. In addition, CD4<sup>+</sup> T cells can also promote cytotoxicity in Th1 type responses by the release of granzyme and perforin as well as other antimicrobial cytokines such as IFN $\gamma$  and TNF $\alpha$  [34]. Finally, CD4<sup>+</sup> T cells can provide help in the activation of CD8<sup>+</sup> T cells. However, activation of CD8<sup>+</sup> T cells can also occur via cross-presentation as described earlier. The cross-priming of CD8<sup>+</sup> T cell with vaccines is an area of particular interest, as these cells can deal with chronic infections and intracellular pathogens. The direct contact of CTLs with a target cell for periods ranging from several minutes to an hour can kill the infected cells while the CD8<sup>+</sup> T cell remains intact for additional killing. Also, activated CD8<sup>+</sup> T cells elicit inflammatory responses against a pathogen through the secretion of cytokines and chemokines that interfere with replication and spreading of the pathogen [35]. A schematic representation of the main functions of CD4<sup>+</sup> and CD8<sup>+</sup> T cells are summarized in Fig. 3, adapted from [36].

The hallmark of a successful T cell-mediated immunization is the generation of long-lived memory cells capable of recognizing and expanding to fight against a re-infection. At least two types of memory T cells exist in mice and human, namely: effector memory (T<sub>EM</sub>) and central memory (T<sub>CM</sub>) T cells. T<sub>EM</sub> and T<sub>CM</sub> are mainly distinguished by the expression of surface markers, their location in the body and their profiles of cytokine secretion [37]. In particular, T<sub>CM</sub> cells reside within lymphoid organs where upon restimulation they expand to resupply the effector T cells at peripheral sites; a process that takes a few days. At their surface, these express the CD62L and CCR7 markers, which distinguishes them from T<sub>EM</sub> that express neither and reside in the peripheral tissues [38, 39]. T<sub>EM</sub>'s role is to provide immediate protection at the sites of infection by cytokine secretion and perforin-mediated killing, without requiring re-differentiation. However, these cells have a limited proliferation

capacity when compared to  $T_{CM}$ .  $CD4^+$  and  $CD8^+$  memory T cells can persist for decades and it is believed that  $CD4^+$  T cells play a role in their maintenance [40].



**Figure 3. The main roles of activated cells in vaccination** (adapted from Haes et. al.[36]). Antigen is taken up by APCs and used to activate  $CD4^+$  T cells which provide help to B cells for antibody production, elicit  $T_H1$  type responses and provide help to  $CD8^+$  T cell activation. The latter are also directly cross-primed by the antigen in a process called cross-presentation

### 1.2.3. $CD8^+$ T cell-inducing vaccines

The important role of T cells, specifically  $CD8^+$  T cells, in the elimination of intracellular infections and tumors has given rise to the study and development of  $CD8^+$  T cell-inducing vaccines (referred to here simply as  $CD8^+$  T cell vaccines), designed to elicit potent CTLs in the context of both prophylactic and therapeutic vaccination. For this reason, there has been growing interest in understanding the key determinants of  $CD8^+$  T cell activation and how to take advantage of these determinants in vaccines. Current  $CD8^+$  T cell vaccines primarily activate CTLs through the use of endogenously produced proteins (i.e. DNA vaccines or viral

vectors) or by cross-presentation of exogenously administered antigens (peptide-based vaccines) to CD8<sup>+</sup> T cells. The maintenance of these activated CD8<sup>+</sup> T cells, however, and their conversion to memory cells remain challenges in vaccine design. Several factors affect the quality of the induced CTLs, the first of these being the nature of the stimulation. CD8<sup>+</sup> T cells can be cross-primed by the cross-presentation of antigen on MHC class I molecules of DCs, while maturation of DCs can be achieved through TLR signaling along with the induction of soluble factors such as IL-12 and type I IFN [41-43] that promote the proliferation of activated CD8<sup>+</sup> T cells [44, 45]. Cross-presentation of antigen by DCs is of the utmost importance for activating CTLs in vaccination, but it requires the induction of co-stimulatory signals to sustain the interactions of DCs with CD8<sup>+</sup> T cells. Furthermore, a number of studies suggest that these vaccines also rely heavily on help from CD4<sup>+</sup> T cells for maintenance of the response and the generation of memory cells [35, 46]. Other factors that impact the quality of induced CTLs include the dose of antigen, the route of administration and the kind of delivery systems used [47]. How these factors affect the development of CTLs is still unclear, and their resolution is critical for the design of better CD8<sup>+</sup> T cell vaccines.

#### **1.2.4. Rational vaccine design**

Three elements are considered key in the design of effective subunit vaccines which, when combined, can potentially lead to induction of an optimal immune response and outcome.

##### *1. Antigen selection*

The antigen against which an immune response is raised is the most important element for raising specific immunity. The antigen in subunit vaccination is a purified or a recombinant protein that retains the immunogenic epitopes of the microbe or pathogen. Regarding the relevance of an antigen for use in a vaccine, two recommended selection criteria are: sequence conservation across the different strains of the pathogen and the levels of protein expression during the normal course of an

infection, especially when considering gene-based vaccination. Choosing the right antigen can be challenging, as most viruses, for example, have multiple epitopes, and more importantly, these epitopes tend to mutate, allowing escape from the immune response. Another significant consideration when designing an effective subunit vaccine is the amount of antigen that will be presented to T cells, as this can have a negative effect on immune activation. Studies have shown, for instance, that low dose vaccination resulted in preferential generation of protective T cells [48, 49]. Finally, susceptibility of the antigen to lysosomal proteolysis should also be taken into consideration when selecting antigens for vaccination, as it has been reported that exacerbated degradation of an antigen after uptake by APCs destroys potential peptides for T cell recognition [50]. Therefore, protection of the antigen against proteolysis can improve the outcome of a vaccination.

## 2. *Adjuvant selection*

In subunit vaccination the antigen alone is typically poorly immunogenic and thus, inclusion of immune potentiators, termed adjuvants, in the vaccine formulation is necessary to enhance the immunogenicity of the antigen. Adjuvants act as PAMPs that bind to the PRRs on APCs and trigger early innate immune responses that aid the generation of robust adaptive immune responses. Co-stimulation provided by adjuvants results in the upregulation of surface molecules on DCs such as CD40, CD80 and CD86, and accelerates the generation of robust T cell responses [51]. Moreover, adjuvants can create a depot effect that allows sustained release of the antigen and increases the duration of the immune response, even in low-inducers [52]. With sustained release, the amount of antigen required for vaccination can be reduced, which also limits the costs of the therapy. In subunit vaccination the most commonly used adjuvants are the TLR agonists. Currently licensed adjuvants include bacterial by-

products, toxins, lipids, nucleic acids, peptidoglycans, cytokines and other small molecules [53]. The most commonly used adjuvant in human vaccines is alum, which mainly induces humoral responses [54], however, many other adjuvants have been licensed for use and are recommended for CD8<sup>+</sup> T cell activation [52, 55]. Of particular interest for the purpose of this thesis are 3 adjuvants: Monophosphoryl lipid-A (MPLA), CpG and poly(I:C). MPLA is a synthetic LPS-derivative, and as such, it is a TLR4 activator that induces Th1 responses and has been approved for use in human vaccines in Europe (AS03 adjuvant by GlaxoSmithKline) [56]. Another adjuvant that is of particular interest is the TLR9 agonist CpG, consisting of nonmethylated cytosine-phosphate-guanosine domains of DNA. CpG is under clinical investigation, as it is a potent Th1 activator that also triggers antibody production [57]. Finally, poly(I:C) is a TLR3 agonist made of double stranded RNA, which mimics replicating viruses. It is a potent IFN inducer and its nontoxic analog has been used in clinical trials of HIV vaccination [58].

### 3. *Delivery system for direct targeting of the antigen*

In subunit vaccines, direct targeting of the antigen to the appropriate cell type *in vivo* is critical for the induction of an immune response. DCs are usually the target in T cell vaccines, and an increasing number of delivery systems have been developed throughout the years to facilitate the transportation of antigen to the proper type of DC for uptake in the lymphoid organs, without prior manipulation *ex vivo*. There are two means of antigen delivery in vaccination that can facilitate the initiation of an immune response:

- direct targeting of APCs with antigen fused to antibodies or chemokines, and
- incorporation of the antigen into a vehicle formulation.



The simplest approach for delivering antigen is to vaccinate with peptides that can bind directly to MHC class I molecules, but this has resulted in limited immunogenicity to the CD8<sup>+</sup> T cell compartments and is dependent upon the specific MHC I allele of the host. Combination of soluble antigen with adjuvants and direct targeting to DCs and/or other APCs has also been a common approach in protein/adjuvant vaccine formulations. DCs express unique surface markers and, as such, fusion of an antigen to an antibody or ligands that can bind these markers is a common vaccination strategy [12, 59, 60]. Examples where CTL responses have been generated by DC-targeted antigens include vaccination with molecules targeting DEC-205 [61], DCIR2 [62, 63], mannose receptor [64], Dectin-1 [65] and Clec9A [66]. Robust CD8<sup>+</sup> T cell responses have also been achieved with the use of dead cells. Studies have shown that DCs and other APCs can collect and process antigens from dead cells [67-69], which suggests that the idea of first targeting antigens to other cell types that will eventually result in the activation of CD8<sup>+</sup> T cells, may be feasible.

For antigen delivery by vehicles, there is an extensive list of tools available, which include the use of DNA vaccines, liposomes, virosomes, water-in-oil-emulsions and micelles [70]. In DNA or viral particles the antigen (protein) is synthesized inside the cell; this is probably the most direct method for loading antigen onto a MHC class I molecule for presentation to CD8<sup>+</sup> T cells. DNA and viral vaccines have been used against cancer, tuberculosis, HIV, influenza virus and other [71, 72]. Other vehicle-based platforms attempt to encapsulate the antigen and deliver the contents to the appropriate cell compartments. Liposomes, for example, can carry viruses, proteins, glycoproteins, nucleic acids, carbohydrates, and lipids, and facilitate their delivery to immune cells [73]. Similarly, virosomes – small spherical vesicles, embedded with viral proteins that can fuse to immune cells – can be used to transport and deliver antigenic cargo [74]. Of particular interest for the purpose of this thesis are micelles that are self-aggregated clusters of amphiphilic surfactant molecules, which can trap antigens and promote their delivery to relevant immunological sites in the body [75].

### 1.3. Accomplishments

In this thesis, we present new methods for T cell activation in subunit vaccination. To target compartments of the innate immune system eligible for raising robust T cell responses in the adaptive immune system, two approaches were undertaken : (1) novel nanoscale vehicles for vaccine delivery were developed, and (2) and recombinant cloning techniques for protein fusion to antibodies and chemical ligands were explored.

In Chapter 2, a novel technology for liver vaccine with direct antigen targeting is presented. We used an antibody technology established in our laboratory for antigen binding to erythrocytes, promoting their cross-presentation to CD8<sup>+</sup> T cells in a tolerogenic context. Using recombinant protein techniques, we inserted an immunogenic signal onto the erythrocyte binding antibody to reverse the tolerogenic outcome, and delivered the antigen to hepatic APCs together with potent adjuvant in a prime-boost vaccine. Direct antigen targeting to liver elicited potent CTL responses for local clearance of pathogen-infected cells. Most importantly, CTLs displayed a long-lasting memory phenotype, currently a significant challenge in hepatic vaccination.

In Chapter 3, a DC vaccine for direct antigen cross-presentation was developed with a novel design to improve cytotoxicity of a currently available technology. In particular, we targeted a subset of DCs known to excel in cross-presentation : CD8<sup>+</sup> DCs. The model antigen OVA was fused with recombinant techniques to the XCL1 ligand, which is uniquely expressed on the surface of this DC subtype. To enhance antigen uptake by CD8<sup>+</sup> DCs, we co-administred XCL1-OVA and a fusion protein of XCL1 with a domain of the extracellular matrix binding protein PIGF-2, produced with recombinat technology. Co-immunization with XCL1-PIGF attracted cross-presenting DCs to the injection site and increased XCL1-OVA uptake efficiency, leading to improved immunogenicity in vaccination. The technology was evaluated in prophylactic and therapeutic tumor models, in which XCL1-OVA mixed with XCL1-PIGF significantly prolonged survival of tumor-bearing mice.

The concept of extracellular matrix binding protein fusion was also tested in Chapter 4, with the fusion protein OVA-PIGF. In this study, we explored whether retaining the fusion protein at the injection site and creating a depot effect would result

in improved immune responses in vaccinations. Our initial hypothesis was not confirmed by the vaccination results, as soluble OVA elicited similar humoral and cellular responses as the OVA-PIGF formulation.

Finally, in Chapter 5, the immunogenicity of a micelle-based vaccine platform, kindly produced by Dr. Carrie Brubaker, was evaluated in a vaccine model. Encapsulation or complexation of different adjuvants and mixtures of adjuvants were used in antigen-bearing micelle formulations to vaccinate animals in a prime-boost-boost study. OVA- and CpG-B-presenting micelles resulted in significant activation of both humoral and cellular responses, suggesting potential for this novel platform in other further studies exploring tumor vaccination or clinically-relevant antigen.

In conclusion, we have developed new technologies for enhancing the CD8<sup>+</sup> T cell response to prophylactic and therapeutic vaccines. Hepatic antigen targeting as well as tumor vaccines remain a challenge in current vaccine technologies and as such, we believe that this work has potential impact in the development of a new generation of rationally designed vaccines with strong CTL activation and long lasting memory.

## References

1. Retief FP, Cilliers L. The epidemic of athens, 430-426 bc. *South African Medical Journal* 1998;88(1): 50-3.
2. Bloch H. Jenner,edward (1749-1823) - the history and effects of smallpox, inoculation, and vaccination. *American Journal of Diseases of Children* 1993;147(7): 772-4.
3. Germain RN. Vaccines and the future of human immunology. *Immunity* 2010;33(4): 441-50.
4. Plotkin SA. Vaccines: Past, present and future. *Nature Medicine* 2005;11(4): S5-S11.
5. Pulendran B, Li S, Nakaya HI. Systems vaccinology. *Immunity* 2010;33(4): 516-29.
6. Pashine A, Valiante NM, Ulmer JB. Targeting the innate immune response with improved vaccine adjuvants. *Nature Medicine* 2005;11(4): S63-S8.
7. Kool M, Soullie T, van Nimwegen M, et al. Alum adjuvant boosts adaptive immunity by inducing uric acid and activating inflammatory dendritic cells. *Journal of Experimental Medicine* 2008;205(4): 869-82.
8. Mangtani P, Abubakar I, Ariti C, et al. Protection by bcg vaccine against tuberculosis: A systematic review of randomized controlled trials. *Clinical Infectious Diseases* 2014;58(4): 470-80.
9. Gerlich WH. Medical virology of hepatitis b: How it began and where we are now. *Virology Journal* 2013;10.

10. Speiser DE, Lienard D, Rufer N, et al. Rapid and strong human cd8(+) t cell responses to vaccination with peptide, ifa, and cpg oligodeoxynucleotide 7909. *Journal of Clinical Investigation* 2005;115(3): 739-46.
11. Speiser DE, Baumgaertner P, Barbey C, et al. A novel approach to characterize clonality and differentiation of human melanoma-specific t cell responses: Spontaneous priming and efficient boosting by vaccination. *Journal of Immunology* 2006;177(2): 1338-48.
12. Kastenmuller W, Kastenmuller K, Kurts C, et al. Dendritic cell-targeted vaccines--hope or hype? *Nature reviews. Immunology* 2014;14(10): 705-11.
13. Reddy ST, van der Vlies AJ, Simeoni E, et al. Exploiting lymphatic transport and complement activation in nanoparticle vaccines. *Tissue Engineering Part A* 2008;14(5): 734-5.
14. Janeway CA, Medzhitov R. Innate immune recognition. *Annual Review of Immunology* 2002;20: 197-216.
15. Medzhitov R, Janeway CJ. Advances in immunology: Innate immunity. *New England Journal of Medicine* 2000;343(5): 338-44.
16. Palm NW, Medzhitov R. Pattern recognition receptors and control of adaptive immunity. *Immunological Reviews* 2009;227: 221-33.
17. Mogensen TH. Pathogen recognition and inflammatory signaling in innate immune defenses. *Clinical Microbiology Reviews* 2009;22(2): 240-+.
18. Beutler BA. Tlrs and innate immunity. *Blood* 2009;113(7): 1399-407.
19. Akira S, Takeda K. Toll-like receptor signalling. *Nature Reviews Immunology* 2004;4(7): 499-511.
20. O'Neill LAJ, Bowie AG. The family of five: Tir-domain-containing adaptors in toll-like receptor signalling. *Nature Reviews Immunology* 2007;7(5): 353-64.
21. Kawai T, Akira S. Signaling to nf-kappa b by toll-like receptors. *Trends in Molecular Medicine* 2007;13(11): 460-9.
22. Akira S, Uematsu S, Takeuchi O. Pathogen recognition and innate immunity. *Cell* 2006;124(4): 783-801.
23. Vyas JM, Van der Veen AG, Ploegh HL. The known unknowns of antigen processing and presentation. *Nature Reviews Immunology* 2008;8(8): 607-18.
24. Roche PA, Furuta K. The ins and outs of mhc class ii-mediated antigen processing and presentation. *Nature Reviews Immunology* 2015;15(4): 203-16.
25. Trapani JA, Smyth MJ. Functional significance of the perforin/granzyme cell death pathway. *Nature Reviews Immunology* 2002;2(10): 735-47.
26. Harty JT, Tvinnereim AR, White DW. Cd8(+) t cell effector mechanisms in resistance to infection. *Annual Review of Immunology* 2000;18: 275-308.
27. Bevan MJ. Cross-priming for a secondary cytotoxic response to minor h-antigens with h-2 congenic cells which do not cross-react in cytotoxic assay. *Journal of Experimental Medicine* 1976;143(5): 1283-8.
28. Kobayashi KS, van den Elsen PJ. Nlrc5: A key regulator of mhc class i-dependent immune responses. *Nature Reviews Immunology* 2012;12(12): 813-20.
29. Li ZQ, Woo CJ, Iglesias-Ussel MD, et al. The generation of antibody diversity through somatic hypermutation and class switch recombination. *Genes & Development* 2004;18(1): 1-11.
30. Vidarsson G, Dekkers G, Rispens T. Igg subclasses and allotypes: From structure to effector functions. *Frontiers in Immunology* 2014;5.
31. Robinson HL, Amara RR. T cell vaccines for microbial infections. *Nature Medicine* 2005;11(4): S25-S32.

32. Esser MT, Marchese RD, Kierstead LS, et al. Memory t cells and vaccines. *Vaccine* 2003;21(5-6): 419-30.
33. Crotty S. Follicular helper cd4 t cells (t<sub>fh</sub>). *Annual Review of Immunology, Vol 29* 2011;29: 621-63.
34. Streeck H, D'Souza MP, Littman DR, et al. Harnessing cd4(+) t cell responses in hiv vaccine development. *Nature Medicine* 2013;19(2): 143-9.
35. Appay V, Douek DC, Price DA. Cd8(+) t cell efficacy in vaccination and disease. *Nature Medicine* 2008;14(6): 623-8.
36. van de Sandt CE, Kreijtz JHCM, Rimmelzwaan GF. Evasion of influenza a viruses from innate and adaptive immune responses. *Viruses-Basel* 2012;4(9): 1438-76.
37. Sallusto F, Lenig D, Forster R, et al. Two subsets of memory t lymphocytes with distinct homing potentials and effector functions. *Journal of Immunology* 2014;192(3): 708-12.
38. Masopust D, Vezys V, Marzo AL, et al. Preferential localization of effector memory cells in nonlymphoid tissue. *Science* 2001;291(5512): 2413-7.
39. Masopust D, Vezys V, Marzo AL, et al. Preferential localization of effector memory cells in nonlymphoid tissue. *Journal of Immunology* 2014;192(3): 2413-7.
40. Reinhardt RL, Khoruts A, Merica R, et al. Visualizing the generation of memory cd4 t cells in the whole body. *Nature* 2001;410(6824): 101-5.
41. Iwasaki A, Medzhitov R. Toll-like receptor control of the adaptive immune responses. *Nature Immunology* 2004;5(10): 987-95.
42. Ito T, Amakawa R, Kaisho T, et al. Interferon-alpha and interleukin-12 are induced differentially by toll-like receptor 7 ligands in human blood dendritic cell subsets. *Journal of Experimental Medicine* 2002;195(11): 1507-12.
43. Palliser D, Ploegh H, Boes M. Myeloid differentiation factor 88 is required for cross-priming in vivo. *Journal of Immunology* 2004;172(6): 3415-21.
44. Curtsinger JM, Schmidt CS, Mondino A, et al. Inflammatory cytokines provide a third signal for activation of naive cd4(+) and cd8(+) t cells. *Journal of Immunology* 1999;162(6): 3256-62.
45. Schmidt CS, Mescher MF. Adjuvant effect of il-12: Conversion of peptide antigen administration from tolerizing to immunizing for cd8(+) t cells in vivo. *Journal of Immunology* 1999;163(5): 2561-7.
46. Castellino F, Germain RN. Cooperation between cd4(+) and cd8(+) t cells: When, where, and how. *Annual Review of Immunology* 2006;24: 519-40.
47. Williams MA, Bevan MJ. Effector and memory ctl differentiation. *Annual Review of Immunology* 2007;25: 171-92.
48. Darrah PA, Patel DT, De Luca PM, et al. Multifunctional th1 cells define a correlate of vaccine-mediated protection against leishmania major. *Nature medicine* 2007;13(7): 843-50.
49. AlexanderMiller MA, Leggatt GR, Berzofsky JA. Selective expansion of high- or low-avidity cytotoxic t lymphocytes and efficacy for adoptive immunotherapy. *Proceedings of the National Academy of Sciences of the United States of America* 1996;93(9): 4102-7.
50. Delamarre L, Couture R, Mellman I, et al. Enhancing immunogenicity by limiting susceptibility to lysosomal proteolysis. *The Journal of experimental medicine* 2006;203(9): 2049-55.
51. Chen LP, Flies DB. Molecular mechanisms of t cell co-stimulation and co-inhibition. *Nature Reviews Immunology* 2013;13(4): 227-42.

52. Bergmann-Leitner ES, Leitner WW. Adjuvants in the driver's seat: How magnitude, type, fine specificity and longevity of immune responses are driven by distinct classes of immune potentiators. *Vaccines* 2014;2(2): 252-96.
53. Mohan T, Verma P, Rao DN. Novel adjuvants & delivery vehicles for vaccines development: A road ahead. *The Indian journal of medical research* 2013;138(5): 779-95.
54. Marrack P, Mckee AS, Munks MW. Towards an understanding of the adjuvant action of aluminium. *Nature Reviews Immunology* 2009;9(4): 287-93.
55. Pasquale A, Preiss S, Silva F, et al. Vaccine adjuvants: From 1920 to 2015 and beyond. *Vaccines* 2015;3(2): 320.
56. Mata-Haro V, Cekic C, Martin M, et al. The vaccine adjuvant monophosphoryl lipid a as a trif-biased agonist of tlr4. *Science* 2007;316(5831): 1628-32.
57. Kobayashi H, Horner AA, Takabayashi K, et al. Immunostimulatory DNA pre-priming: A novel approach for prolonged th1-biased immunity. *Cellular immunology* 1999;198(1): 69-75.
58. Moyle PM, Toth I. Modern subunit vaccines: Development, components, and research opportunities. *ChemMedChem* 2013;8(3): 360-76.
59. Ueno H, Klechevsky E, Schmitt N, et al. Targeting human dendritic cell subsets for improved vaccines. *Seminars in immunology* 2011;23(1): 21-7.
60. Steinman RM. Dendritic cells in vivo: A key target for a new vaccine science. *Immunity* 2008;29(3): 319-24.
61. Bonifaz LC, Bonnyay DP, Charalambous A, et al. In vivo targeting of antigens to maturing dendritic cells via the dec-205 receptor improves t cell vaccination. *Journal of Experimental Medicine* 2004;199(6): 815-24.
62. Dudziak D, Kamphorst AO, Heidkamp GF, et al. Differential antigen processing by dendritic cell subsets in vivo. *Science* 2007;315(5808): 107-11.
63. Soares H, Waechter H, Glaichenhaus N, et al. A subset of dendritic cells induces cd4+ t cells to produce ifn-gamma by an il-12-independent but cd70-dependent mechanism in vivo. *The Journal of experimental medicine* 2007;204(5): 1095-106.
64. He LZ, Crocker A, Lee J, et al. Antigenic targeting of the human mannose receptor induces tumor immunity. *Journal of immunology* 2007;178(10): 6259-67.
65. Carter RW, Thompson C, Reid DM, et al. Preferential induction of cd4+ t cell responses through in vivo targeting of antigen to dendritic cell-associated c-type lectin-1. *Journal of immunology* 2006;177(4): 2276-84.
66. Sancho D, Mourao-Sa D, Joffre OP, et al. Tumor therapy in mice via antigen targeting to a novel, dc-restricted c-type lectin. *The Journal of clinical investigation* 2008;118(6): 2098-110.
67. Schulz O, Reis e Sousa C. Cross-presentation of cell-associated antigens by cd8alpha+ dendritic cells is attributable to their ability to internalize dead cells. *Immunology* 2002;107(2): 183-9.
68. Iyoda T, Shimoyama S, Liu K, et al. The cd8+ dendritic cell subset selectively endocytoses dying cells in culture and in vivo. *The Journal of experimental medicine* 2002;195(10): 1289-302.
69. Schnorrer P, Behrens GM, Wilson NS, et al. The dominant role of cd8+ dendritic cells in cross-presentation is not dictated by antigen capture. *Proceedings of the National Academy of Sciences of the United States of America* 2006;103(28): 10729-34.
70. Saroja C, Lakshmi P, Bhaskaran S. Recent trends in vaccine delivery systems: A review. *International journal of pharmaceutical investigation* 2011;1(2): 64-74.
71. Khan KH. DNA vaccines: Roles against diseases. *Germes* 2013;3(1): 26-35.

72. Robert-Guroff M. Replicating and non-replicating viral vectors for vaccine development. *Current opinion in biotechnology* 2007;18(6): 546-56.
73. Zaks K, Jordan M, Guth A, et al. Efficient immunization and cross-priming by vaccine adjuvants containing tlr3 or tlr9 agonists complexed to cationic liposomes. *Journal of immunology* 2006;176(12): 7335-45.
74. Moser C, Metcalfe IC, Viret JF. Virosomal adjuvanted antigen delivery systems. *Expert review of vaccines* 2003;2(2): 189-96.
75. Eby JK, Dane KY, O'Neil CP, et al. Polymer micelles with pyridyl disulfide-coupled antigen travel through lymphatics and show enhanced cellular responses following immunization. *Acta biomaterialia* 2012;8(9): 3210-7.





## **Chapter 2:**

### **Hepatic Targeting of Vaccinal Antigens**

Vasiliki Panagiotou, Eleonora Simeoni, Jeffrey Hubbell

Manuscript in preparation for submission

## 2.1 Abstract

A challenge in liver-targeted subunit vaccines is the activation of local cytotoxic responses with long-lasting memory. Previously we demonstrated that intravenous injected antigens bearing the TER119 erythrocyte-binding domain target the liver and crosspresent very efficiently to CD8<sup>+</sup> T cells. Here, we present a tri-domain fusion protein of TER119, OVA as a model antigen, and the BBOX domain of high mobility group box-1 (HMGB1) as an adjuvant (TER119-BBOX-OVA), which, when co-administered with CpG-B, we show elicits robust cytotoxic T lymphocyte (CTL) responses with a memory phenotype intrahepatically. Following a prime-boost immunization, we found that TER119-BBOX-OVA + CpG resulted in 6-fold higher IFN- $\gamma$  secretion in the liver of vaccinated mice compared with OVA + CpG vaccinations. Mice immunized with TER119-BBOX-OVA + CpG overcame the tolerogenic fate of activated CD8<sup>+</sup> T cells in the liver and developed memory cells that responded to a recall 5 weeks after the vaccination. Also, immunizations with TER119-BBOX-OVA + CpG resulted in clearance of the *Listeria monocytogenes* infected cells in the liver within 72 hr after infection. Overall, we designed a novel vaccine platform that efficiently cross-primes CD8<sup>+</sup> T cells and, when combined with adjuvants, activates CD8<sup>+</sup> T cells intrahepatically. Considering the simplicity of recombinant production of practically any fusion antigen, this strategy has potential to treat hepatic diseases where a strong, local cytotoxic response is required and the infected cells are difficult to approach by standard vaccination.

## 2.2. Introduction

Effective vaccines against viruses and tumors must induce the activation and expansion of antigen-specific CD8<sup>+</sup> T cells [1]. Accordingly, many efforts in vaccine design have focused on the induction of robust cellular responses. The ability to generate such immune responses in the disease-relevant organs is likewise essential to the efficacy of vaccines. However, organ-specific targeting has largely eluded vaccine designs to date. Common examples of infections where traditional vaccines are unable to raise sufficient CD8<sup>+</sup> T cell responses include liver infections [2]. In hepatitis B, a prophylactic vaccine has been available for years but adult infections or perinatal/postnatal mother-to-child infections still occur, emphasizing the need for improved vaccines from the standpoint of inducing cellular responses for therapeutic treatments [3]. Also, chronic hepatitis B patients with exhausted immune cells fail to initiate responses against the virus, a situation that can lead to hepatocellular carcinomas. Finally in malaria, the sporozites released in the blood harness the tolerogenic environment of the liver and escape immune surveillance. Thus, strong CD8<sup>+</sup> T cells raised in the liver are required to achieve protection with vaccination [4]. Efforts in liver vaccination focus on the induction of effective CD8<sup>+</sup> T cells with long lasting memory [5-7]. Recent studies have shown that the liver plays a major role in local immune responses and, more specifically, that induction of high numbers of memory CD8<sup>+</sup> T cells in the liver is a prerequisite for virus protection [8].

Raising effective CD8<sup>+</sup> T cell responses in the liver is challenging due to its role in promoting T cell tolerance [9-11]. Intrahepatic activated CD8<sup>+</sup> T cells can soon become defective in the liver after immunization and are cleared by apoptotic mechanisms [12]. However, contradictory studies support that the liver plays an important role in the defense against blood-borne pathogens, suggesting that generating and supporting strong intrahepatic CD8<sup>+</sup> T cell responses is possible [13-15]. The main challenge for liver immunity is to prevent the exhaustion of activated CD8<sup>+</sup> T cells, expand their number locally and directly target and kill the infected cells. Current vaccine approaches targeting liver focus on the induction of CD8<sup>+</sup> T cell responses with a memory phenotype that can be used as a preventive or therapeutic approach in liver infections and the treatment of chronic infections.

Traditional vaccination approaches include immunization with live or attenuated viruses, the preparation of which is difficult and requires the maintenance of the viability of the virus throughout the whole process. Such technical limitations have opened the field to the development of subunit vaccines with synthetic peptides or whole protein antigens. The successful design and development of liver subunit CD8<sup>+</sup> vaccines would require effective activation of CD8<sup>+</sup> T cells with a memory phenotype [16]. Prolonged antigen presentation and thus enhanced uptake by antigen presenting cells (APCs) is mandatory for such activation. Another prerequisite for effector CD8<sup>+</sup> T cells is the efficient cross-presentation of the antigen by loading on to MHC class I molecules on the surface of the appropriate APC. In addition to antigen cross-presentation, a potent TLR agonist that can activate costimulatory molecules and engage the T cells is necessary for the APCs to provide the appropriate signal that will prevent tolerogenic outcomes, which can exist in the absence of costimulation. Direct and prolonged targeting of the antigen to the liver, crosspresentation to CD8<sup>+</sup> T cells and sufficient costimulation would raise robust immune responses that would further initiate local immunity.

The purpose of this study was to design a vaccine platform that can induce antigen specific CD8<sup>+</sup> T cell responses inside the liver and overcome the tolerogenic fate of CD8<sup>+</sup> T cell activation that is frequently associated with the liver. Our laboratory has previously engineered antigens bearing antibody fragments that upon intravenous injection bind to erythrocytes [17]. Targeting antigens to erythrocytes improves the circulation half-life of the antigen and, more importantly, dramatically increases the (tolerogenic) cross-presentation of the antigen to CD8<sup>+</sup> T cells in the spleen and liver [18]. We hypothesized that coupling the enhanced antigen cross-presentation of our erythrocyte binding technology with a powerful danger signal would activate immunity and induce robust CD8<sup>+</sup> T cell responses. To examine the potential benefits of our approach in the context of vaccination, we engineered a fusion protein consisting of an erythrocyte binding, glycophorin A-specific scFv called TER119 [19], the danger signal domain BBOX from the endogenous adjuvant high mobility group box 1 (HMGB-1) [20] and the model antigen ovalbumin (OVA). The HMGB-1 protein is released by necrotic cells and activates dendritic cells via its BBOX domain only when a critical cysteine in the 193 position is present [21, 22]. In our experiments, the fusion protein TER119-BBOX-OVA was mixed with the strong

CpG-B adjuvant to further enhance the cytotoxic responses. Moreover, we took advantage of the intravenous route of administration to directly target the antigen to the liver and raise local responses.

We found that TER119-BBOX-OVA, when administered i.v. with CpG, induces strong Th1 cytotoxic responses in the liver that led to the clearance of pathogen-infected cells and generation of long-lasting CD8<sup>+</sup> T cell memory.

## 2.3. Materials and Methods

**Animals.** Female C57BL/6J mice were purchased from Harlan, and female Ly5.1 (CD45.1) mice were purchased from Charles River Laboratories. All mice were aged between 8-12 weeks and kept under pathogen free conditions at the animal facility of Ecole Polytechnique Fédéral Lausanne (EPFL). Female C57BL/6-Tg(TcraTcrb) 1100Mjb (OTI) mice between 8-15 weeks that were used for isolation of splenocytes were bred under specific pathogen-free (SPF). The Veterinary Authority of the Canton de Vaud has approved all procedures and experiments.

### **Recombinant production of proteins. Design and cloning of TER119-BBOX-OVA.**

The altered pSecTag plasmid carrying the DNA sequence coding for the TER119 scFv antibody fragment fused with the OVA antigen at the 3' end, was previously developed in our laboratory [18]. The HMGB1 vector was purchased from HMGBiotech; the forward primer “accggtgacttcaaggacccaatgcaccaagaggcctc” and the reverse primer “gatattgctgcctacagagctaaaggtggcggttctggtggcggttctggatcc” were used to amplify the BBOX sequence of HMGB1. A GGSGGS linker was added upstream and downstream of the BBOX sequence to allow proper folding of the protein after translation. A 6 Histidine tag sequence was further added to the 3' end to facilitate purification. HEK cells were transfected with the TER119-BBOX-OVA construct under serum free conditions with 3.75 mM valproic acid (Sigma-Aldrich) [23], and after 7 days the protein in suspension was purified with immobilized metal affinity chromatography using a HiTrap HP His-tag column (GE Healthcare). The purified protein was analyzed for purity using SDS/PAGE, endotoxin levels were assessed in THP-1 x Blue cells (InvivoGen), and concentration was measured using bicinchoninic acid assays

(Thermo Scientific). The final product was sterile-filtered, and stored at  $-80\text{ }^{\circ}\text{C}$  in working aliquots.

**Pharmacokinetic and pharmacodynamic studies.** To measure the TER119-BBOX-OVA dissociation constant  $k_d$  with the erythrocyte surface TER119-BBOX-OVA was diluted in a range of concentrations varying from 0.1 nM to 5000 nM in a total of 10  $\mu\text{L}$  PBS with 10 mg/ml BSA, whereas 20  $\mu\text{L}$  of diluted erythrocytes (1  $\mu\text{L}$  of blood in 100  $\mu\text{L}$  PBS mixed with 10 mg/ml BSA) were added in a total volume of 180  $\mu\text{L}$  PBS mixed with 10 mg/ml BSA. After incubation for 1 hr at  $37^{\circ}\text{C}$ , the cells were washed, centrifuged and labeled with 100  $\mu\text{L}$  of OVA-FITC antibody (Abcam) in a dilution of 1:100 for 20 min on ice. The geometric mean fluorescence intensity of the antibody binding was measured by flow cytometry and analyzed by Prism (One site-total binding).

For *in vivo* binding measurements, 34  $\mu\text{g}$  TER119-BBOX-OVA mixed with 20  $\mu\text{g}$  OVA were injected *i.v.* into the tail vein of C57BL/6 mice. At predetermined time points, 1  $\mu\text{L}$  of blood obtained by tail incision was diluted 100-fold into PBS mixed with 10 mg/ml BSA, washed 3 times and incubated with 100  $\mu\text{L}$  of OVA-FITC antibody (dilution 1:100) for 20 min on ice. The OVA content of the samples was analyzed by flow cytometry and calculations of the  $t_{1/2}$  were done in Prism (One phase decay).

**Labeling of proteins.** The TER119-OVA, TER119-BBOX-OVA and OVA proteins were labeled with the Alexa 647 fluorophore (Dyomics). All proteins were mixed with the fluorophore in a protein:dye molar ratio of 1:10, and incubated for 1 hr at room temperature. The free dye was removed by centrifugation with Zeba columns (Thermo Scientific). All reactions were performed under sterile conditions to protect from endotoxin contamination.

**Biodistribution studies and liver processing for uptake.** The fluorescently conjugated proteins TER119-OVA A647, TER119-BBOX-OVA A647 and OVA A647 were injected *i.v.* in equimolar amounts of 0.45 nmoles with or without 5  $\mu\text{g}$  CpG, and were allowed to circulate *in vivo* for 17 hr. Female C57BL/6L mice 8 weeks old were used for this experiment. The mice were euthanized by cervical dislocation, and the

liver was perfused with 10 ml Hanks' Balanced Salt Solution media (Gibco) mixed with 0.5mg/ml Collagenase D (Roche) through the inferior vena cava with a 25 Ga needle. The portal vein was cut to release the pressure in the liver and allow the blood to exit. Subsequently, it was cut and homogenized to single cell suspension. The hepatocytes were removed first via centrifugation at 20xg, and stained with antibodies against CD45 (1:200), MHCII (1:800) and CD1d (1:200) for flow cytometry. The remaining homogenate was mixed in a 70% Percoll (VWR) layer, overlaid by a 20% layer of PBS, and centrifuged for 20 min. The hepatic stellate cells (HSCs) were removed from the 20-PBS surface, whereas the liver dendritic cells (DCs), Kupffer cells (KCs), and liver sinusoidal endothelial cells (LSECs) from the 20-70 layer, washed and stained with the following antibodies: HSCs: CD45, MHCII, CD1d and CD146 (1:200); liver DCs: CD45 and CD11c (1:200); KCs: CD45 and F4/80 (1:200); LSECs: CD45, CD146 and CD31 (1:200). All the aforementioned antibodies were purchased from eBiosciences.

**Adoptive transfer of OTI T cells.** Female CD45.2+ cells were isolated from splenocytes of OTI mice, between 12-16 weeks old, using a CD8 magnetic bead negative selection kit (Miltenyi Biotec). The isolated CD8+ OTI cells were incubated with 1  $\mu$ M CFSE (Invitrogen) for 6 min at room temperature, and the reaction was quenched with an equal volume of Iscove's modified Dulbecco's medium (IMDM) with 10% (vol/vol) FBS (Gibco). Before injection, cells were resuspended in pure IMDM to a final concentration of  $10^7$  cells/ml. A total of 100  $\mu$ l were injected i.v. into the tail vein of recipient female Ly5/ CD45.1+ mice, 8 weeks old. The following day the mice received an i.v. injection of equimolar (0.45 nmoles) amounts of TER119-OVA, TER119-BBOX-OVA or OVA with or without 10  $\mu$ g CpG, and they were sacrificed 4 days later. The liver and spleen were collected and processed and stained for flow cytometry as described previously.

**Immunizations, and memory recall experiments.** Female C57BL/6 mice, 8 weeks old, were immunized under isoflurane anesthesia on day 0 (i.v. injection of 100  $\mu$ l total mixture) and on day 14 (s.c. injection of 200  $\mu$ l total mixture volume) with 32  $\mu$ g TER119-OVA, 32  $\mu$ g TER119-OVA + 5  $\mu$ g CpG, 34  $\mu$ g TER119-BBOX-OVA, 34  $\mu$ g TER119-BBOX-OVA + 5  $\mu$ g CpG, 20  $\mu$ g OVA (endotoxin free, Hyglos), 20  $\mu$ g OVA + 5  $\mu$ g CpG or just saline. 5 days later the mice were euthanized, and the liver and

spleen were collected for *ex vivo* restimulation. For the memory recall, the mice were immunized as described above, and 5 weeks after the boost injection they all received a s.c. injection of 10 µg OVA + 20 µg CpG. A control group of mice that was not originally vaccinated also received the recall boost. All mice were euthanized, and their organs (spleen, liver and the axillary, branchial and inguinal lymph nodes) were processed and restimulated as described previously.

***Listeria monocytogenes* infection.** *Listeria monocytogenes* bacteria expressing OVA (*Listeria* strain 10403; modified by the Dietmar Lab (UNIL, Lausanne) to express OVA as described here [24]) were grown at 37°C in Brain Heart Infusion (Fulka) media without antibiotics until the OD reached 0.3. The cells were subsequently diluted with PBS to a final concentration of 10<sup>5</sup> CFU/ml, and C57BL/6 mice were injected with 100 µl of the bacterial cell suspension via i.v. injection in the tail vein. 3 days after the infection the mice were euthanized, and their organs were processed as described elsewhere [25]. Briefly, the liver and spleen were homogenized through a 100-µm cell sieve and a 70-µm cell sieve correspondingly, and PBS was added to a final volume of 40 ml. 100 µl of the homogenate were plated in brain heart infusion agar plates (Fulka) prepared 1 day before, and the number of bacteria colonies was assessed after overnight incubation at 37°C.

**Tissue and cell preparation for *ex vivo* restimulation of lymphocytes.** The liver was perfused with 10 ml HBSS through the inferior vena cava, and gently homogenized through a 100 µm cell sieve. Hepatocytes were removed by centrifuge for 5 min at 20xg, and lymphocytes were separated from other hepatic cells with a 30% Percoll (VWR) gradient. Remaining red blood cells were lysed for 5 min with 0.155M NH<sub>4</sub>Cl. Splenocytes were obtained by disruption of the spleen through a 70-µm cell sieve, and subsequent red blood cell lysis with 0.155M NH<sub>4</sub>Cl. The lymph nodes were digested for 30 min with 2 mg/mL Collagenase D (Roche) in IMDM, and passed through a 70-µm cell sieve to obtain single cell suspensions. All organs were kept in Dulbecco's Modified Eagle Medium (DMEM) (Gibco) supplemented with 10% FBS and 1% penicillin, streptomycin (Invitrogen). For CD8<sup>+</sup> T-cell-specific restimulation and intracellular cytokine staining, cells were first cultured for 3 hr at 37 °C in the presence of 1 µg/mL SIINFEKL, 10<sup>4</sup> U/ml IL2, and 0.5 µg anti-CD28 (eBioscience), and subsequently for 3 hr with the addition of 250 µg/mL brefeldin A (SigmaAldrich). For



CD4<sup>+</sup> T-cell restimulation, 10<sup>4</sup> U/ml IL2, 0.5 µg anti-CD28 and 100 µg/mL of OVA grade VI (Sigma-Aldrich) were added to the cells for 3 hr, followed by incubation with 50 µg/mL brefeldin A for another 12 hr. Alternatively, cells were restimulated for 4 days in the presence of 100 µg/mL OVA or 1 µg/mL SIINFEKL for the analysis of cytokine production in the supernatant.

**Flow cytometry and ELISA.** For the detection of live cells, cells were suspended at a concentration of 1 mio cells in 200 µl, washed with PBS, and labeled with live/dead fixable cell viability reagent (Invitrogen). Subsequently, the cells were incubated for 20 min on ice with PBS/2% FBS solutions of the surface markers CD3 (1:100) and CD8 (1:200) or CD4 (1:200). For intracellular cytokine staining, cells were fixed in 2% paraformaldehyde solution, washed with 0.5% saponin (SigmaAldrich) in PBS/2% FBS, and incubated with the IFN $\gamma$  (1:200) antibody diluted in saponin solution for 30 min on ice. Finally, the cells were resuspended in PBS/2% FBS for analysis. Samples were processed on CyAn ADP Analyzer (Beckman Coulter), and data were analyzed with FlowJo software (Tree Star). The antibodies against mouse CD3, CD4, CD8, IFN $\gamma$  and TNF $\alpha$  were purchased from eBioscience.

For the detection of cytokines in the supernatant of incubated cells, Ready-SET-go! ELISA kits were purchased from eBioscience, and the manufacturer's instructions were followed for a sandwich ELISA.

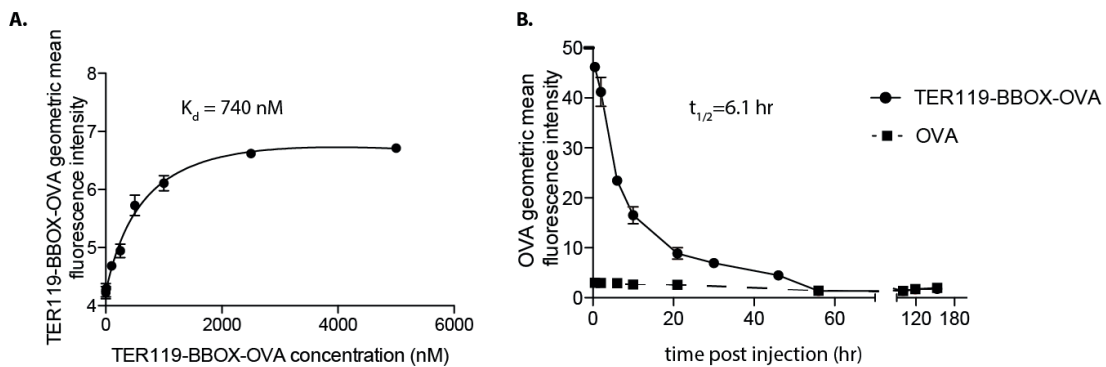
**Data Analysis.** All flow cytometry data were analyzed using FlowJo (v8.8.6). Graphs and statistical analyses of worked-up data were performed using Prism (v5, GraphPad). The statistical significance was determined by one way ANOVA – Bonferoni test or t-test with Welch correction. The asterisks indicate the significance as follows: \*p<0.05, \*\*p < 0.01, \*\*\*p < 0.001.

## 2.4. Results and Figures

### 2.4.1. Production and characterization of erythrocyte-binding antigens.

Engineering proteins to bind to erythrocytes improves their pharmacokinetic properties and increases the circulation half life [17]. We generated a tri-domain fusion protein consisting of an erythrocyte-binding antibody fragment, an adjuvant domain,

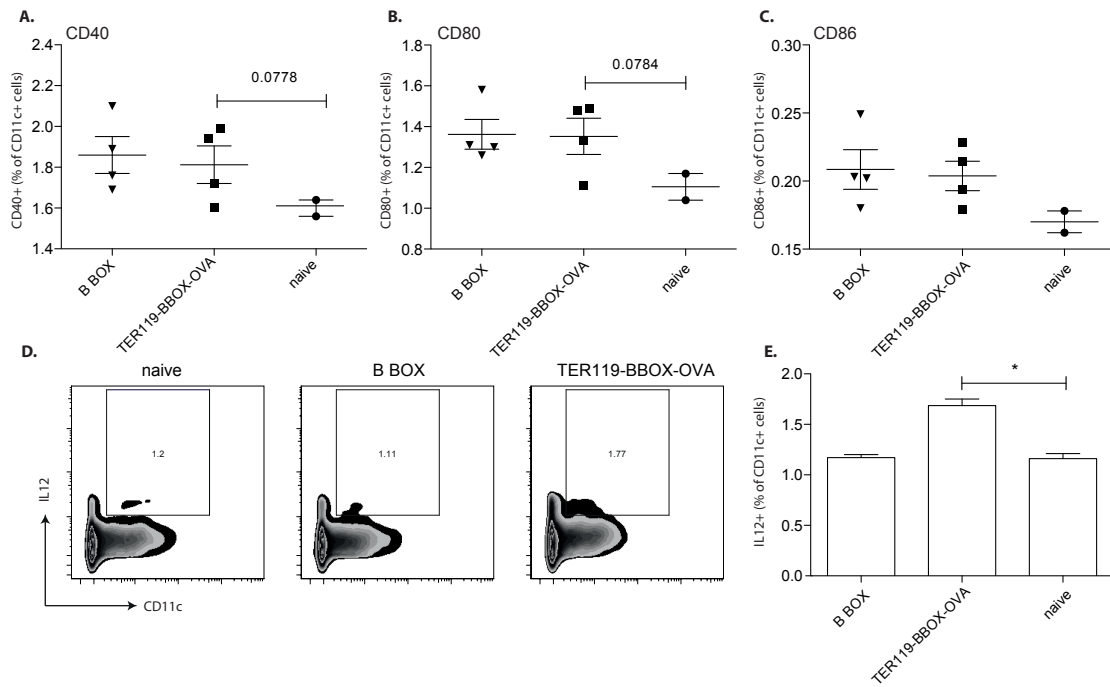
and an antigen domain. In particular we used the TER119 antibody that binds to glycophorin-A on the surface of erythrocytes in mice [19], the BBOX active domain of the endogenous necrotic signal HMGB1 [20], and the model antigen OVA, and we cloned the TER119-BBOX-OVA fusion protein. We evaluated the pharmacokinetic properties of the protein compared to the non-erythrocyte binding OVA-only protein and found that the former binds to red blood cells and circulates *in vivo* longer than OVA only. The binding affinity of TER119-BBOX-OVA to red blood cells was validated *in vitro* by equilibrium binding measurements using varying concentrations of the protein. TER119-BBOX-OVA binds to red blood cells with high affinity and an equilibrium dissociation constant ( $k_d$ ) of 740 nM (Fig. 1A), whereas OVA-only does not bind (data not shown). We also performed pharmacokinetic measurements to characterize the *in vivo* circulation time of TER119-BBOX-OVA. Following a single i.v. injection of 32  $\mu$ g TER119-BBOX-OVA, we sampled the blood frequently and used flow cytometry to determine the amount of TER119-BBOX-OVA bound to the surface of erythrocytes as a function of time. TER119-BBOX-OVA exhibits a cell surface half life ( $t_{1/2}$ ) of 6 h and remains in circulation for a few days after the injection as opposed to OVA that is cleared immediately from the body (Fig. 1B). The above results confirm the binding of TER119-BBOX-OVA to red blood cells and show the improved pharmacokinetic parameters of the molecule compared to OVA-only.



**Figure 1: TER119-BBOX-OVA binds to erythrocytes and circulates *in vivo* for a few hours.** **A)** The equilibrium dissociation constant of TER119-BBOX-OVA to erythrocytes was determined by flow cytometry, using an anti-HIStag PE antibody (Analysis with Prism 5: One site- total,  $R^2=0.9827$ ). **B)** The half life ( $t_{1/2}$ ) of equimolar amounts (0.45 nmoles) of TER119-BBOX-OVA and OVA administered i.v. with a single dose were measured by flow cytometry using an anti-OVA FITC antibody (Analysis with Prism 5: One phase decay,  $R^2=0.9844$ ).

#### **2.4.2. TER119-BBOX-OVA bears a danger signal.**

Erythrocytes undergo physiological death associated with immune suppressive and tolerogenic signals, whereas cells dying under stress release damage-associated molecular patterns (DAMPs) that can activate the immune system [26]. We aimed to force an artificial danger signal on dying erythrocytes by introducing BBOX within the tri-domain fusion protein and activating DCs to uptake the erythrocyte debris and initiate further immune responses. To confirm that the BBOX retains its adjuvant properties within the TER119-BBOX-OVA protein, we injected C57BL/6 mice with TER119-BBOX-OVA or BBOX-only and compared the upregulation of costimulatory molecules on CD11c<sup>+</sup> DCs, in their spleens. We found that the BBOX within TER119-BBOX-OVA retains the adjuvant properties of free BBOX. In particular, we looked for upregulation of common costimulatory molecules on DCs such as CD40, CD80 and CD86. All 3 molecules were equally upregulated both with TER119-BBOX-OVA and BBOX compared to naïve untreated mice (Fig. 2A, B and C correspondingly). In addition, we searched for the proinflammatory cytokines IL12 and TNF $\alpha$  by intracellular staining. The secretion of IL12 by TER119-BBOX-OVA was higher than BBOX or naïve mice; 1.77% of IL12 positive cells in TER119-BBOX-OVA group compared to 1.11% and 1.2% for BBOX and naïve groups correspondingly (Fig. 2D and 2E). The secretion of TNF $\alpha$  was similar in all groups (data not shown). Even though the secretion levels are not very high, these findings confirm the presence of a danger signal inside the tri-domain fusion protein and support our initial hypothesis that antigens circulating on red blood cells and bearing danger signals can be used as initiators of immune responses in vaccination.



**Figure 2: TER119-BBOX-OVA retains the adjuvant properties of BBOX.** C57BL/6 mice were injected with equimolar amounts of BBOX and TER119-BBOX-OVA and the spleens were harvested 12 hr later. The cells were stained and analyzed by flow cytometry **A,B,C**) Upregulation of costimulatory molecules **A**) CD40, **B**) CD80 and **C**) CD86 on CD11c+ gate. **D**) Intracellular staining for IL12 expression. Representative plots with positive gate on CD11c<sup>+</sup>, IL12<sup>+</sup> cells. **E**) The graph shows IL12 expression in all groups; gate on CD11c<sup>+</sup> cells (Analysis with t test, \*p<0.05)

### 2.4.3. Uptake of TER119-BBOX-OVA by hepatic cells and upregulation of antigen presenting cells in the liver.

The generation of antigen-specific effector T cell responses requires that antigens are taken up by APCs and further presented to T cells in the presence of costimulatory molecules. We are particularly interested in the liver uptake because it hosts different types of antigen presenting cells, which can be immunogenic or tolerogenic, depending on the stimulant. Therefore, we explored the hepatic cellular uptake targets of the TER119-BBOX-OVA protein and compared it to the equivalent erythrocyte-binding antigen TER119-OVA without the BBOX and OVA-only protein. All proteins were tested with and without CpG. To show that the injected constructs reach the liver, are taken up by APCs and activate them, we treated C57BL/6 mice with Alexa-647 fluorophore-labeled proteins. After 17 h, we analyzed the cellular distribution of the injected proteins and the presence of co-stimulatory molecules.

Flow cytometry analysis revealed preferred uptake of the TER119-BBOX-OVA with and without CpG by hepatocytes, as seen by CD45<sup>-</sup> MHCII<sup>low</sup> CD1d<sup>-</sup> staining in all groups (Fig 3A). In particular, there is a 2-fold increase in the uptake of TER119-BBOX-OVA compared to TER119-OVA and almost 2-fold compared to OVA alone. Similarly, hepatic stellate cells (HSCs), known to express molecules required for antigen presentation (MHC I, MHC II and costimulatory molecules), were stained with CD45<sup>+</sup> MHCII<sup>+</sup> CD1d<sup>+</sup> CD146<sup>-</sup> and showed preferential uptake of the TER119-BBOX-OVA protein both with and without CpG (Fig 3B). In particular, the uptake by TER119-BBOX-OVA was increased by 4-fold compared to TER119-OVA and 2-fold compared to OVA, in the presence of CpG. Further processing of the liver homogenate allowed the separation of the non-parenchymal liver cells in a homogenous solution that included KCs, liver DCs and LSECs. The uptake by the different cell types within this layer is represented in pie charts in Figure 3C. TER119-OVA (Fig. 3C top left) is mostly distributed among KCs (CD45<sup>+</sup>, F4/80<sup>+</sup>) with 49.2% uptake, a small percentage (4.2%) of liver DCs (CD45<sup>+</sup>, CD11c<sup>+</sup>) and the rest (46.6%) of the protein is taken up by other unstained populations. The addition of CpG to TER119-OVA (Fig. 3C top right) only slightly increased the percentages of KCs and DCs that uptake the protein but does not change drastically the uptake distribution percentages. Interestingly, in addition to Kupffer cells, TER119-BBOX-OVA (Fig. 3C middle left) is taken up also by LSECs (1.3%) labeled as CD45<sup>-</sup>, CD31<sup>-</sup>, CD146<sup>+</sup> cells and higher percentages (7.7%) of liver DCs compared with TER119-OVA. The addition of CpG to TER119-BBOX-OVA (Fig. 3C middle right) further increases the uptake percentages by LSECs (4%) and DCs (14%). Finally, OVA-only that does not bind to erythrocytes has the biggest percentage of KCs uptake (59.9%) as well as some uptake by LSECs (1%) and liver DCs (6.1%) (Fig. 3C bottom left). The distribution of OVA changes with the addition of CpG (Fig. 3C bottom right) between KCs (39.2%) and other unstained populations (51.6%) but no big differences are observed between LSECs uptake (0.8%) and DCs (8.2%) in this group.

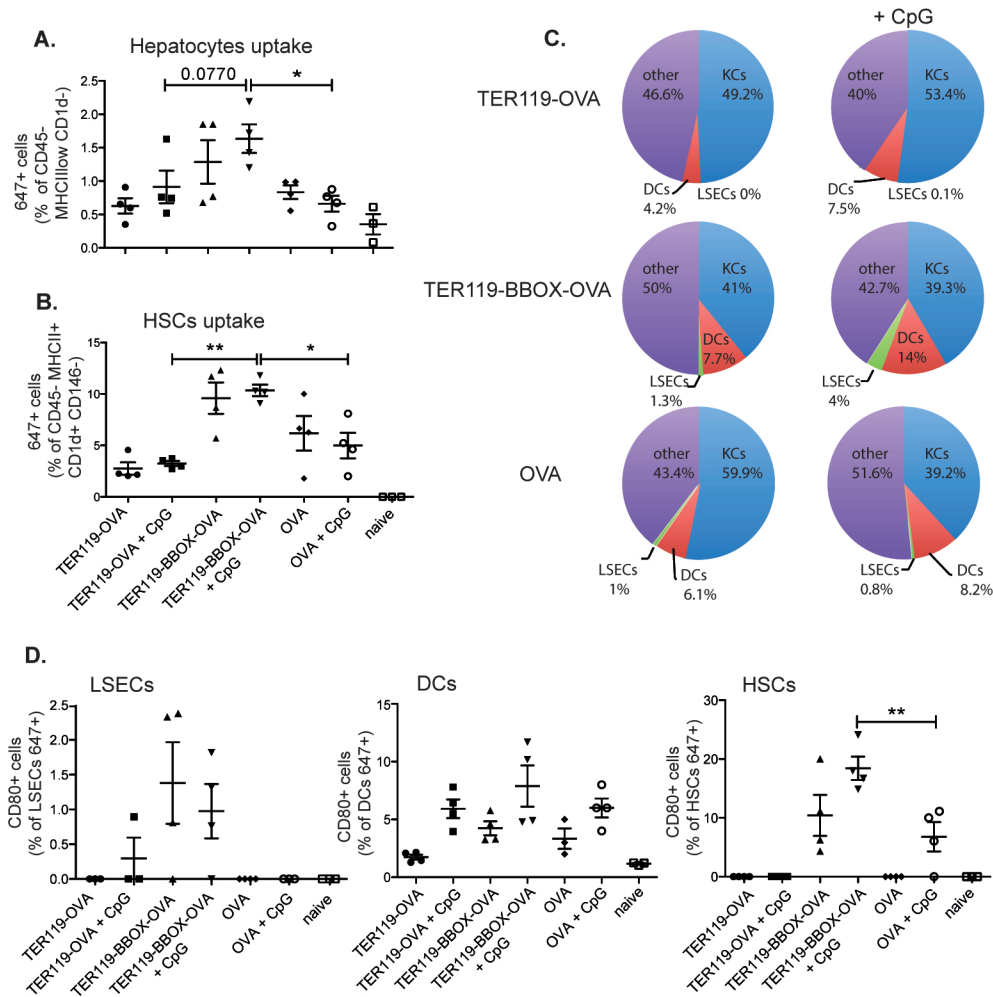
Finally, we confirmed by flow cytometry the upregulation of costimulatory molecules in AF-647 positive cells, which have taken up the antigen (Fig. 3D). We found that CD80 is upregulated in LSECs, DCs and HSCs that are positive for uptake of TER119-BBOX-OVA or TER119-BBOX-OVA + CpG. This result supports the capacity of these cells to activate T cells. In particular, 1.5% and 1% of LSECs positive

for TER119-BBOX-OVA and TER119-BBOX-OVA + CpG uptake correspondingly are positive for CD80 upregulation compared to no upregulation by OVA, OVA + CpG, TER119-OVA and TER119-OVA + CpG with the exception of one mouse in the last group (Fig. 3D left). The upregulation of CD80 in liver DCs is present in all groups injected with CpG; 6% with TER119-OVA + CpG, 7.5% with TER119-BBOX-OVA + CpG and 6% with OVA + CpG as well as in TER119-BBOX-OVA (4%) and OVA (3%) (Fig. 3D middle). In HSCs 10% of the cells positive for TER119-BBOX-OVA are positive for CD80 upregulation and more interestingly 20% of TER119-BBOX-OVA + CpG cells are positive which represents a 3-fold increase compared to OVA + CpG (Fig. 3D right).

Taken together, the above data support that TER119-BBOX-OVA mixed with CpG can reach the liver, initiate local immune responses and thus be further used as a potent vaccine candidate.

#### **2.4.4. Efficient crosspresentation of TER119-BBOX-OVA + CpG improves the proliferation of OVA-specific CD8<sup>+</sup> T cells.**

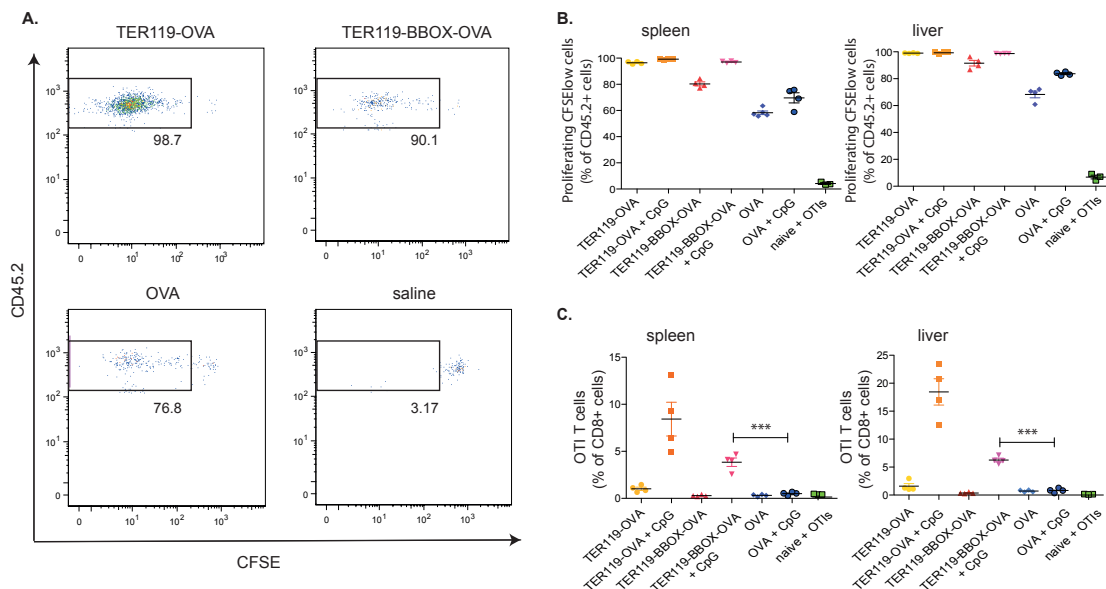
In principle, the design of potent CD8 vaccines, able to kill viruses and tumors, requires effective crosspresentation of the antigen to CD8<sup>+</sup> T cells and a strong adjuvant. We further explored whether TER119-BBOX-OVA can crosspresent OVA to CD8<sup>+</sup> T cells using an established adoptive transfer model. Carboxyfluorescein succinimidyl ester (CFSE)-labeled OTI CD8<sup>+</sup> T cells (CD45.2<sup>+</sup>) were injected into CD45.1<sup>+</sup> mice, followed 24 h later by i.v. injections of equimolar amounts of TER119-BBOX-OVA, OVA or TER119-OVA, used as a positive control as shown elsewhere [18]. All formulations were injected with or without 10 µg CpG. The proliferation of CD45.2<sup>+</sup> cells was measured 4 days later in the spleen and liver by the dilution of CFSE, using flow cytometry. TER119-BBOX-OVA mixed with CpG crosspresents to CD8<sup>+</sup> T cells more efficiently than OVA, as it is seen by increased proliferation of OTI T cells (Fig.4). Representative gating on proliferating OTI T cells shows enhanced dilution of CFSE in TER119-OVA and TER119-BBOX-OVA injected mice in the spleen (98.7% and 90.1%, respectively) compared to OVA (76.8%) or saline-injected mice (3.17%), in which no proliferation was observed (Fig 4A). The average dilution of CFSE-labeled OTI T cells in all groups for both spleen (Fig. 4B left) and liver (Fig. 4B right) clearly shows that antigens fused to the scFv antibody TER119, with or



**Figure 3: TER119-BBOX-OVA reaches the liver more efficiently than OVA alone and is taken up by different APCs in the liver.** Equimolar amounts (0.45nmoles) of Alexa-647 fluorophore labeled TER119-OVA, TER119-BBOX-OVA and OVA with or without 5 $\mu$ g CpG were administered i.v. The liver was harvested 17 hr later. Uptake by **A)** hepatocytes (percentage of MHCII<sup>low</sup>, CD45<sup>-</sup> CD1d<sup>-</sup> cells) and **B)** hepatic stellate cells (percentage of MHCII<sup>+</sup> CD45<sup>-</sup> CD1d<sup>+</sup> CD146<sup>-</sup> cells) quantified by flow cytometry. **C)** Uptake by nonparenchymal liver cells represented in a pie chart as a percentage of total A647<sup>+</sup> cells in the nonparenchymal layer of liver cells after separation with Percoll. Each pie chart represents the distribution among KCs (CD45<sup>+</sup>F4/80<sup>+</sup> cells), LSECs (CD45<sup>-</sup>CD31<sup>+</sup>CD146<sup>+</sup> cells), DCs (CD45<sup>+</sup>CD11c<sup>+</sup> cells) and other (unstained) for each group as follows: TER119-OVA, TER119-BBOX-OVA and OVA on the left column from top to bottom and TER119-OVA + CpG, TER119-BBOX-OVA + CpG and OVA + CpG on the right column from top to bottom. **D)** Upregulation of CD80 costimulatory molecule as a percentage of A647<sup>+</sup> LSECs (left), DCs (middle) and HSCs (right). (Analysis with one way ANOVA ("Bonferroni's Multiple Comparison Test", \*p<0.05, \*\*p<0.001

without CpG, have significantly high percentages (up to 98% for both TER119-OVA + CpG and TER119-BBOX-OVA + CpG) of CFSE diluted cells, and thus increased proliferation compared to the non-fused OVA antigen mixed with CpG (70%

proliferation in spleen and 80% in liver). We also measured the expansion of the OTI T cells by the increase of the CD45.2<sup>+</sup> cell population. TER119-BBOX-OVA mixed with CpG crosspresents the antigen to OTI T cells, thus promoting their proliferation by 4-fold in the spleen (Fig. 4C left) and more than 5-fold in the liver (Fig. 4C right), as compared to soluble OVA mixed with CpG. Interestingly, the BBOX insertion decreased the proliferation capacity of TER119-BBOX-OVA compared to TER119-OVA, most probably due to the lower binding affinity of the former onto erythrocytes related with folding properties of the two molecules. Overall, treatment with TER119-BBOX-OVA + CpG results in efficient cross presentation to CD8<sup>+</sup> T cells as measured by proliferation and expansion of OTI cells, as compared to the OVA + CpG control.



**Figure 4: TER119-BBOX-OVA mixed with CpG crosspresents to CD8<sup>+</sup> T cells and enhances the proliferation of adoptively transferred OTI T cells.** A total of 10<sup>6</sup> CFSE labeled OTI T cells were adoptively transferred into naive Bl6 mice by i.v. injections in 100 $\mu$ l solutions. A day later the mice were immunized i.v. with equimolar amounts (0.45nmoles) of TER119-OVA, TER119-BBOX-OVA or OVA with or without 10 $\mu$ g CpG and the spleen and liver were harvested 4 days later. **A)** Representative CFSE dilution of OTI proliferating (CD8<sup>+</sup> CD45.2<sup>+</sup>) spleen cells injected with TER119-OVA (top left), TER119-BBOX-OVA (top right), OVA (bottom left) and saline (bottom right). The numbers display the percentage of proliferating cells in CD45.2<sup>+</sup> cells. **B)** Proliferating CFSE<sup>low</sup> OTI T cells (gate from A) in spleen (left) and liver (right) for all groups. **C)** Quantified expansion of OTI CD8<sup>+</sup> CD45<sup>+</sup> T cells in spleen (left) and liver (right). All data were determined by multiparameter flow cytometry and analyzed with Prism 5 ("Bonferroni's Multiple Comparison Test", \*\*\*p value < 0.0001)



#### **2.4.5. Immunization with TER119-BBOX-OVA mixed with CpG leads to enhanced cytotoxicity of CD8<sup>+</sup> T cells mainly in the liver of vaccinated mice.**

The activation of CD8<sup>+</sup> T cells and their differentiation to CTLs is crucial for CD8 vaccine development. We next evaluated the induction of cytotoxic CD8<sup>+</sup> T cell responses in mice immunized on day 0 and 14 with TER119-BBOX-OVA + CpG compared to TER119-OVA + CpG and OVA + CpG, as described in Fig. 5A. The cytotoxicity of CD8<sup>+</sup> T cells was assessed in the spleen and liver of vaccinated mice 6 days after the boost. Overall, more cytotoxic CD8<sup>+</sup> T cells were measured in the group of mice vaccinated with TER119-BBOX-OVA + CpG compared with any other group.

A single i.v. injection was sufficient to raise effective CD8<sup>+</sup> T cells in all mice injected with TER119-BBOX-OVA + CpG, TER119-OVA + CpG and OVA + CpG measured by SIINFEKL pentamer staining in the blood of mice 8 days after the injection (Fig 5B). It is very interesting that only the mice injected with TER119-BBOX-OVA+ CpG had an effector phenotype characterized by a CD44<sup>+</sup>CD62L<sup>-</sup> staining on CD8<sup>+</sup> SIINFEKL pentamer<sup>+</sup> blood cells, that was 4-fold and 8-fold higher compared with TER119-OVA + CpG and OVA + CpG correspondingly on day 8 of the experiment (Fig. 5C). On day 20, the spleen and liver of all mice were harvested and the lymphocytes were stained *ex vivo* for OVA specific SIINFEKL pentamer<sup>+</sup> cells. There were 0.4% of pentamer<sup>+</sup> cells in the spleen of TER119-BBOX-OVA + CpG mice compared with 0.2% for both TER119-OVA + CpG and OVA + CpG (Fig. 5D) and 2.1% in the liver of TER119-BBOX-OVA + CpG compared with 1.7% and 1.5% for TER119-OVA + CpG and OVA + CpG correspondingly (Fig. 5F). The crosspresentation efficiency of both TER119-BBOX-OVA + CpG and TER119-OVA seen in Fig. 4 explains the close values of OVA specific cells in these two groups. The frequency of effector phenotype of the cells in the TER119-BBOX-OVA + CpG group remained high (45% effector positive cells both in spleen and liver), as measured by CD44<sup>+</sup> CD62L<sup>-</sup> staining (Fig. 5 E&G).

The cytotoxicity of activated CD8<sup>+</sup> T cells was further investigated by examining the cytokine secretion profile of lymphocytes taken from the spleens and livers of vaccinated animals. Consistent with the above data, *ex vivo* restimulation of splenocytes and liver lymphocytes with SIINFEKL for 6 hr led to a significant increase in the percentage of cytotoxic IFN $\gamma$ -secreting cells in the spleen and liver of TER119-

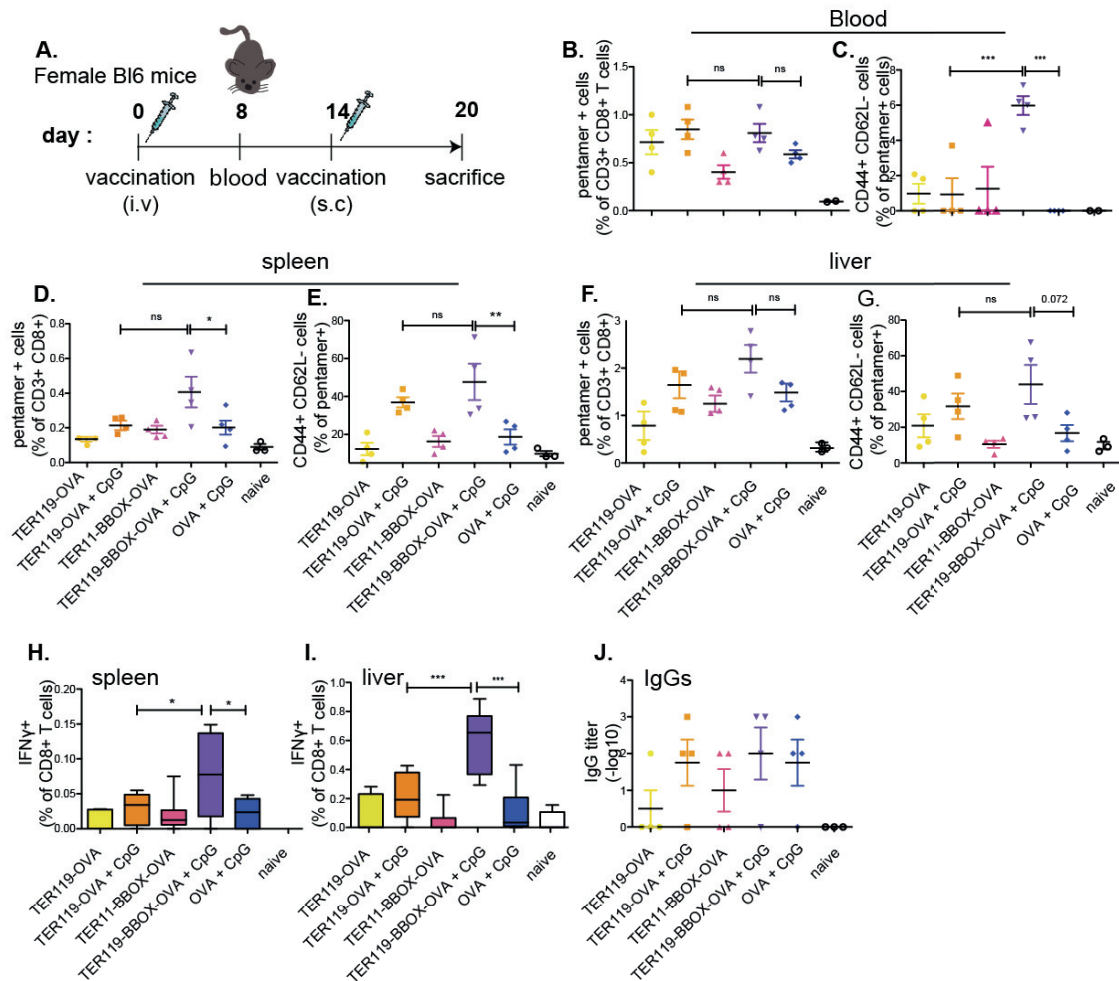
BBOX-OVA + CpG-vaccinated mice. In particular, 2-fold higher responses, as compared to TER119-OVA + CpG and OVA + CpG were seen in the spleen of mice vaccinated with TER119-BBOX-OVA + CpG (Fig. 5H). In the liver, TER119-BBOX-OVA + CpG had 3-fold and 6-fold higher responses in IFN $\gamma$  secretion compared with TER119-OVA + CpG and OVA + CpG, respectively (Fig. 5I). The above observations were also confirmed by *ex vivo* restimulation of the organs for 4 days with SIINFEKL, following ELISA measurements in the supernatant (data not shown).

Effective vaccines that elicit simultaneous activation of cytotoxic CD8<sup>+</sup> T cells and neutralizing antibodies are favored. The humoral responses were assessed by antibody titer measurements in all mice after vaccination. All groups of mice immunized with CpG displayed antibody titers around 2 with no significant differences between them. Interestingly, 2 out of 4 mice in the TER119-BBOX-OVA group without CpG and 1 out of 4 in the TER119-OVA group also created antibody titers of 2, in the absence of strong adjuvant (Fig 5J).

Overall, TER119-BBOX-OVA + CpG was very effective in activating CD8<sup>+</sup> T cells for the production of cytokines after vaccination with much stronger responses than TER119-OVA + CpG or OVA + CpG, especially in the liver of immunized mice.

#### **2.4.6. Immunization with TER119-BBOX-OVA mixed with CpG creates memory CD8<sup>+</sup> T cells that can be activated upon recall in the liver.**

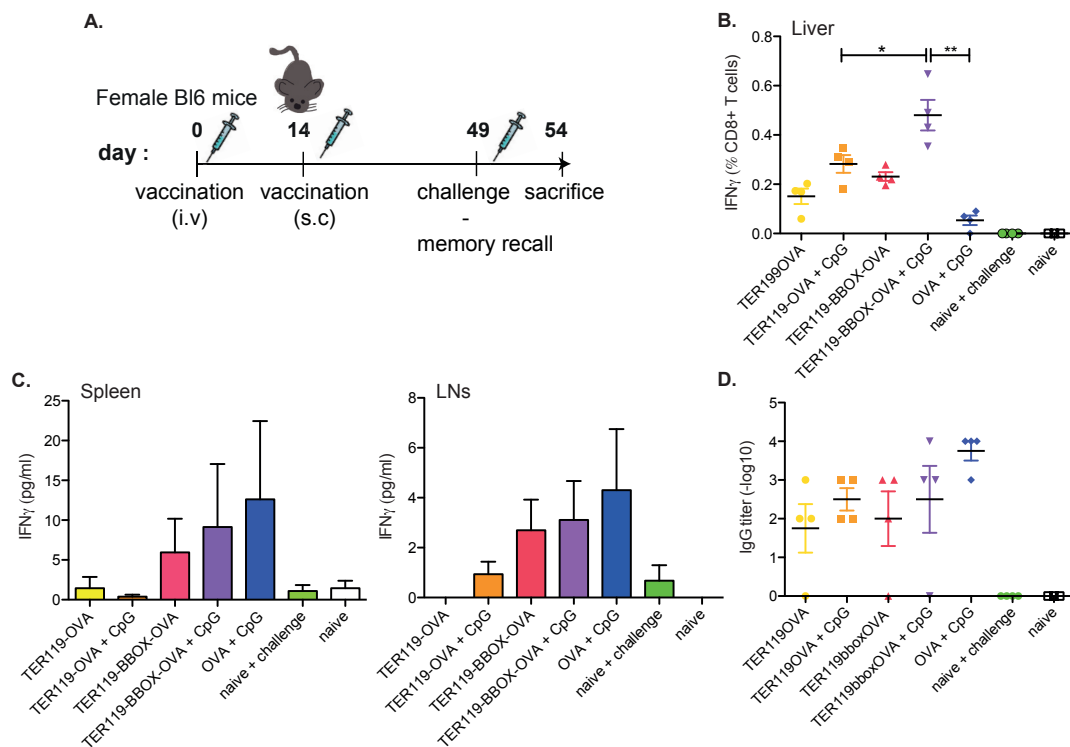
A feature of a vaccine that confers long-term immunity is its ability to induce long-lasting memory T cells, which can be reactivated upon recall with the same antigen. Following the same vaccination protocol as described above, we explored whether the induced CD8<sup>+</sup> T cells can differentiate into memory cells and expand upon recall with the OVA antigen. The mice were vaccinated on day 0 and 14, and the pool of CD8<sup>+</sup> T cells after immunization was allowed to develop memory for 5 weeks. Subsequently, all groups of animals, including one group with naïve non-immunized mice, were injected s.c. with 10  $\mu$ g OVA mixed with 20  $\mu$ g CpG, and allowed another 5 days for the cells to become activated (Fig. 6A). We evaluated the cytotoxicity of CD8<sup>+</sup> T cells in the spleen, liver and pooled LNs (Axillary, Branchial and Inguinal) by *ex vivo* restimulation of the lymphocytes with SIINFEKL peptide and found that only TER119-BBOX-OVA + CpG was capable of inducing memory CD8<sup>+</sup> T cells with the capacity to expand and display cytotoxic activity. In particular, after 6 hr of



**Figure 5: TER119-BBOX-OVA + CpG differentiates CD8+ T cells into effector cells mainly in the liver of immunized mice.** A) Immunization schedule ; Female C57BL/6 mice were immunized with 20 $\mu$ g OVA + 5 $\mu$ g CpG or equimolar amounts of TER119-OVA, TER119-OVA + CpG, TER119-BBOX-OVA and TER119-BBOX-OVA + CpG on day 0 and 14. Induction of effector CD8+ T-cell immune responses was measured in the spleen and in the liver on day 20. B) OVA-specific CD8+ T cells were assessed by SIINFEKL pentamer stain and flow cytometry in blood 8 days after the prime injection. C) The pentamer+ cell's effector phenotype was assessed by CD44<sup>+</sup> CD62L<sup>-</sup> staining by flow cytometry. D) Spleen pentamer stain on day 20 and E) effector phenotype of pentamer+ splenocytes. F) Liver pentamer stain on day 20 and E) effector phenotype of pentamer+ liver lymphocytes. H) Splenocytes and I) liver lymphocytes were isolated and restimulated ex vivo for 6 h in the presence of SIINFEKL; IFN- $\gamma$  expression by CD8+ T cells was determined by intracellular cytokine staining and flow cytometry. J) Total IgG titers in the serum of all vaccinated mice on day 20 of the experiment measured by ELISA. All data were analyzed with Prism 5 ("Bonferroni's Multiple Comparison Test", \*p<0.05, \*\*p<0.001, \*\*\*p<0.0001)

restimulation with SIINFEKL, only the liver lymphocytes of mice immunized with TER119-BBOX-OVA + CpG responded to the stimulation by a 5-fold increase in IFN $\gamma$  secretion (Fig. 6B) compared to OVA + CpG, whereas no active T cells were

found in the spleen or the LNs (data not shown), indicating that the long-lasting CD8<sup>+</sup> T cell immunity is not systemic but rather localized in the liver. Interestingly, restimulation of liver CD8<sup>+</sup> T cells with antigen *ex vivo* did not yield an increase in cytokine production. In contrast, we were able to measure IFN $\gamma$  secretion by CD4<sup>+</sup> T cells after 4 days of restimulation with the OVA antigen both in the spleen (Fig. 6C left) and the LNs (Fig. 6C right) in all groups mixed with CpG as well as the TER119-BBOX-OVA group without CpG. We also measured the total IgG titers in the serum of all mice and found that, in accordance to the IFN $\gamma$  secretion by CD4 T cells, all the groups displayed high antibody titers, without significant differences between them (Fig. 6D).



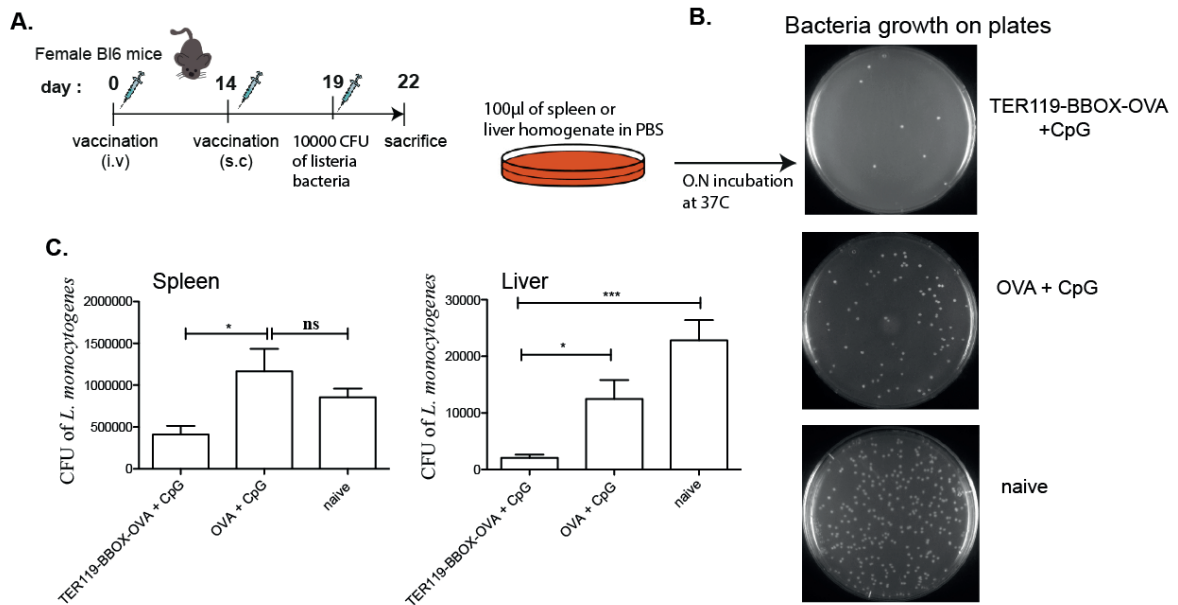
**Figure 6: T cells activated by TER119-BBOX-OVA + CpG differentiate to antigen specific memory T cells that survive in the liver and can be reactivated upon challenge with the same antigen.** **A)** Experimental timeline; Mice were immunized as in Fig. 4, and 5 weeks after the boost injection the mice in all groups, including a control group with non-vaccinated mice, were challenged with a s.c. injection of 10 $\mu$ g OVA + 20 $\mu$ g CpG. The presence and the cytotoxic capacity of memory cells in the spleen, liver and LNs was assessed 5 days later. **B)** Liver lymphocytes restimulated *ex vivo* with SIINFEKL for 6hr and stained for IFN $\gamma$  secretion in CD8<sup>+</sup> T cells. Gate on live cells, CD3<sup>+</sup> CD8<sup>+</sup>. **C)** *Ex vivo* restimulation with OVA of spleen and LNs lymphocytes for 4 days. The IFN $\gamma$  secretion in the supernatant of spleen (left) and LNs (right) was determined by ELISA. **D)** Total IgG titers in the serum of all vaccinated mice on day 54 of the experiment measured by ELISA. Statistical analysis of data with “Bonferroni’s Comparison test” \*p<0.05, \*\*p<0.001

The above results confirm that the cytotoxic CD8<sup>+</sup> T cells in the liver generated after the prime-boost vaccination develop memory and can be recalled into an effector phenotype, escaping the toerogenic fate of activated CD8<sup>+</sup> T cells that is associated with activation in the liver without costimulation.

#### **2.4.7. Effector CD8<sup>+</sup> T cells induced after TER119-BBOX-OVA + CpG immunization kill *Listeria monocytogenes*-infected cells.**

To evaluate the ability of cytotoxic T cells produced after vaccination to recognize and kill infected cells we challenged the mice with the pathogen *Listeria monocytogenes*, more specifically with a recombinant strain that expresses OVA antigen (*Listeria*-OVA). *Listeria* is a gram positive bacteria that can grow and reproduce inside the host's cells and is one of the most virulent food-borne pathogens, with 20 to 30 percent of clinical infections resulting in death [27]. In mice it infects the liver and spleen, and if it is not cleared, is lethal in high doses. Based on the previous vaccination data, we chose to compare the best vaccine approach, the TER119-BBOX-OVA + CpG to the most relevant control, the OVA + CpG, to reduce the number of mice used in the experiment. The mice were vaccinated following the regular vaccination protocol and 5 days after the boost they were challenged with an i.v. injection of *Listeria* (Fig. 7A). Three days after challenge, the organs were harvested, homogenized and 100 µl of the homogenates were grown on agar plates overnight. No or minimum bacteria colonies on the plates was considered as successful clearance of the bacteria infection. Overall, mice immunized with TER119-BBOX-OVA+CpG were very efficient in clearing the bacteria within 72 hr after infection. In particular, in the liver between 0-25 colonies grew in the TER119-BBOX-OVA + CpG agar plate compared to 60-280 in the OVA + CpG and over 300 in the non-vaccinated mice. Representative images of agar plates with bacteria colonies from liver homogenates are shown in Fig. 7B, and the total bacteria counts in all groups for both organs are shown in Fig. 7C. Consistent with the earlier vaccine and vaccine-memory data, the cytolytic activity of CD8<sup>+</sup> T cells is more powerful in the liver of TER119-BBOX-OVA+CpG vaccinated mice where the infection was almost eradicated.

Taken together, the above data demonstrate that vaccination with TER119-BBOX-OVA + CpG induces effective cytotoxic CD8<sup>+</sup> T cell immunity and raises potent CD8<sup>+</sup> T cells in the liver that can respond rapidly to an infection and clear the organs from the pathogen.



**Figure 7: *Listeria monocytogenes* clearance in the spleen and liver of mice immunized with TER119-BBOX-OVA + CpG.** **A)** Infection timeline; Mice were first immunized as in Fig. 4 and a week after the last boost all mice including naive untreated mice were infected with 10000CFU bacteria expressing the OVA antigen. The spleens and livers were harvested 3 days later. **B)** Bacteria growth on agar plates. The organs were homogenized to single cell suspensions in PBS and 100µl of the homogenate was plated on Brain Heart Infusion agar plates. Representative liver plates from mice immunized with TER119-BBOX-OVA + CpG (top) OVA + CpG (middle) and untreated naive mice (bottom) are shown. **C)** Absolute numbers of bacteria in spleen (left) and liver (right) based on the number of colonies on the plates calculated by the following formula: CFU total= (number of colonies \* 40ml total homogenate)/0.1ml homogenate plated. Statistical analysis of data with “Bonferroni’s Comparison test” \*\*\*p<0.0001 \*p<0.05

## 2.5. Discussion

Targeting hepatic cells and raising local, cytotoxic specific responses that can overcome the tolerogenic environment of the liver is challenging. In this study we explored the effect of recombinant proteins bound to erythrocytes in liver vaccination. We show that a fusion protein composed of an erythrocyte binding domain, a danger signal and an antigen co-administered with a strong adjuvant can activate cytotoxic T cells in the liver. These cells have a memory phenotype and the capacity to clear

intracellular hepatic pathogens. Our results demonstrate that a prime-boost vaccination with TER119-BBOX-OVA + CpG significantly improves the IFN $\gamma$  secretion in the liver by 6-fold compared with the non-erythrocyte bound antigen OVA + CpG and by 3-fold compared with TER119-OVA + CpG without BBOX. The potency of TER119-BBOX-OVA + CpG in vaccination is further proved by the clearance of the *Listeria* infected cells in the liver within 72 hrs after infection, which precedes the time required for infiltration of T cells from other organs. Most importantly, TER119-BBOX-OVA + CpG induces effective memory cells in the liver that last for at least 5 weeks and can be reactivated upon recall with the same antigen. Overall, we were able to overcome the tolerogenic fate of activated CD8<sup>+</sup> T cells and to promote the cytotoxic activation of CD8<sup>+</sup> T cells with a memory phenotype intrahepatically.

Our technology uses the i.v. route to deliver the antigen directly to the liver. Recent studies have shown that the i.v. route of immunization induces a more robust response in the liver and the spleen compared to other routes of administration [28]. The main challenge with i.v. injections is to prevent the free protein from immediate clearance, as it is the case with soluble OVA. Binding the antigen onto erythrocytes prolongs its circulation in the blood and in combination with the slow blood flow in the liver, increases the exposure time to hepatic immune cells and thus the uptake and the activation of the CD8<sup>+</sup> T cells locally. To further enhance the cytotoxic CD8<sup>+</sup> T cells responses and prevent the cells from exhaustion and apoptosis, we gave a subcutaneous boost injection that resulted in increased cytokine secretion of the activated CD8<sup>+</sup> T cells and developed an effector memory phenotype, seen by CD44<sup>+</sup> CD62L<sup>-</sup> populations in CD8<sup>+</sup> T cells in the spleen and liver. Overcoming the obstacle of liver tolerance and the clearance by apoptosis of the activated CD8<sup>+</sup> T cells is of great importance and adds significant value to our erythrocyte-binding platform.

The choice of BBOX and the co-administration of the protein with the CpG-B adjuvant were critical for the immunogenic outcome of the vaccine. HMGB1 and its active domain BBOX are endogenous DAMPs released by necrotic cells that can induce maturation of DCs. Uptake of BBOX by APCs causes the release of proinflammatory cytokines such as TNF $\alpha$ , IL-6, IL-8 and IL-12 *in vivo* by RAGE binding and signaling, leading to activation of the NF- $\kappa$ b pathway [29]. According to the literature, HMGB1 triggers a sustained and strong inflammation only when it forms

complexes with PAMPs (LPS, TLR9 agonists) or cytokines (IL-1 $\beta$ ) [30]. Our results confirm the above as TER119-OVA + CpG (a TLR9 ligand) produced 3 times less IFN $\gamma$  in the liver of vaccinated mice than TER119-BBOX-OVA + CpG, and TER119-BBOX-OVA without the CpG was not sufficient to raise cytotoxic CD8<sup>+</sup> T cells both in the spleen and the liver. Only the combination of the two danger signals in TER119-BBOX-OVA + CpG vaccinations activated cytotoxic CD8<sup>+</sup> T cells, as seen by the vaccine experiment in Fig. 4 and the memory recall in Fig. 5.

One of the limitations in subunit vaccines compared with live vaccines is that they are poor activators of CD8<sup>+</sup> T cells, mainly due to insufficient crosspresentation of the antigen by the appropriate APC type. We overcame this obstacle with our erythrocyte-binding platform, which, according to previous studies, enables very efficient crosspresentation to CD8<sup>+</sup> T cells. In particular, TER119-BBOX-OVA + CpG is crosspresented to CD8<sup>+</sup> T cells both in the spleen and the liver and enhances the proliferation of adoptively transferred OTI T cells by increasing their population by 4 fold as compared to OVA + CpG. Interestingly, the addition of BBOX within TER119-BBOX-OVA decreases the proliferation capacity compared to TER119-OVA, most probably due to less efficient binding of the first protein to red blood cells related with the folding properties of the two proteins. In addition to effective crosspresentation, the advantage of the erythrocyte-binding platform is the direct targeting of the antigen to the liver and the uptake of the protein by different APC types. Biodistribution studies showed that TER119-BBOX-OVA with or without CpG was preferentially taken up by the APCs in the liver and upregulated the costimulatory molecule CD80.

Uptake by the appropriate cell type determines the crosspresentation to CD8<sup>+</sup> T cells and their activation to effector cytotoxic T cells [31]. In particular, hepatocytes take up TER119-BBOX-OVA and TER119-BBOX-OVA + CpG better than any other treatment. Although the primary role of hepatocytes is in metabolism, there is evidence that hepatocytes express MHC I and under inflammatory conditions also MHC II [32, 33] and as such they can participate in T cell activation[34, 35]. Also, uptake by hepatic stellate cells is increased in these two groups. This is particularly interesting since the role of HSCs in activating T cells is controversial, but one study has demonstrated that HSC can activate CD8<sup>+</sup> T cells within the liver [36, 37]. The upregulation of CD80 in HSCs by TER119-BBOX-OVA and TER119-BBOX-OVA +



CpG further supports their possible role in activation of CD8<sup>+</sup> T cells in our studies. Interestingly, reduced uptake in the BBOX groups compared to other groups is observed by KCs, which represent the biggest phagocytic population in the liver [38] and as such they have the potential to be good APCs [39]. Furthermore, we could not detect upregulation of costimulatory molecules in this subset. The uptake by liver DCs is enhanced in TER119-BBOX-OVA and even more in TER119-BBOX-OVA + CpG mice with simultaneous upregulation of costimulatory molecules (CD80). Liver DCs can internalize blood-derived pathogens and, depending on the subtype, they can stimulate T cells [40]; however, the activation is less efficient compared to DCs from other tissues [41, 42]. Finally, we believe that the preferential uptake of TER119-BBOX-OVA proteins by LSECs is critical for the activation of CD8<sup>+</sup> T cells in the liver. LSECs can internalize cellular debris, and they express MHC I and II [43]. As such, they can directly present to T cells [44, 45]. Uptake by these cells and simultaneous upregulation of the CD80 costimulatory molecule in the TER119-BBOX-OVA and TER119-BBOX-OVA + CpG groups indicates their possible contribution of this cell type in CD8<sup>+</sup> T cell activation.

Immunization with TER119-BBOX-OVA + CpG is very efficient in CD8<sup>+</sup> T cell activation in the liver but less so in CD4<sup>+</sup> T cell activation in the liver compartment. *Ex vivo* restimulation with the full OVA protein resulted in minimal cytokine secretion by CD4<sup>+</sup> T cells indicating their non-effective status in the liver, a result that requires further exploration as CD4<sup>+</sup> T cells are required to ensure the survival of CD8<sup>+</sup> T cells [46]. However, CD4<sup>+</sup> T cells are activated in other organs raising antibodies against OVA in all groups, adding value to the potency of our vaccine platform. A vaccine that can raise both humoral and cellular responses has great potential in dealing with viruses infecting cells as well as viruses circulating systemically.

Other approaches from other groups have been explored to raise CD8<sup>+</sup> T cells in subunit vaccination. A similar study has used short peptide epitopes, not the full protein, and conjugated them to TLR ligands prior to injection to raise immune responses in the liver without though the induction of IgGs [15]. Also in malaria vaccination trials, the originally raised CD8<sup>+</sup> T cells by a CD8 epitope of the CS malaria antigen of *P.yoelii* proliferated but did not survive in the liver without the help

of CD4<sup>+</sup> T cells [46]. Peptide and protein based therapeutic vaccine formulations have also failed in inducing CD8<sup>+</sup> T cell responses in patients with chronic hepatitis B infection mostly due to the insufficient CD8<sup>+</sup> T cell activation [47].

Overall, we have developed a novel vaccine platform that can efficiently target the liver, crosspresent the antigen to CD8<sup>+</sup> T cells and raise local antigen specific immune responses. Furthermore, we have succeeded in retaining the effector phenotype of these activated cells and preventing them from clearance; a challenge for most CD8 liver vaccines that need to deal with persistent infections. The simplicity in recombinant production allows any antigen to be cloned and produced as a fusion TER119 protein not only in mice but also in human with a different scFv (TER119 binds only murine glycoporphin A). The erythrocyte binding technique serves as a potential approach for the development of hepatic vaccines both for prophylactic and therapeutic treatment. Given the fast clearance of *listeria*-infected cells within 72 hr, we believe that this vaccine may find application in malaria, where the mosquito bite infection resembles that of *listeria*. Also, the direct liver targeting and the induction of local responses suggests that a TER119-BBOX-Ag immunization may be sufficient to deal with established infections, such as chronic hepatitis B, or liver carcinomas in therapeutic cancer vaccination.

## References

1. Appay V, Douek DC, Price DA. Cd8(+) t cell efficacy in vaccination and disease. *Nature Medicine* 2008;14(6): 623-8.
2. Hilleman MR. Critical overview and outlook: Pathogenesis, prevention, and treatment of hepatitis and hepatocarcinoma caused by hepatitis b virus. *Vaccine* 2003;21(32): 4626-49.
3. Gerlich WH. Medical virology of hepatitis b: How it began and where we are now. *Virology Journal* 2013;10.
4. Bertolino P, Bowen DG. Malaria and the liver: Immunological hide-and-see or subversion of immunity from within? (vol 6, pg 41, 2015). *Frontiers in Microbiology* 2015;6.
5. Tse SW, Radtke AJ, Zavala F. Induction and maintenance of protective cd8(+) t cells against malaria liver stages: Implications for vaccine development. *Memorias Do Instituto Oswaldo Cruz* 2011;106: 172-8.
6. Schmidt NW, Podyminogin RL, Butler NS, et al. Memory cd8 t cell responses exceeding a large but definable threshold provide long-term immunity to malaria. *Proceedings of the National Academy of Sciences of the United States of America* 2008;105(37): 14017-22.

7. Ewer KJ, O'Hara GA, Duncan CJA, et al. Protective cd8(+) t-cell immunity to human malaria induced by chimpanzee adenovirus-mva immunisation. *Nature Communications* 2013;4.
8. Keating R, Yue W, Rutigliano JA, et al. Virus-specific cd8(+) t cells in the liver: Armed and ready to kill. *Journal of Immunology* 2007;178(5): 2737-45.
9. Bowen DG, McCaughan GW, Bertolino P. Intrahepatic immunity: A tale of two sites? *Trends in Immunology* 2005;26(10): 512-7.
10. Crispe IN. Hepatic t cells and liver tolerance. *Nature Reviews Immunology* 2003;3(1): 51-62.
11. Wick MJ, Leithauser F, Reimann J. The hepatic immune system. *Critical Reviews in Immunology* 2002;22(1): 47-103.
12. Bowen DG, Zen M, Holz L, et al. The site of primary t cell activation is a determinant of the balance between intrahepatic tolerance and immunity. *Journal of Clinical Investigation* 2004;114(5): 701-12.
13. Huang LR, Wohlleber D, Reisinger F, et al. Intrahepatic myeloid-cell aggregates enable local proliferation of cd8+t cells and successful immunotherapy against chronic viral liver infection. *Nature Immunology* 2013;14(6): 574-+.
14. Dikopoulos N, Jomantaite L, Schirmbeck R, et al. Specific, functional effector/memory cd8(+) t cells are found in the liver post-vaccination. *Journal of Hepatology* 2003;39(6): 910-7.
15. Dikopoulos N, Riedl P, Schirmbeck R, et al. Novel peptide-based vaccines efficiently prime murine "help"-independent cd8(+) t cell responses in the liver. *Hepatology* 2004;40(2): 300-9.
16. Heit A, Schmitz F, O'Keefe M, et al. Protective cd8 t cell immunity triggered by cpg-protein conjugates competes with the efficacy of live vaccines. *Journal of Immunology* 2005;174(7): 4373-80.
17. Kontos S, Hubbell JA. Improving protein pharmacokinetics by engineering erythrocyte affinity. *Molecular pharmaceuticals* 2010;7(6): 2141-7.
18. Kontos S, Kourtis IC, Dane KY, et al. Engineering antigens for in situ erythrocyte binding induces t-cell deletion. *Proceedings of the National Academy of Sciences of the United States of America* 2013;110(1): E60-8.
19. Kina T, Ikuta K, Takayama E, et al. The monoclonal antibody ter-119 recognizes a molecule associated with glycophorin a and specifically marks the late stages of murine erythroid lineage. *British Journal of Haematology* 2000;109(2): 280-7.
20. Messmer D, Yang H, Telusma G, et al. High mobility group box protein 1: An endogenous signal for dendritic cell maturation and th1 polarization. *Journal of Immunology* 2004;173(1): 307-13.
21. Lotze MT, Tracey KJ. High-mobility group box 1 protein (hmgb): Nuclear weapon in the immune arsenal. *Nature Reviews Immunology* 2005;5(4): 331-42.
22. Yang HA, Hreggvidsdottir HS, Palmblad K, et al. A critical cysteine is required for hmgb1 binding to toll-like receptor 4 and activation of macrophage cytokine release. *Proceedings of the National Academy of Sciences of the United States of America* 2010;107(26): 11942-7.
23. Baldi L, Hacker DL, Meerschman C, et al. Large-scale transfection of mammalian cells. *Methods in molecular biology* 2012;801: 13-26.
24. Zehn D, Lee SY, Bevan MJ. Complete but curtailed t-cell response to very low-affinity antigen. *Nature* 2009;458(7235): 211-4.
25. Nancy Wang RS, Odilia Wijburg, Thomas Brodnicki Measuring bacteria load and immune responses in mice infected with listeria monocytogenes. *Journal of visualized experiments* 2011.

26. Green DR, Ferguson T, Zitvogel L, et al. Immunogenic and tolerogenic cell death. *Nature reviews. Immunology* 2009;9(5): 353-63.
27. Wing EJ, Gregory SH. Listeria monocytogenes: Clinical and experimental update. *Journal of Infectious Diseases* 2002;185: S18-S24.
28. Epstein JE, Tewari K, Lyke KE, et al. Live attenuated malaria vaccine designed to protect through hepatic cd8(+) t cell immunity. *Science* 2011;334(6055): 475-80.
29. Luan ZG, Zhang H, Yang PT, et al. Hmgb1 activates nuclear factor-kappa b signaling by rage and increases the production of tnf-alpha in human umbilical vein endothelial cells. *Immunobiology* 2010;215(12): 956-62.
30. Bianchi ME. Hmgb1 loves company. *Journal of Leukocyte Biology* 2009;86(3): 573-6.
31. Jenne CN, Kubes P. Immune surveillance by the liver. *Nature Immunology* 2013;14(10): 996-1006.
32. Franco A, Barnaba V, Natali P, et al. Expression of class-i and class-ii major histocompatibility complex antigens on human hepatocytes. *Hepatology* 1988;8(3): 449-54.
33. Chen M, Tabaczewski P, Truscott SM, et al. Hepatocytes express abundant surface class i mhc and efficiently use transporter associated with antigen processing, tapasin, and low molecular weight polypeptide proteasome subunit components of antigen processing and presentation pathway. *Journal of Immunology* 2005;175(2): 1047-55.
34. Bertolino P, Bowen DG, McCaughan GW, et al. Antigen-specific primary activation of cd8(+) t cells within the liver. *Journal of Immunology* 2001;166(9): 5430-8.
35. Bertolino P, McCaughan GW, Bowen DG. Role of primary intrahepatic t-cell activation in the 'liver tolerance effect'. *Immunology and Cell Biology* 2002;80(1): 84-92.
36. Bomble M, Tacke F, Rink L, et al. Analysis of antigen-presenting functionality of cultured rat hepatic stellate cells and transdifferentiated myofibroblasts. *Biochemical and Biophysical Research Communications* 2010;396(2): 342-7.
37. Winau F, Hegasy G, Weiskirchen R, et al. Ito cells are liver-resident antigen-presenting cells for activating t cell responses. *Immunity* 2007;26(1): 117-29.
38. Bilzer M, Roggel F, Gerbes AL. Role of kupffer cells in host defense and liver disease. *Liver International* 2006;26(10): 1175-86.
39. You Q, Cheng LL, Kedl RM, et al. Mechanism of t cell tolerance induction by murine hepatic kupffer cells. *Hepatology* 2008;48(3): 978-90.
40. Kingham TP, Chaudhry UI, Plitas G, et al. Murine liver plasmacytoid dendritic cells become potent immunostimulatory cells after flt-3 ligand expansion. *Hepatology* 2007;45(2): 445-54.
41. Tokita D, Sumpter TL, Ralmondi G, et al. Poor allostimulatory function of liver plasmacytoid dc is associated with pro-apoptotic activity, dependent on regulatory t cells. *Journal of Hepatology* 2008;49(6): 1008-18.
42. Pillarisetty VG, Shah AB, Miller G, et al. Liver dendritic cells are less immunogenic than spleen dendritic cells because of differences in subtype composition. *Journal of Immunology* 2004;172(2): 1009-17.
43. Knolle PA, Limmer A. Control of immune responses by scavenger liver endothelial cells. *Swiss medical weekly* 2003;133(37-38): 501-6.
44. Lohse AW, Knolle PA, Bilo K, et al. Antigen-presenting function and b7 expression of murine sinusoidal endothelial cells and kupffer cells. *Gastroenterology* 1996;110(4): 1175-81.

45. Knolle PA, Uhrig A, Hegenbarth S, et al. Il-10 down-regulates t cell activation by antigen-presenting liver sinusoidal endothelial cells through decreased antigen uptake via the mannose receptor and lowered surface expression of accessory molecules. *Clinical and Experimental Immunology* 1998;114(3): 427-33.
46. Overstreet MG, Chen YC, Cockburn IA, et al. Cd4(+) t cells modulate expansion and survival but not functional properties of effector and memory cd8(+) t cells induced by malaria sporozoites. *Plos One* 2011;6(1).
47. Batdelger D, Dandii D, Dahgwahdorj Y, et al. Clinical experience with therapeutic vaccines designed for patients with hepatitis. *Current Pharmaceutical Design* 2009;15(11): 1159-71.



## **Chapter 3:**

Enhanced CD8<sup>+</sup> T Cell-Targeting Vaccination by  
Prolonged Binding of XCL1 Fusion Proteins at the  
Injection Site

### 3.1. Introduction

The idea that cells of the immune system can suppress tumor development was first proposed by Paul Ehrlich in the early 1900s [1] and led to the cancer immune surveillance hypothesis of Burnet [2], that the immune system can suppress cancerous cells and prevent tumor progression before they cause harm to the body. Since then, research in the field has revealed that cytotoxic T lymphocyte (CTL) responses play a major role in tumor eradication, and it is widely accepted that CD8<sup>+</sup> T cells are necessary in dealing with transformed cells [3]. As a result, current research focuses on eliciting strong antitumor CD8<sup>+</sup> T cell responses for the prevention as well as the treatment of malignancies, using different vaccination strategies. A large variety of different methodologies has been tried in the past years both in prophylactic and therapeutic vaccination, including – but not limited to – immunization with peptides and recombinant proteins [4]. Examples of protein vaccines that are prepared based on tumor-associated antigens (TAAs) include vaccination with prostatic acid phosphatase (PAP) fused to the human cytokine GM-CSF [5, 6], fusion of the MAGE-A3 tumor antigen with lipoprotein D from *H. influenza* [7] and epitope like IgG antibody vaccination with the ovarian tumor associated antigen CA-125 [8].

The mechanisms required to mount effective antitumor responses can be described in three steps. First, antigen presenting cells (APCs) must capture and present TAAs. Key players in these mechanisms are the dendritic cells (DCs), where different cellular subtypes can process the antigen, load on either MHC class I or II and display to CD8<sup>+</sup> or CD4<sup>+</sup> T cells respectively. Studies have shown that the DC subtypes have different functional specializations and, in particular, that specific DC subtypes can determine the type of immune response generated [9]. Following antigen uptake by the appropriate cell type, maturation of DCs in response to stimuli such as Toll-like receptors is required for migration to the T cell areas of lymphoid organs and presentation of antigen to naïve T cells. Finally, activation and expansion of T cells in sufficient numbers is necessary to recognize and eliminate tumor cells. These antigen-educated T cells must then exit the lymph node (LN), traffic to the tumor and kill the malignant cells. Tumor immunotherapy studies aim to induce immune responses against TAAs following these mechanisms [10].



Recent advances in CD8<sup>+</sup> vaccines focus towards induction of Th1 responses by direct cross-presentation of an antigen to CD8<sup>+</sup> T cells [11]. A subset of lymphoid DCs, called CD8<sup>+</sup> DCs, resides in the spleen and LNs and, together with the skin migratory CD103<sup>+</sup> DCs, excels in cross-presentation and cross-priming of CD8<sup>+</sup> T cells [12-14]. Studies have shown that these subsets can take up exogenous antigens and present them on class I MHC. Through this process, CD8<sup>+</sup> DCs directly cross prime CD8<sup>+</sup> T cells and induce a CTL response. The CD8<sup>+</sup> DC subset exists both in mice and humans and is distinguished by the specific markers expressed on the surface of the cells, namely CD8, DEC205, Clec9A and XCR1 [15].

Elegant strategies in the past have employed methods for targeting CD8<sup>+</sup> DCs using antibodies against the molecules expressed on the surface of the cross-presenting DCs. The first example comes from the Ralph Steinmann group where monoclonal antibodies (mAbs) were fused with antigens and were targeted to the DEC205 endocytosis receptor [16]. Co-administration of the  $\alpha$ DEC205:OVA fusion protein with an agonistic  $\alpha$ CD40 antibody to mature DCs resulted in efficient activation and cytokine release of CD8<sup>+</sup> T cells after a single s.c. injection. However, DEC205 is not only expressed in CD8 $\alpha$ <sup>+</sup> DCs but also in other conventional DCs (cDCs), Langerhans cells, interstitial DCs and thymic epithelial cells, and as such the efficiency of the vaccine was not optimal [17]. Similar studies were performed with the surface C-type lectin-like molecule Clec9A, which is selectively expressed by mouse CD8<sup>+</sup> cDCs. In particular, it was first shown that targeted delivery of antigen fused mAbs against mClec9A raised antigen-specific antibodies and resulted in proliferation of adoptively transferred OTI (transgenic CD8<sup>+</sup> T cells with a T cell receptor specific for an ovalbumin epitope SIINFEKL) and OTII (transgenic CD4<sup>+</sup> T cells with a T cell receptor specific for an ovalbumin epitope ISQAVHAAHAEINEAGR) cells, without the normal activation of DCs [18]. Similar studies targeting short peptides to the same molecule (called by them DNGR-1 that is also expressed in humans) showed enhanced cytotoxicity of CD8<sup>+</sup> T cells and tumor regression after vaccination [19]. While Clec9a is mainly expressed on CD8 $\alpha$ <sup>+</sup> DCs, it is also found at low levels on plasmacytoid DCs (pDCs) [20, 21].

More recent studies have focused on targeting the chemokine receptor XCR1 receptor that is exclusively expressed on lymphoid tissue (LT) derived resident CD8<sup>+</sup> DCs and migratory CD103<sup>+</sup> DCs of mice (and the expression is conserved on the

CD141<sup>+</sup> DCs in humans [22, 23]); all known to excel in cross-presentation of antigen to CD8<sup>+</sup> T cells. XCL1, the specific chemokine ligand for XCR1, is a chemoattractant of CD8<sup>+</sup> DCs [24, 25] and has been used by several groups as a target molecule for direct delivery to cross-presenting DCs in tumor regression experiments and influenza virus protection. In a recent study, XCL1-OVA fusion proteins were used to target CD8<sup>+</sup> DCs in the spleen and LNs of C57BL/6 mice, in a prophylactic vaccine [26]. Together with the co-administration of lipopolysaccharide (LPS), potent cytotoxic CD8<sup>+</sup> T cells responses resulted in IFN $\gamma$  secretion and prevention of EL4 tumor (a murine T cell lymphoma) growth in a prophylactic vaccine context. In another study, dimeric fusions of XCL1 and the PR8 influenza virus antigen were used in DNA vaccination [27]. A single intradermal injection resulted in effective IFN $\gamma$  cytokine production and protection after challenge with the influenza virus. Overall, these recent studies have shown very promising results for CD8<sup>+</sup> T cell-targeted vaccination by targeting the cross-presenting CD8<sup>+</sup> DCs.

Given the positive results presented in the literature with the XCL1 fusion proteins, we aimed to further improve the efficacy of the XCR1-targeting vaccines by increasing the number of CD8<sup>+</sup> DCs at the injection site and thus enhance the uptake of antigen. In particular, we fused XCL1 to the placenta growth factor-2 (PlGF-2) growth factor (GF) domain (PlGF-2<sub>123-144</sub>) that binds the extracellular matrix (ECM) with high affinity [28]. Our hypothesis was based on previous studies that showed prolonged retention of the fusion proteins comprising this PlGF-2 domain in the ECM by non-covalent binding with dissociation constants in the 1-10 nM range [29, 30]. Fusion of XCL1 to this PlGF-2 domain promoted the chemotaxis of cross-presenting DCs at the skin site following an intradermal injection. Direct targeting of the antigen to the cross-presenting DCs was then accomplished by co-administration of XCL1-PlGF-2<sub>123-144</sub> (referred to hereinafter simply as XCL1-PlGF) with a fusion protein of XCL1 and the model protein antigen ovalbumin (XCL1-OVA). Following two intradermal immunizations of XCL1-OVA + XCL1-PlGF with the adjuvant polyI:C (an agonist for Toll-like receptor 3, TLR3), CD8<sup>+</sup> T cells were activated in the secondary immune organs of C57BL/6 mice and cytolytic antigen-specific immune responses were raised. We evaluated our platform by a prophylactic and therapeutic B16-OVA (the murine melanoma line B16F10 expressing OVA as a model TAA) treatment, and we found prolonged survival of tumor-bearing mice in both cases. Overall, attraction of CD8<sup>+</sup>

DCs to the injection site and simultaneous targeting of the antigen to the cross-presenting DCs enhanced the cytolytic activity of CD8<sup>+</sup> T cells and raised potent immune responses in a vaccination context, showing promising results for tumor treatment.

## 3.2. Materials and Methods

**Animals.** Female C57BL/6J mice were purchased from Harlan and female Balb/c and Ly5.1 (CD45.1) mice were purchased from Charles River Laboratories. All mice were aged between 8-12 weeks and kept under pathogen free conditions at the animal facility of Ecole Polytechnic Fédéral de Lausanne. Female C57BL/6-Tg(Tcr $\alpha$ Tcr $\beta$ ) 1100Mjb (OTI) mice between 8-15 weeks that were used for isolation of splenocytes were bred under specific pathogen-free conditions (SPF). The Veterinary Authority of the Canton de Vaud has approved all procedures and experiments.

**Proteins and Recombinant protein production.** Murine XCL1 was purchased from SinoBiological. The DNA sequences coding for XCL1-OVA and XCL1-PIGF were purchased from Mircrosynth DNA. The PIGF sequence includes the amino acids in positions 123-144 described by Martino et. al. [28] and is the following: “RRRPKGRGKRRREKQRPTDCHL”. Both XCL1-OVA and XCL1-PIGF sequences were introduced into the pXLG plasmid for mammalian expression. A 6 histidine tag sequence was inserted to the 3' end of XCL1-OVA to facilitate purification. No tags were inserted in the XCL1-PIGF sequence. HEK cells were transfected with either XCL1-OVA or XCL1-PIGF constructs under serum free conditions with 3.75 mM valproic acid (Sigma-Aldrich), and after 7 days the proteins in suspension were purified with immobilized metal affinity chromatography. XCL1-OVA was processed using a HiTrap HP His-tag column (GE Healthcare) and XCL1-PIGF was purified with a heparin-binding column (GE Healthcare) using 1 M NaCl for elution. The purified proteins were analyzed for purity using SDS/PAGE, endotoxin levels were assessed in THP-1 x Blue cells (InvivoGen), and concentration was measured using bicinchoninic acid assays (Thermo Scientific). The final product was sterile-filtered, and stored at -80 °C in working aliquots.

**XCL1-PIGF binding to ECM *in vitro* and *in vivo*.** For *in vitro* binding, ELISA plates (Nunc Max- iSorp; Thermo Fisher Scientific) were coated with 50 nM of XCL1-PIGF or XCL1 overnight at 4 °C and subsequently blocked with 2% (wt/vol) BSA (Enzyme Research Laboratories) in PBS-Tween 20 (PBS-T, 0.05%) for 1 h at room temperature. Wells were washed with PBS-T and further incubated with 100 nM fibrinogen in PBS-T with 0.1% BSA for 45 min at room temperature. After three washes with PBS-T, wells were incubated with anti-fibrinogen antibody conjugated to HRP (ab7539; Abcam) for 45 min. The binding was detected with tetramethylbenzidine substrate (Thermo Scientific) and the absorbance was measured at 450 nm. For *in vivo* binding, XCL1-PIGF and XCL1 were labeled with an Alexa 750 fluorophore (Dyomics) in a protein:dye molar ratio of 1:10, and incubated for 1hr at room temperature. The free dye was removed by centrifugation with Zeba columns (Thermo Scientific). All reactions were performed under sterile conditions to protect from endotoxin contamination. The Balb/c mice were injected with 3 µg of XCL1-A750 on one footpad and 3,3 µg of XCL1-PIGF-A750 on the opposite. Live imaging with the IVIS spectrum was performed at different timepoints, namely 0, 4, 12, 24, 48 hr post injection. The emission and excitation wavelengths were set at 800 and 745nm respectively and the exposure time at 0.5 s. The images were analyzed with the IVIS software.

**CD8<sup>+</sup> DCs skin count and antigen uptake.** C57BL/6 mice were injected in all 4 footpads with 3 µg XCL1 or 3.3 µg XCL1-PIGF and were sacrificed 4 and 12 hr after the injection. The skin around the injection site was cut and digested for further processing. Briefly, the skin tissues were incubated at 37 °C for 1 hr with 10<sup>5</sup> units/ml of Liberase DH mixed with 10% FBS and 1% penicillin, streptomycin (Invitrogen) in Dulbecco's Modified Eagle Medium (DMEM) (Gibco). The tissue was smashed with a syringe plunger and was passed through a 70 µm strainer for a final resuspension in DMEM medium and preparation for staining. The draining LNs were collected and processed for staining as described in the tissue preparation section. For the uptake experiment, XCL1-OVA, XCL1-PIGF and OVA were labelled with the Alexa 488 fluorophore (Dyomics) as described above. The mice were injected with 20 µg OVA + 20 µg CpG-B, 23 µg XCL1-OVA + 20 µg CpG-B or 23 µg XCL1-OVA + 3.3 µg XCL1-PIGF + 20 µg CpG-B and the LNs (axillary, branchial and inguinal) and spleen were collected for processing and staining 48 hr later, as described in other sections.

Briefly, skin DCs were labeled with CD103 (1:200), CD11c (1:200), CD11b (1:200) and CD3 (1:100) antibodies purchased from eBioscience. Similarly, LNs were labelled with CD8 (1:200), CD11c (1:200), CD11b (1:200) and CD3 (1:100) antibodies.

**Adoptive transfer experiment.** OTI T cells were isolated from splenocytes of female CD45.2<sup>+</sup> mice, between 12-16 weeks old, using a CD8 magnetic bead negative selection kit (Miltenyi Biotec). The isolated CD8<sup>+</sup> OTI cells were incubated with 1  $\mu$ M CFSE (Invitrogen) for 6 min at room temperature, and the reaction was quenched with an equal volume of Iscove's modified Dulbecco's medium (IMDM) with 10% (vol/vol) FBS (Gibco). Before injection, cells were resuspended in pure IMDM to a final concentration of 10<sup>7</sup> cells/ml. A total of 100  $\mu$ l were injected i.v. into the tail vein of recipient female Ly5/ CD45.1<sup>+</sup> mice, 8 weeks old. The following day the mice received an i.d. injection of 20  $\mu$ g OVA, 23  $\mu$ g XCL1- OVA or 23  $\mu$ g XCL1-OVA + 3.3  $\mu$ g XCL1-PIGF all mixed with 10  $\mu$ g polyI:C, and were sacrificed 4 days later. The axillary, branchial and inguinal LNs and spleen were collected, processed and stained with CD45.2 (1:200), CD8 (1:200) and CD3 (1:300) for flow cytometry as described in other sections.

**Immunizations.** 8 week old female C57BL/6 mice were immunized under isoflurane anesthesia (5% for induction and 2% for maintenance) on day 0 and 14 with an intradermal injection of 20  $\mu$ g OVA + 20  $\mu$ g polyI:C, 23  $\mu$ g XCL1-OVA + 20  $\mu$ g polyI:C, 20  $\mu$ g OVA + 3  $\mu$ g XCL1 + 20  $\mu$ g polyI:C, 20  $\mu$ g OVA + 3.3  $\mu$ g XCL1-PIGF + 20  $\mu$ g polyI:C or 23  $\mu$ g XCL1-OVA + 3.3  $\mu$ g XCL1-PIGF + 20  $\mu$ g polyI:C or just saline. 5 days after the boost mice were euthanized, and the axillary, branchial and inguinal LNs and spleen were collected for *ex vivo* restimulation and staining as described in other sections.

**Tissue and cell preparation for ex vivo restimulation of lymphocytes.** Splenocytes were obtained by disruption of the spleen through a 70- $\mu$ m cell sieve and subsequent red blood cell lysis with 0.155 M NH<sub>4</sub>Cl. The lymph nodes were digested for 30 min with 2 mg/mL Collagenase D (Roche) in IMDM, and passed through a 70- $\mu$ m cell sieve to obtain single cell suspensions. All organs were kept in Dulbecco's Modified Eagle Medium (DMEM) (Gibco) supplemented with 10% FBS and 1% penicillin, streptomycin (Invitrogen). For CD8<sup>+</sup> T cell-specific restimulation and intracellular cytokine staining, cells were first cultured for 3 hr at 37 °C in the presence of 1  $\mu$ g/mL

SIINFEKL,  $10^4$  U/ml IL2, and 0.5  $\mu\text{g}$  anti-CD28 (eBioscience), and subsequently for 3 hr with the addition of 250  $\mu\text{g}/\text{mL}$  brefeldin A (SigmaAldrich). For CD4<sup>+</sup> T cell restimulation,  $10^4$  U/ml IL2, 0.5  $\mu\text{g}$  anti-CD28 and 100  $\mu\text{g}/\text{mL}$  OVA VI (Sigma-Aldrich) protein were added to the cells for 3 h, followed by incubation with 50  $\mu\text{g}/\text{mL}$  brefeldin A for another 12 hr.

**Flow cytometry staining.** For the detection of live cells, cells were suspended at a concentration of  $10^6$  cells in 200 $\mu\text{l}$ , washed with PBS, and labeled with live/dead fixable cell viability reagent (Invitrogen). Subsequently, the cells were incubated for 20 min on ice with PBS/2% FBS solutions of the surface markers CD3 (1:100) and CD8 (1:200) or CD4 (1:200). For intracellular cytokine staining, cells were fixed in 2% paraformaldehyde solution, washed with 0.5% saponin (SigmaAldrich) in PBS/2% FBS, and incubated with the IFN $\gamma$  (1:200) or TNF $\alpha$  (1:200) antibody diluted in saponin solution for 30 min on ice. Finally, the cells were resuspended in PBS/2% FBS for analysis. Samples were processed on CyAn ADP Analyzer (Beckman Coulter) and data were analyzed with FlowJo software (Tree Star). The antibodies against mouse CD3, CD4, CD8, IFN $\gamma$  and TNF $\alpha$  were purchased from eBioscience.

**Tumor inoculations.** Mice were anesthetized with isoflurane (5% for induction and 2% for maintenance) and their backs were shaved. For the therapeutic treatment,  $2.5 \times 10^5$  B16-OVA melanoma cells were injected i.d. on the back of each mouse followed by 7 consecutive injections every 4 days of 20  $\mu\text{g}$  OVA + 20  $\mu\text{g}$  polyI:C, 23  $\mu\text{g}$  XCL1-OVA + 20  $\mu\text{g}$  polyI:C or 23  $\mu\text{g}$  XCL1-OVA + 3.3  $\mu\text{g}$  XCL1-PIGF + 20  $\mu\text{g}$  polyI:C. For the prophylactic treatment mice were vaccinated with 20  $\mu\text{g}$  OVA + 20  $\mu\text{g}$  polyI:C, 23  $\mu\text{g}$  XCL1-OVA + 20  $\mu\text{g}$  polyI:C or 23  $\mu\text{g}$  XCL1-OVA + 3.3  $\mu\text{g}$  XCL1-PIGF + 20  $\mu\text{g}$  polyI:C on day 0 and 14 and 5 days later  $2.5 \times 10^5$  B16-OVA melanoma cells were injected i.d. on the back of each mouse. Tumors were measured every 2 days with a digital caliper starting 4 d post-inoculation, and volumes (**V**) were calculated as ellipsoids ( $V = \pi/6 \times \text{length} \times \text{width} \times \text{height}$ ). Mice were sacrificed when tumor volumes reached 1  $\text{cm}^3$  as required by Swiss law.

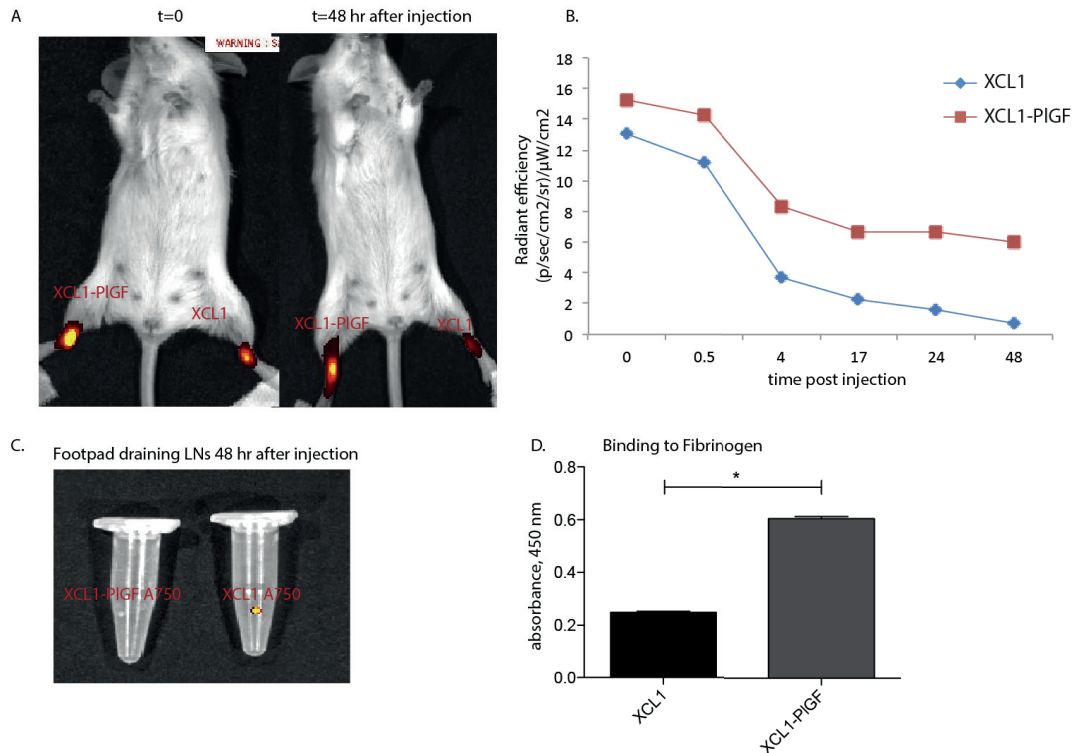
**Data Analysis.** All flow cytometry data were analyzed using FlowJo (v8.8.6). Graphs and statistical analyses of data were performed using Prism (v5, GraphPad). The statistical significance was determined by one way ANOVA – Bonferoni test or t-test

with Welch correction, as indicated in each figure separately. The asterisks indicate the significance as follows: \* $p < 0.05$ , \*\* $p < 0.01$ , \*\*\* $p < 0.001$ .

### 3.3 Results and Figures

#### 3.3.1. PIGF-2<sub>123-144</sub> fusion prolongs XCL1 retention at injection site through ECM binding.

The heparin-binding sequence of placenta growth factor-2, PIGF-2<sub>123-144</sub>, binds strongly to the ECM with an equilibrium dissociation constant  $K_d$  of 1.9nM, as shown in previous studies [28]. We hypothesized that we could form a reservoir for attracting CD8<sup>+</sup> DCs by maintaining the presence of the XCL1 chemokine ligand at the site of injection through ECM binding. Thus, we engineered a fusion of PIGF-2<sub>123-144</sub> with XCL1 and expressed the recombinant protein, XCL1-PIGF, in HEK cells. To assess *in vivo* ECM binding, XCL1-PIGF was conjugated with Alexa 750 fluorophore and injected i.d. into the footpad of Balb/c mice. As a control, XCL1 alone was conjugated with Alexa 750 fluorophore and injected i.d. into the opposite footpad of the same Balb/c mouse, as seen in Figure 1A. The fluorescence intensity of both proteins was measured using an IVIS Spectrum imaging system at various time points over 48 hours (Fig 1B). XCL1-PIGF binds to the ECM and remains at the injection site for at least 2 days, whereas the fluorophore intensity of XCL1 diffuses during time, indicating limited binding to the site of the injection. Imaging of the footpad draining LNs with the IVIS Spectrum 48 hr after the injection confirmed the diffusion of XCL1 towards the LNs as seen by the fluorescent XCL1-LNs versus fluorescence-absent XCL1-PIGF LNs (Fig. 1C). *In vitro*, XCL1-PIGF binds to an example ECM molecule, fibrinogen, 3 times better than XCL1 alone as confirmed by ELISA measurements (Fig. 1D). The above data suggest that XCL1-PIGF can remain at the site of the injection for at least 48 hr and potentially allow XCR1<sup>+</sup> DCs to sense and migrate locally.



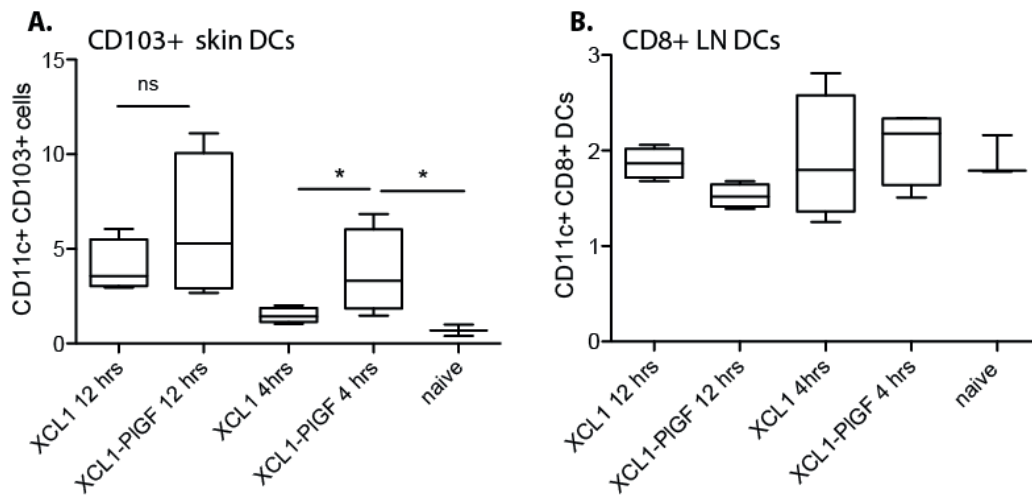
**Figure 1: XCL1-PIGF binds to the extracellular matrix in vitro and in vivo and remains bound at the injection site for at least 48 hr.** **A)** Live imaging by IVIS spectrum of Balb/c mice injected with 3μg XCL1 on the right footpad and equimolar amount of XCL1-PIGF on the left footpad, both conjugated to Alexa 750 fluorophore. Images at injection time t=0 (left mouse) and t=48 hr (right mouse) show the fluorescence intensity of XCL1-PIGF (left footpad) and XCL1 (right footpad). **B)** Median fluorescence intensity calculated at different time points by the IVIS spectrum software. **C)** XCL1-A750 drainage to the popliteal lymph node (right tube). XCL1-PIGF remains at the injection site (left tube) 48 hr after injection (fluorescent free LN). **D)** In vitro binding of XCL1-PIGF to the ECM protein fibrinogen, measured by an ELISA assay.

### 3.3.2. XCL1-PIGF recruits cross-presenting DCs to the site of injection.

The cross-presenting DCs of the epidermis that express the CD11c and CD103 surface markers represent 1% of the total skin DC population of naïve C57BL/6 mice [14]. Therefore, the competition for antigen uptake by other APCs is a limiting factor for the CD8<sup>+</sup> T cell-targeting vaccine efficacy. We hypothesized that the prolonged presence of the XCL1 chemokine ligand bound to the ECM would allow skin CD8<sup>+</sup> DCs to sense and migrate towards the XCL1 location and that this would enhance the preferred uptake of the antigen by the concentrated cross presenting DCs. We tested our hypothesis by measuring the skin DC populations at different time points after injection of either XCL1-PIGF or XCL1 alone. We found that 4 and 12 hr after the injection of XCL1-PIGF, the percentage of CD103<sup>+</sup> cross-presenting skin DCs



increased by 2 and 5-fold, respectively, compared to the naïve C57BL/6 untreated mice. Fewer cells accumulated at the site of XCL1 injection (Fig. 2A). Similar measurements of CD8<sup>+</sup> DCs in the LNs of the same mice revealed no differences among the populations at any time point indicating migration of DCs only at the skin site and not towards the LNs. (Fig. 2B).



**Figure 2: XCL1-PIGF attracts crosspresenting DCs to the site of injection.** Naive C57BL/6 mice where injected i.d. with equimolar XCL1 or XCL1-PIGF. 12 and 4 hr post injection, skin and skin draining LNs were stained for cross-presenting DCs. **A.** Skin samples were cut around the injection site and stained for CD11c<sup>+</sup> CD103<sup>+</sup> live cells. **B.** Skin draining LNs from all 4 footpads were harvested and stained for CD3- CD11c<sup>+</sup> CD8<sup>+</sup> live cells.

### 3.3.3. XCL1-PIGF mixed with XCL1-OVA enhances antigen uptake by cross-presenting DCs and promotes cross-priming of CD8<sup>+</sup> T cells.

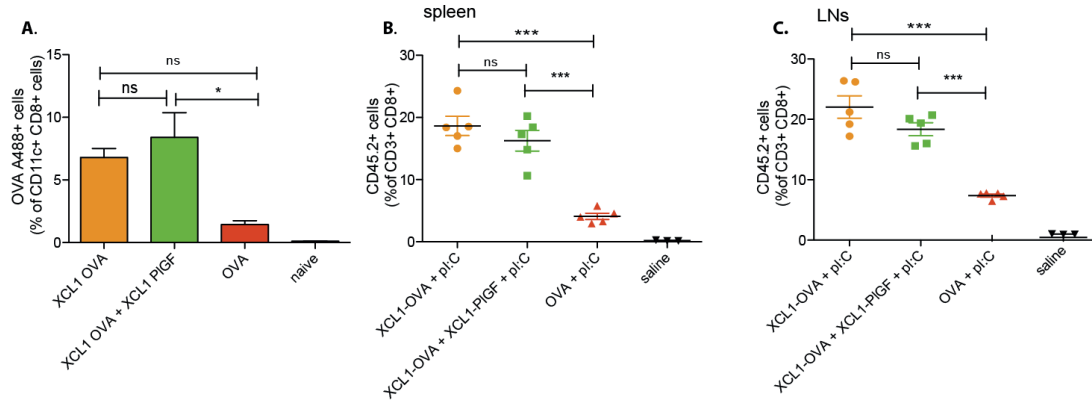
Given the positive results for attraction of CD8<sup>+</sup> DCs at the skin site, we further investigated whether the increased number of DCs capable for cross-presentation at the site of injection would lead to enhanced uptake of the antigen and further promote the cross-presentation to CD8<sup>+</sup> T cells. In order to target the antigen directly to the cross-presenting DCs, OVA was fused to the XCL1 ligand and the XCL1-OVA fusion protein was expressed in HEK cells. XCL1-OVA was labeled with Alexa 488 fluorophore and injected i.d. with or without XCL1-PIGF. As control, OVA alone was conjugated with Alexa Fluor 488 and injected as above. Consistent with previous studies, the XCL1-OVA fusion protein increased the uptake of the antigen by 3.5-fold compared with OVA. Co-administration of XCL1-PIGF with XCL1-OVA further enhanced the uptake by CD8<sup>+</sup> DCs in the LNs resulting in a 4-fold increase compared

to OVA (Fig. 3A) but without significant difference compared to the XCL1-OVA group .

It has been previously demonstrated that uptake of an antigen by cross-presenting DCs promotes cross-priming of CD8<sup>+</sup> T cells [24, 31]. Given the effective uptake of the OVA antigen by the XCL1-OVA and XCL1-OVA + XCL1-PIGF administration, we evaluated the cross-presentation efficiency of our fusion proteins following an adoptive transfer experiment with OTI CD8<sup>+</sup> T cells. In particular, we adoptively transferred OTI T cells into Ly5<sup>+</sup> CD45.2 mice and 24 hr later we immunized the mice with 23 µg XCL1-OVA, 23 µg XCL1-OVA mixed with 3.3 µg XCL1-PIGF or 20 µg OVA alone; all groups were co-administered with 20 µg polyI:C. The increase in the OTI population in the spleen and LNs of all mice 4 days after the immunization was measured as an indicator of effective cross-presentation to CD8<sup>+</sup> T cells. OTI populations in both the XCL1-OVA and the XCL1-OVA + XCL1-PIGF groups had quadrupled in the spleen (Fig. 3B) and tripled in the LNs (Fig. 3C), compared with the OVA-injected mice. However, no differences in OTI population were observed between XCL1-OVA and XCL1-OVA + XCL1-PIGF immunizations. Collectively, the above results suggest that immunization with XCL1-PIGF mixed with XCL1-OVA may lead to enhanced uptake of the antigen and promote cross-presentation to CD8<sup>+</sup> T cells; a desirable effect for CD8<sup>+</sup> T cell-targeted vaccination.

#### **3.3.4. Enhanced cytolytic activity of CD8<sup>+</sup> T cells in the LNs of mice vaccinated with XCL1-OVA + XCL1-PIGF.**

Effective vaccination for the prevention or therapeutic treatment of viral infections and tumors requires potent activation of cytolytic responses from CD8<sup>+</sup> T cells. XCL1-OVA mixed or not with XCL1-PIGF is effectively taken up by CD8<sup>+</sup> DCs and promotes cross-presentation to CD8<sup>+</sup> T cells. We evaluated whether the addition of XCL1-PIGF to XCL1-OVA immunizations would further increase the cytotoxicity of the activated CD8<sup>+</sup> T cells compared to XCL1-OVA alone that has been shown by others to excel in CD8<sup>+</sup> T cell-targeted vaccines. Female C57BL/6 mice were immunized with a prime-boost vaccination on day 0 and 14 with 20 µg OVA, 23 µg XCL1-OVA, 20 µg OVA + 2 µg XCL1, 20 µg OVA + 3 µg XCL1-PIGF or 23 µg XCL1-OVA + 3 µg XCL1-PIGF all mixed with 20 µg polyI:C (Fig. 4A). A single i.d. immunization increased by 3-fold the population of SIINFEKL pentamer<sup>+</sup> cells in the



**Figure 3: XCL1-PIGF + XCL1-OVA enhances the uptake of antigen by CD8+ DCs and cross-priming to CD8+ T cells.** **A)** OVA and XCL1-OVA were conjugated with an Alexa 488 fluorophore. The mice were injected i.d. with 20 $\mu$ g OVA or equimolar amounts of XCL1-OVA or XCL1-OVA + XCL1-PIGF and all groups were mixed with 20 $\mu$ g CpG. The uptake of the antigen by CD8<sup>+</sup> DCs in the LNs was measured by flow cytometry 48hrs later. Gate on live cells, CD11c<sup>+</sup> CD8<sup>+</sup> (\*P<0.05). **B** and **C)** 106 OTI splenocytes were adoptively transferred to naive Ly5 C57Bl/6 mice and 24 hours later the mice were injected i.d. with 20 $\mu$ g OVA or equimolar amounts of XCL1-OVA or XCL1-OVA + XCL1-PIGF. The proliferation of OTI T cells was measured by flow cytometry as a percentage of CD45.2<sup>+</sup> cells (gate on CD3<sup>+</sup> CD8<sup>+</sup> live cells) in the **(B)** spleen and **(C)** LNs (\*\*\*P<0.0001)

circulation of mice injected with XCL1-OVA + XCL1-PIGF compared with XCL1-OVA 7 days after the injection (Fig. 4B). Furthermore, the activated SIINFEKL pentamer<sup>+</sup> cells displayed an effector phenotype, as measured by CD44<sup>+</sup> CD62L<sup>-</sup> staining of pentamer<sup>+</sup> cells and flow cytometry (Fig. 4C). These results show an advantage in cross-presentation to CD8<sup>+</sup> T cells in the presence of XCL1-PIGF.

Processing of the LNs 6 days after the boost injection revealed enhanced cytotoxicity of the CD8<sup>+</sup> T cells in the mice vaccinated with XCL1-OVA + XCL1-PIGF. In particular, the axillary, branchial, popliteal and inguinal LNs of the mice were collected and restimulated *ex vivo* with SIINFEKL for 6 hr followed by staining for IFN $\gamma$  and TNF $\alpha$  CD8<sup>+</sup> T cells. Vaccination with XCL1-OVA + XCL1-PIGF caused a significant increase in the cytolytic activity of CD8<sup>+</sup> T cells in the LNs as indicated by the 1.5- and 2-fold enhanced secretion of IFN $\gamma$  (Fig, 4D) and TNF $\alpha$  (Fig, 4E) populations, respectively, compared with XCL1-OVA immunization. Overall, XCL1-OVA + XCL1-PIGF had a clear benefit in stimulation of cytotoxic CD8<sup>+</sup> T cell responses, making it an appealing platform for CD8 vaccines.

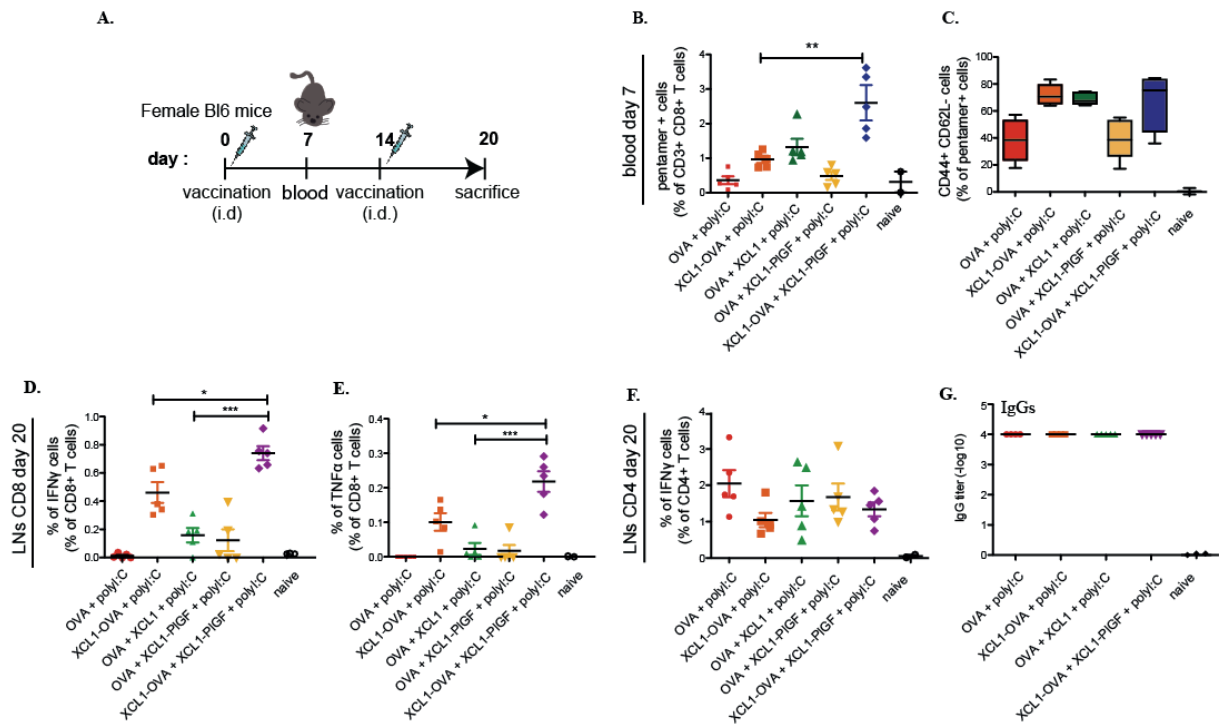
The activation of CD4<sup>+</sup> T cells was further evaluated, as humoral responses and antibody production largely depends on this subset. The pool of LNs was restimulated with the full OVA protein for 12 hr and stained for IFN $\gamma$ <sup>+</sup> and TNF $\alpha$ <sup>+</sup> CD4<sup>+</sup> T lymphocytes. Interestingly, we found that the OVA restimulation failed to activate CD4<sup>+</sup> T cells as displayed by no differences in cytokine secretion among the groups. More importantly, all the groups vaccinated with XCL1 alone or an XCL1 fusion protein had lower cytotoxicity than the OVA + polyI:C group showing no benefit of the XCL1 ligand in CD4<sup>+</sup> T cell activation (Fig. 4F). Finally, the OVA specific antibodies were measured in the serum of vaccinated mice at the end of the experiment. No differences were observed among the groups, consistent with the equal CD4<sup>+</sup> T cell activation (Fig. 4G). This result emphasizes the clear specificity of the XCL1 fusion proteins in activation of CD8<sup>+</sup> T cells. Taken together, the above suggest that XCL1-PIGF mixed with XCL1-OVA is very effective in raising cytolytic T cell responses by cross-presenting the antigen directly to CD8<sup>+</sup> DCs and not by the classical MHC II antigen presentation pathway for extracellular antigens.

### **3.3.5. XCL1-PIGF enhances the efficacy of XCL1-OVA tumor vaccines in both a prophylactic and a therapeutic manner.**

In current cancer research for vaccines that can either prevent or treat tumors, targeting and activating CD8<sup>+</sup> T cells is crucial for the development of effective antitumor therapies. Having demonstrated the clear superiority in cytotoxicity of the XCL1-PIGF + XCL1-OVA vaccine, we further evaluated its potency in tumor regression. In particular, we tested the XCL1-OVA + XCL1-PIGF vaccine formulation in a therapeutic and a prophylactic model of B16-OVA tumor treatment and found that it shows a benefit in tumor regression and overall survival compared to other groups.

Following an established protocol for therapeutic vaccine treatment [32] naïve C57BL/6 mice were inoculated with 2x10<sup>5</sup> tumor cells and 4 days later the mice received consecutive i.d injections of OVA, XCL1-OVA or XCL1-OVA + XCL1-PIGF, all mixed with 20  $\mu$ g polyI:C at frequent time points; namely day 4, 7, 11, 15, 19 and 23 (Fig. 5A). Tumor growth was followed for over a month and the volume was measure by a caliper using an ellipsoid formula every other day. Delay of growth (Fig. 5B) and improved overall survival by 4 days (Fig. 5C) was observed in the XCL1-

OVA + XCL1-PIGF group compared to the other groups, indicating the benefit of XCL1-PIGF in therapeutic treatment.

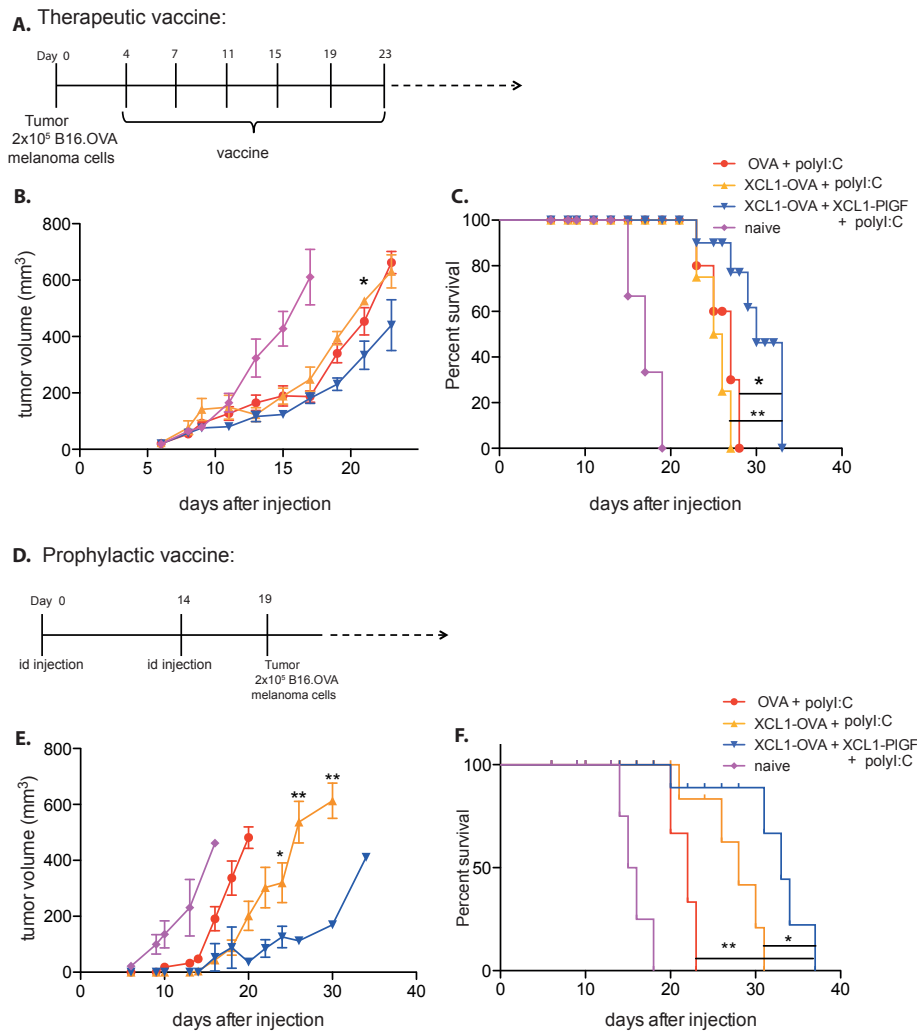


**Figure 4: XCL1-PIGF mixed with XCL1-OVA significantly increases the cytotoxicity of CD8<sup>+</sup> T cells.** **A)** Immunization schedule; Female C57BL/6 mice were injected i.d. with 20μg OVA + 20μg pI:C, 23μg XCL1-OVA + 20μg pI:C, 20μg OVA + 3μg XCL1 + 20μg pI:C, 20μg OVA + 3μg XCL1-PIGF + 20μg pI:C or 20μg XCL1-OVA + 3μg XCL1-PIGF + 20μg pI:C on day 0 and 14 and were sacrificed 6 days after the last boost. Blood samples were collected on day 7 after the first immunization. **B)** Activation of OVA-specific CD8<sup>+</sup> T cells in the blood 7 days after the prime injection, assessed by SIINFEKL pentamer stain and flow cytometry (\*\*p<0.001). **C)** Activation phenotype of pentamer<sup>+</sup> cells measured by CD44<sup>+</sup>, CD62L<sup>-</sup> staining in flow cytometry. **D)** LN lymphocytes were isolated and restimulated ex vivo for 6 h in the presence of SIINFEKL; IFN-γ and **E)** TNFα expression by CD8<sup>+</sup> T cells was measured by intracellular cytokine staining and flow cytometry (\*p<0.01, \*\*\*p<0.0001). **F)** Ex vivo restimulation of lymphocytes with OVA for 12 hr followed by intracellular cytokine stain and flow cytometry, Representative data of IFNγ secretion by CD4<sup>+</sup> T cells. **G)** Antibody titers in the serum of mice at the end of the experiment, measured by ELISA

In prophylactic treatment, the mice were vaccinated first on day 0 and 14 with the same groups as in the therapeutic model, and on day 19 2x10<sup>5</sup> tumor cells were inoculated in the back of all groups, including an untreated naïve group (Fig. 5D). Consistent with the vaccination data and the therapeutic treatment, the tumor growth in the XCL1-OVA + XCL1-PIGF group was significantly delayed compared to XCL1-OVA vaccination, as it remain almost at the same volume for 30 days post inoculation

(Fig. 5E). Consequently, the survival of the mice in this group was prolonged by 7 and 16 days compared to the XCL1-OVA and OVA, respectively (Fig. 5F).

Overall co-administration of XCL1-PIGF with XCL1-OVA has a beneficial effect in tumor treatment both therapeutically and prophylactically compared to XCL1-OVA immunization alone and can potentially serve as a useful platform in improving the current CD8<sup>+</sup> T cell-targeting vaccine design



**Figure 5: XCL1-OVA +XCL1-PIGF prolongs tumor growth both in therapeutic and prophylactic treatments.** A) Therapeutic vaccination schedule; B16-OVA melanoma tumor cells were inoculated on day 0 and after 4 days the mice were vaccinated with 20μg OVA + 20μg pI:C, 23μg XCL1-OVA + 20μg pI:C or 23μg XCL1-OVA + 3μg XCL1-PIGF + 20μg pI:C, following 5 consecutive boosts every 4 days. B) Tumor volumes calculated as ellipsoids ( $V = \pi/6 \times \text{length} \times \text{width} \times \text{height}$ ) and C) survival curves in all groups. D) Prophylactic vaccination schedule; Mice were vaccinated with the same groups as in A on day 0 and 14 and on day 19 B16-OVA tumors cells were inoculated in mice. E) Tumor volume and H) survival curves. (\*p<0.01, \*\*p<0.001)

### 3.4. Discussion

The aim of cancer immunotherapy is to elicit strong CTL responses against tumor infected cells. This has been challenging and one of the main reasons is due to the limited frequency of cross presenting DCs that will activate the CD8<sup>+</sup> T cells. Therefore, the general aim of this study was to explore a novel platform for antigen targeting to cross-presenting DCs. Novel vaccines that target the antigen directly to cross-presenting DCs to promote cross-priming of CD8<sup>+</sup> T cells have shown promising results in tumor treatment with potential application in humans. In this study we improved the current methodology by providing a platform for sustained attraction of XCR1-expressing DCs to the site of antigen administration. In particular, we fused the XCL1 chemokine ligand to the PlGF-2<sub>123-144</sub> ECM-binding domain and succeeded in prolonging the presence of XCL1 at the injection site. Intradermal administration of XCL1-PlGF resulted in migration of skin cross-presenting DCs (CD103<sup>+</sup>) locally and promoted the targeted take up of the antigen when co-administered with XCL1-OVA fusion proteins. The enhanced cross-presentation and activation of CD8<sup>+</sup> T cells resulted in improved cytokine release following a prime-boost vaccination study. Furthermore, the XCL1-OVA mixed with XCL1-PlGF significantly increased the survival of tumor bearing mice both in a prophylactic and a therapeutic approach, supporting further use of the PlGF platform as a standard approach for enhancement of antigen uptake in vaccination.

The implementation of XCL1-PlGF in the vaccine platform aimed at creating a sustained reservoir of cross-presenting DCs at the injection site that would allow enhanced uptake of the antigen directly targeted to this DC subtype. The physiological role of XCL1 secreted by activated NK cells and CD8<sup>+</sup> T cells *in vivo* is to chemoattract DCs that express XCR1 on their surface [33]. Following previous studies from our laboratory, we used the PlGF-2 engineered domain, which displayed the strongest binding to the ECM, in order to maintain XCL1 at the injection site. We took advantage of the prolonged retention of the molecule at the injection site and used it in a fusion protein with XCL1 (XCL1-PlGF) to attract the cross-presenting DCs locally. As seen by the fluorescent images in Fig. 1, XCL1-PlGF can maintain its presence at the injection site for longer than 48 hr, whereas XCL1 alone did not bind adequately and rapidly diffused to the draining LNs. The prolonged presence of the fusion protein

resulted in attraction of cross-presenting DCs at the injection site, as compared with the naïve CD103<sup>+</sup> population. Interestingly, as seen in Fig. 2A, XCL1 alone also attracted cross-presenting DCs to the injection site, although at a slower rate than PIGF-fused XCL1. This could be explained by studies showing binding of XCL1 to heparin [34] and in particular that XCL1 (also called lymphotactin) exists in two different forms in physiological conditions, that interconvert between each other. One conformation that binds to glycosaminoglycans (heparin) and one that activates the XCR1 [35]. These studies refer to human XCL1, but it is possible that this is also the case in mice, where heparan sulfate proteoglycan is present at the skin epidermis.

Our initial hypothesis was that the prolonged presence of the chemokine and the increased recruiting of the DCs locally would result in enhanced uptake of the antigen by cross-presenting DCs and improved cross-priming of CD8<sup>+</sup> T cells. As seen by the uptake experiment in Fig. 3, 48 hr after the injection of XCL1-OVA, XCL1-OVA + XCL1-PIGF or OVA enhanced uptake is observed only in the groups containing XCL1-OVA, as expected. The addition of XCL1-PIGF only slightly improves the uptake compared with XCL1-OVA alone although the difference between the two groups is not statistically significant. This can possibly be explained by the timing of the experiment, as 48 hr exceed the time required for an antigen to drain to the LNs and be processed by the APCs locally [36]. According to Fig. 2, 4 hr after the injection the XCL1-PIGF injected mice had significantly higher numbers of cross-presenting DCs concentrated at the injection site and as such we believe that administration of XCL1-OVA 4 hr after the XCL1-PIGF injection and processing of the LNs 8-16 hr later would help in observing better differences between the groups containing XCL1-PIGF or not. Injecting the antigen after the local migration of cross-presenting DCs would also improve the activation of OTI transferred CD8<sup>+</sup> T cells. Similar to the uptake experiment, better differences among the groups including or not the XCL1-PIGF could have been observed at different time points in the adoptive transfer experiment. In particular, 2-3 days after the immunization should be adequate to develop an OTI proliferated pool of cells in the LNs and 5 days should allow for a detectable population in the spleen. Considering the above, future studies should be performed using a different timeline that would allow better observation of the differences among the groups.



Although the enhanced uptake and cross-presentation are not confirmed by our experiments with XCL1-PIGF immunization, we still observe enhanced cytotoxicity of CD8<sup>+</sup> T cells and improved cytokine secretion in our vaccination studies. Following a prime-boost vaccination, the cytokine secretion in the LNs of mice injected with XCL1-OVA + XCL1-PIGF was significantly enhanced compared to XCL1-OVA vaccination, implying an improved mechanism in CD8<sup>+</sup> T cell activation by XCL1-PIGF. This advantage is preserved also in tumor treatment, as seen by slower rate of tumor growth both in the therapeutic and the prophylactic setting. Prolonged survival of mice immunized with XCL1-OVA + XCL1-PIGF implies that our approach is of biological relevance in vaccines, since the XCR1 expression is preserved in human cross-presenting DCs [22] and can be a target in vaccination using this methodology. Overall, these results suggest that our initial hypothesis for local skin attraction and enhanced cross-presentation may not be the explanation for the positive outcome in vaccination, using the XCL1-PIGF protein, and further mechanism studies should be conducted.

The Kroczek group has used a similar strategy in targeting the antigen directly to the CD8<sup>+</sup> T cells with an XCL1-OVA fusion protein [26]. In our studies we could observe the same trend as the Kroczek group of enhanced XCL1-OVA activity compared to OVA alone after the adoptive transfer and the vaccination experiments. Direct comparison between the two methods though is not possible, as different dosing and immunization approaches have been used. In particular, the Kroczek group used LPS as an adjuvant in vaccination, that is a TLR4 agonist not adequately expressed on CD8<sup>+</sup> DCs. Instead, we used polyI:C, which is a TLR3 agonist abundantly expressed on cross-presenting DCs together with TLR9. We believe that this approach is advantageous, as we limited the diffusion of the danger signals to other cell types to specifically promote the activation of the CD8<sup>+</sup> DCs. The drawback in our experiments is loss in the classical pathway of CD4<sup>+</sup> T cell activation as seen by limited cytotoxicity in this cell type and low antigen specific antibody titers. Overall, we believe that our contribution by the addition of XCL1-PIGF to the XCL1-OVA platform adds value to the current methodologies as it significantly improves the cytotoxic efficacy in vaccination compared to XCL1-OVA alone group. To further improve the immune responses raised by the XCL1-PIGF platform mixed with XCL1-OVA and polyI:C, we can proceed with double adjuvant treatments and, more

specifically, use together with polyI:C a TLR9 agonist such as CpG to vaccinate mice. This could have an additive effect in activation and cytokine secretion of CD8<sup>+</sup> T cells and at the same time also contribute in humoral responses, since CpG has been used by us and by others for inducing humoral responses.

Targeting the XCR1 surface molecule of cross-presenting DCs is a very promising approach in CD8<sup>+</sup> DC vaccination so far, compared to failures of similar methodologies targeting other surface markers of CD8<sup>+</sup> DCs. The DEC205 approach has been challenging, as this receptor is also expressed on other cell lineages, such as conventional DCs (cDCs), Langerhans cells, interstitial DCs and thymic epithelial cells resulting in loss of the desired specificity. Also, the specificity of the Clec9A molecule is questioned by one study [21] as its presence has been reported in other cell types. In contrast, XCR1 is uniquely expressed on cross-presenting CD8<sup>+</sup> DCs of the secondary immune organs and the CD103<sup>+</sup> DCs of skin. Targeting the antigen directly to these DCs by binding the XCR1 receptor has shown very promising results in CD8<sup>+</sup> T cell activation by recent studies [26, 27, 37]. We succeeded in further improving the already existing platforms for direct targeting of an antigen to XCR1 bearing cross-presenting DCs by implementing new strategies to enhance the cytotoxicity of CD8<sup>+</sup> T cell inducing vaccines. Our platform can be translated to human vaccination and, to our knowledge, the PIGF protein is not immunogenic and does not have side effects. Thus, we believe that our improved platform has biological relevance in human vaccines and can enhance the efficacy of existing methodologies.

## References

1. Ehrlich P. On the present state of chemotherapy. *Berichte Der Deutschen Chemischen Gesellschaft* 1909;42: 17-47.
2. Burnet FM. The concept of immunological surveillance. *Progress in experimental tumor research* 1970;13: 1-27.
3. Pedersen SR, Sorensen MR, Buus S, et al. Comparison of vaccine-induced effector cd8 t cell responses directed against self- and non-self-tumor antigens: Implications for cancer immunotherapy. *Journal of Immunology* 2013;191(7): 3955-67.
4. Speiser DE, Romero P. Molecularly defined vaccines for cancer immunotherapy, and protective t cell immunity. *Seminars in Immunology* 2010;22(3): 144-54.
5. Higano CS, Schellhammer PF, Small EJ, et al. Integrated data from 2 randomized, double-blind, placebo-controlled, phase 3 trials of active cellular immunotherapy with sipuleucel-t in advanced prostate cancer. *Cancer* 2009;115(16): 3670-9.

6. Small EJ, Schellhammer PF, Higano CS, et al. Placebo-controlled phase iii trial of immunologic therapy with sipuleucel-t (apc8015) in patients with metastatic, asymptomatic hormone refractory prostate cancer. *Journal of Clinical Oncology* 2006;24(19): 3089-94.
7. Kruit WHJ, van Ojik HH, Brichard VG, et al. Phase 1/2 study of subcutaneous and intradermal immunization with a recombinant mage-3 protein in patients with detectable metastatic melanoma. *International Journal of Cancer* 2005;117(4): 596-604.
8. Sabbatini P, Dupont J, Aghajanian C, et al. Phase i study of abagovomab in patients with epithelial ovarian, fallopian tube, or primary peritoneal cancer. *Clinical Cancer Research* 2006;12(18): 5503-10.
9. Caminschi I, Lahoud MH, Shortman K. Enhancing immune responses by targeting antigen to dc. *European Journal of Immunology* 2009;39(4): 931-8.
10. Sharma P, Wagner K, Wolchok JD, et al. Novel cancer immunotherapy agents with survival benefit: Recent successes and next steps. *Nature Reviews Cancer* 2011;11(11): 805-12.
11. Burgdorf S, Kautz A, Bohnert V, et al. Distinct pathways of antigen uptake and intracellular routing in cd4 and cd8 t cell activation. *Science* 2007;316(5824): 612-6.
12. Lin ML, Zhan YF, Villadangos JA, et al. The cell biology of cross-presentation and the role of dendritic cell subsets. *Immunology and Cell Biology* 2008;86(4): 353-62.
13. Shortman K, Heath WR. The cd8+dendritic cell subset. *Immunological Reviews* 2010;234: 18-31.
14. Henri S, Poulin LF, Tamoutounour S, et al. Cd207(+) cd103(+) dermal dendritic cells cross-present keratinocyte-derived antigens irrespective of the presence of langerhans cells (vol 207, pg 189, 2010). *Journal of Experimental Medicine* 2010;207(2): 445-.
15. Crozat K, Tamoutounour S, Vu Manh TP, et al. Cutting edge: Expression of xcr1 defines mouse lymphoid-tissue resident and migratory dendritic cells of the cd8alpha+ type. *Journal of immunology* 2011;187(9): 4411-5.
16. Bonifaz LC, Bonnyay DP, Charalambous A, et al. In vivo targeting of antigens to maturing dendritic cells via the dec-205 receptor improves t cell vaccination. *Journal of Experimental Medicine* 2004;199(6): 815-24.
17. Jiang WP, Swiggard WJ, Heufler C, et al. The receptor dec-205 expressed by dendritic cells and thymic epithelial-cells is involved in antigen-processing. *Nature* 1995;375(6527): 151-5.
18. Caminschi I, Proietto AI, Ahmet F, et al. The dendritic cell subtype-restricted c-type lectin clec9a is a target for vaccine enhancement. *Blood* 2008;112(8): 3264-73.
19. Sancho D, Mourao-Sa D, Joffre OP, et al. Tumor therapy in mice via antigen targeting to a novel, dc-restricted c-type lectin. *Journal of Clinical Investigation* 2008;118(6): 2098-110.
20. Schraml BU, van Blijswijk J, Zelenay S, et al. Genetic tracing via dngr-1 expression history defines dendritic cells as a hematopoietic lineage. *Cell* 2013;154(4): 843-58.
21. Huysamen C, Willment JA, Dennehy KM, et al. Clec9a is a novel activation c-type lectin-like receptor expressed on bdca3(+) dendritic cells and a subset of monocytes. *Journal of Biological Chemistry* 2008;283(24): 16693-701.
22. Bachem A, Guttler S, Hartung E, et al. Superior antigen cross-presentation and xcr1 expression define human cd11c(+)cd141(+) cells as homologues of mouse cd8(+) dendritic cells. *Journal of Experimental Medicine* 2010;207(6): 1273-81.

23. Haniffa M, Shin A, Bigley V, et al. Human tissues contain cd141(hi) cross-presenting dendritic cells with functional homology to mouse cd103(+) nonlymphoid dendritic cells. *Immunity* 2012;37(1): 60-73.
24. Dorner BG, Dorner MB, Zhou X, et al. Selective expression of the chemokine receptor xcr1 on cross-presenting dendritic cells determines cooperation with cd8+ t cells. *Immunity* 2009;31(5): 823-33.
25. Lei Y, Takahama Y. Xcl1 and xcr1 in the immune system. *Microbes and infection / Institut Pasteur* 2012;14(3): 262-7.
26. Hartung E, Becker M, Bachem A, et al. Induction of potent cd8 t cell cytotoxicity by specific targeting of antigen to cross-presenting dendritic cells in vivo via murine or human xcr1. *Journal of Immunology* 2015;194(3): 1069-79.
27. Fossum E, Grodeland G, Terhorst D, et al. Vaccine molecules targeting xcr1 on cross-presenting dcs induce protective cd8(+) t-cell responses against influenza virus. *European Journal of Immunology* 2015;45(2): 624-35.
28. Martino MM, Briquez PS, Ranga A, et al. Heparin-binding domain of fibrin(ogen) binds growth factors and promotes tissue repair when incorporated within a synthetic matrix. *Proceedings of the National Academy of Sciences of the United States of America* 2013;110(12): 4563-8.
29. Martino MM, Briquez PS, Guc E, et al. Growth factors engineered for super-affinity to the extracellular matrix enhance tissue healing. *Science* 2014;343(6173): 885-8.
31. Belz GT, Smith CM, Kleinert L, et al. Distinct migrating and nonmigrating dendritic cell populations are involved in mhc class i-restricted antigen presentation after lung infection with virus. *Proceedings of the National Academy of Sciences of the United States of America* 2004;101(23): 8670-5.
32. Jeanbart L, Ballester M, de Titta A, et al. Enhancing efficacy of anticancer vaccines by targeted delivery to tumor-draining lymph nodes. *Cancer immunology research* 2014;2(5): 436-47.
33. Yoshida T, Imai T, Kakizaki M, et al. Identification of single c motif-1/lymphotactin receptor xcr1. *The Journal of biological chemistry* 1998;273(26): 16551-4.
34. Peterson FC, Elgin ES, Nelson TJ, et al. Identification and characterization of a glycosaminoglycan recognition element of the c chemokine lymphotactin. *Journal of Biological Chemistry* 2004;279(13): 12598-604.
35. Tuinstra RL, Peterson FC, Kutlesa S, et al. Interconversion between two unrelated protein folds in the lymphotactin native state. *Proceedings of the National Academy of Sciences of the United States of America* 2008;105(13): 5057-62.
36. Allan RS, Waithman J, Bedoui S, et al. Migratory dendritic cells transfer antigen to a lymph node-resident dendritic cell population for efficient ctl priming. *Immunity* 2006;25(1): 153-62.
37. Terhorst D, Fossum E, Baranska A, et al. Laser-assisted intradermal delivery of adjuvant-free vaccines targeting xcr1(+) dendritic cells induces potent antitumoral responses. *Journal of Immunology* 2015;194(12): 5895-902.

## **Chapter 4:**

### **Depot Effect Investigation of Antigen Affinity With the Injection Site in Vaccination**

## 4.1. Introduction

A goal in vaccination is to induce strong immune responses that can protect the host against infectious diseases in the long-term. An effective vaccine must support the recognition of an antigen and the consequent activation of the immune system to induce antigen-specific immunity. Different mechanisms, including the efficient uptake and delivery of antigen to appropriate sites, are responsible for inducing immune responses in secondary immune organs. Several immunostimulators are used in vaccination, along with antigens, to facilitate initiation of the appropriate mechanisms for development of immunity, the most common being adjuvants[1]. In most cases, and mainly in the non-live vaccines, different adjuvants are included in vaccine formulations to induce a more robust immune response. Although different roles of adjuvants have been proposed by several groups [2], their exact mechanisms of action and roles in stimulating innate, and later adaptive immunity, is still unclear; some function by stimulating particular molecular pathways for activation of dendritic cells (DCs), whereas others are less direct in their mode of action. .

The oldest, and probably the most popular theory for the role of adjuvants, is the depot effect, first described by Glenny [3]. According to this theory, antigens are trapped and slowly released at the site of injection, when co-administered with an adjuvant. It was later shown that this ensures the constant stimulation of the immune system, and allows enhanced uptake and maturation of antigen presenting cells (APCs) to further elicit an immune response [4]. In one study, it was shown that antigen remained at the site of injection for at least 2-3 weeks, and resulted in activation of the immune system when co-administered with an alum adjuvant [5]. Similarly, in a different antigen-adjuvant formulation, Hebert showed that the model antigen OVA can result in antibody production that is forty times higher when administered in water-in-oil emulsions [6]. Since then, many adjuvant formulations, such as complete Freund's adjuvant (CFA) [7] or AS04 – an adjuvant combination of monophosphoryl lipid A (MPLA) and alum – were shown to have a depot effect on the release of antigen [8].

In order to explore further improvement of current vaccine strategies and also avoid complications such as severe local and systemic side-effects, including sterile

abscesses, eosinophilia and myofascitis [9], which strong adjuvants can cause, different approaches to enhance immunogenicity and support the sustained release of antigen in vaccines have been tried. Delivery of antigen in a sustained manner has been shown to be advantageous in vaccination, as the prolonged presence and interaction of an antigen with cells of the immune system increases the efficiency of uptake, and thus promotes an effective immune response [10]. In addition, the sustained release of antigen may allow a reduction in the number of immunizations required, as the presence of the antigen is maintained locally [11]. Towards this end, significant effort has been made to provide novel vaccine platforms for sustained antigen release. Aside from synthetic materials such as virus-like particles, nanoparticles, liposomes and biodegradable polymers [12-14] that have been vastly used for antigen delivery, methods that trap antigen at the site of injection, allowing for sustained release, and thus enhanced uptake by APCs, are of particular interest. The skin and, in particular, the epidermis have a large number of epidermal Langerhans cells (skin-resident dendritic cells) that can capture antigens and transport them to draining lymph nodes. Therefore, the skin is an attractive immunological site for vaccination [15].

There are several examples in the literature with skin-based vaccination approaches. Vaccine-loaded microneedles on skin patches have been used in vaccination against influenza to enhance protection against the virus, with positive results when compared to free, soluble antigen [16]. Also, the use of antigen-loaded depot technologies have shown positive results for the sustained release of antigen at the site of injection [17]. The use of hydrogels is another means of trapping antigen for enhanced immunogenicity in skin vaccination. For example, it has been shown that a liquid solution of chitosan can form a hydrogel *in vivo*, after injection, and can support the sustained release of OVA antigen for > 24 days. This resulted in enhanced activation of CD4<sup>+</sup> and CD8<sup>+</sup> T cells, compared to the results of activation with soluble OVA. There was also greater antibody production, with titers equal to those produced by OVA vaccination with an alum adjuvant [18].

While the technologies described above have shown positive results in sustaining the release of antigen and immunogenicity, these methods, however, require manufacturing that is costly and could potentially damage the antigen. To overcome these complications we evaluated and present here an alternative approach to trap

antigen at the site of injection. Specifically, we engineered a recombinant protein consisting of antigen fused to the extracellular matrix binding (ECM) domain of the growth factor placenta growth factor-2 (PlGF-2), specifically the domain PlGF-2<sub>123-144</sub> [19], using ovalbumin (OVA) as a model antigen, thus creating the fusion protein OVA-PlGF-2<sub>123-144</sub> (abbreviated hereinafter as OVA-PlGF). It was hypothesized that the presence of OVA-PlGF could be maintained at the site of injection by direct binding of PlGF to the ECM of the skin. This would allow more APCs to approach the site of injection and take up the antigen. Furthermore, in the presence of a potent adjuvant, the APCs would mature and drain to the lymph nodes LNs to elicit antigen-specific immune responses. The OVA-PlGF fusion protein was produced in HEK293 cells and was used in a prime-boost vaccine experiment with female C57BL/6 mice. Both the humoral and cellular responses were assessed in the spleens and LNs of vaccinated animals, and these were compared to responses elicited by immunizations with free OVA. Contrary to the hypothesis of our design, no significant benefit from binding to the ECM could be observed with OVA-PlGF vaccinations when compared to vaccinations with free OVA antigen.

## 4.2. Materials and Methods

**Animals** Female C57BL/6J mice were purchased from Harlan and female Balb/c and Ly5.1 (CD45.1) mice were purchased from Charles River laboratories. All mice were aged between 8-12 weeks and kept under pathogen free conditions at the animal facility of Ecole Polytechnique Fédérale de Lausanne. The Veterinary Authority of the Canton de Vaud approved all procedures and experiments.

**OVA-PlGF recombinant production.** OVA-PlGF was produced as previously described for the engineering of other growth factors [20]. Briefly, the sequence encoding for PlGF-2<sub>(123-144)</sub> was subcloned in a pSecTagA mammalian vector engineered to express the OVA protein. The PlGF sequence was added at the C-terminus together with a 6 histidine tag for purification at the N-terminus. The sequence for the OVA-PlGF was as follows: “HHHHHH – OVA – RRRPKGRGKRRREKQRPTDCHL”. The protein was expressed in a HEK293 cells under serum free conditions with 3.75 mM valproic acid (Sigma-Aldrich), and after 7



days the protein in suspension was purified using a HisTrap HP column (GE Healthcare) with immobilized metal affinity chromatography. The purified protein was analyzed for purity using SDS/PAGE, endotoxin levels were assessed in THP-1 x Blue cells (InvivoGen), and concentration was measured using bicinchoninic acid assays (Thermo Scientific). The final product was sterile-filtered, and stored at -80 °C in working aliquots.

**Immunizations.** 8-week old female C57BL/6 mice were immunized under isofluorane anesthesia (5% for induction and 2% for maintenance) on day 0 and 14 with an intradermal injection of 20 µg OVA, 20 µg OVA + 20 µg CpG-B, 20 µg OVA-PIGF, 20 µg OVA-PIGF + 20 µg CpG-B or just saline. 7 days after the boost mice were euthanized, and the axillary, branchial and inguinal LNs and spleen were collected for *ex vivo* restimulation and staining as described in other sections.

**Pentamer staining.** While mice were under anesthesia, 50 µl of blood was collected from their facial vein and stored in EDTA containing tubes. Blood was spun at 2000xg for 5 min and the serum was collected from the supernatant. The remaining cells were lysed for 5 min at room temperature with 0.155M NH<sub>4</sub>Cl and were further processed in preparation for analysis by flow cytometry as described in other sections. Following the live dead staining, the cells were incubated at room temperature for 12 min with 1:10 dilution of SIINFEKL pentamer (Bioscience). The cells were further stained for CD3 (1:100), CD8 (1:200), CD44 (1:200), CD62L (1:200), CD19 (1:800) and acquired by flow cytometry. For the pentamer stain of LNs and spleen, 10<sup>6</sup> cells from both organs were stained as described above.

**Tissue and cell preparation for ex vivo restimulation of lymphocytes.** Splenocytes were obtained by disruption of the spleen through a 70-µm cell sieve and subsequent red blood cell lysis with 0.155M NH<sub>4</sub>Cl. The lymph nodes were digested for 30 min with 2 mg/mL Collagenase D (Roche) in IMDM, and passed through a 70-µm cell sieve to obtain single cell suspensions. All organs were kept in Dulbecco's Modified Eagle Medium (DMEM) (Gibco) supplemented with 10% FBS and 1% penicillin, streptomycin (Invitrogen). For CD8<sup>+</sup> T cell-specific restimulation and intracellular cytokine staining, cells were first cultured for 3 hr at 37 °C in the presence of 1 µg/mL SIINFEKL, 10<sup>4</sup> U/ml IL2, and 0.5 µg anti-CD28 (eBioscience), and subsequently for 3

hr with the addition of 250 µg/mL brefeldin A (SigmaAldrich). For CD4<sup>+</sup> T cell restimulation, 10<sup>4</sup> U/ml IL2, 0.5 µg anti-CD28 and 100 µg/mL OVA grade VI (SigmaAldrich) protein were added to the cells for 3 h, followed by incubation with 50 µg/mL brefeldin A for another 12 hr.

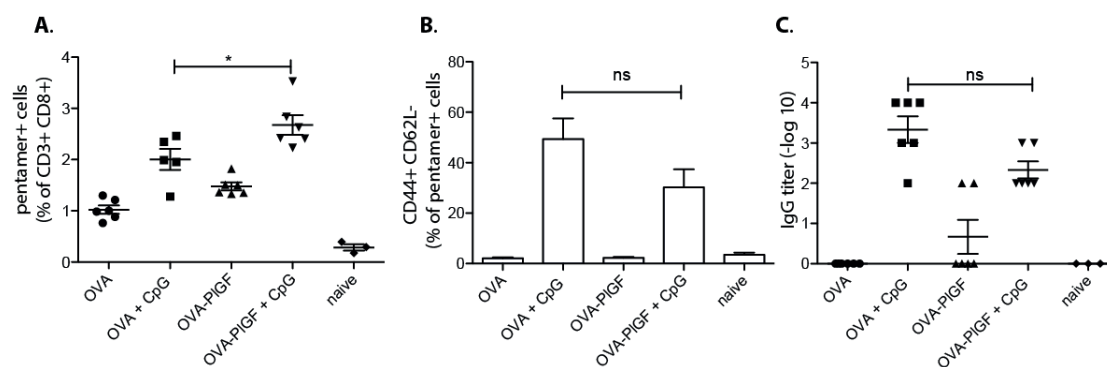
**Flow cytometry staining.** For the detection of live cells, cells were suspended at a concentration of 10<sup>6</sup> cells in 200µl, washed with PBS, and labeled with live/dead fixable cell viability reagent (Invitrogen). Subsequently, the cells were incubated for 20 min on ice with PBS/2% FBS solutions of the surface markers CD3 (1:100) and CD8 (1:200) or CD4 (1:200). For intracellular cytokine staining, cells were fixed in 2% paraformaldehyde solution, washed with 0.5% saponin (SigmaAldrich) in PBS/2% FBS, and incubated with the IFN $\gamma$  (1:200) or TNF $\alpha$  (1:200) antibody diluted in saponin solution for 30 min on ice. Finally, the cells were resuspended in PBS/2% FBS for analysis. Samples were processed on CyAn ADP Analyzer (Beckman Coulter) and data were analyzed with FlowJo software (Tree Star). The antibodies against mouse CD3, CD4, CD8, IFN $\gamma$  and TNF $\alpha$  used were purchased from eBioscience.

**Antibody titers measurement.** Blood was collected from the facial vein of all mice and was spun at 2000xg for 10 min. The serum was collected from the supernatant and was stored at -20 °C for later analysis. ELISA plates (Nunc MaxiSorp, Thermo Fisher Scientific) were coated with 10 µg/ml OVA antigen in phosphate buffer saline (PBS) and were incubated at 4 °C over night. Next, the plates were blocked with 2% bovine serum albumin (BSA) in PBS with 0.05% Tween 20 (PBS-T) for 2 h at room temperature (RT). Wells were then washed with PBS-T and further incubated with the following dilution of the serum: 1:100, 1:200, 1:300, 1:400 in BSA for 2 hr at RT. After washes, the anti-IgG antibody was added in a 1:8000 dilution in BSA for 1hr at RT and was detected with tetramethylbenzidine substrate by measurement of the absorbance at 450 nm.

**Data Analysis.** All flow cytometry data were analyzed using FlowJo (v8.8.6). Graphs and statistical analyses of data were performed using GraphPad<sup>®</sup> Prism (v5). Statistical significance was determined by pair-wise Student's t-test with Welch correction. The asterisks indicate the significance as follows: \* implies p<0.05, \*\*\* implies p < 0.001.

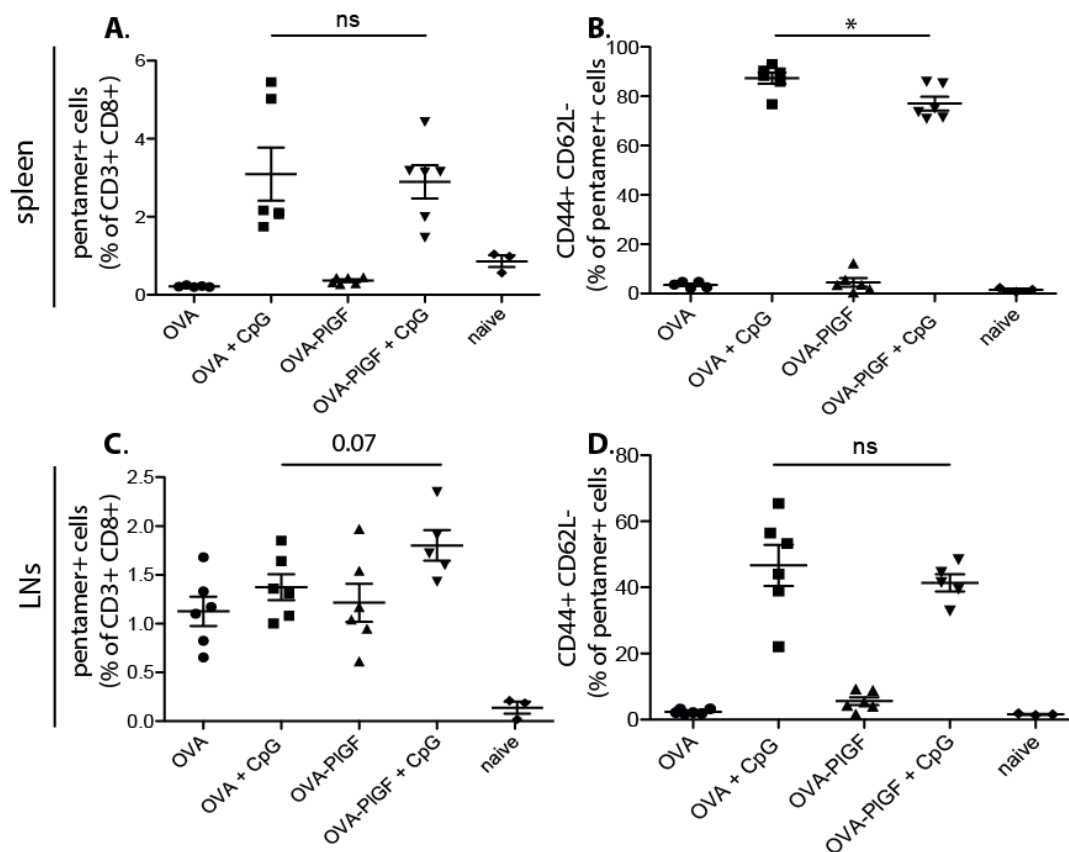
### 4.3. Results and Figures

A potent vaccine elicits antigen-specific antibodies through CD4<sup>+</sup> T cells and activates cytolytic CD8<sup>+</sup> T cells. We evaluated the immune responses raised after a prime-boost intradermal vaccination with OVA, OVA + CpG-B, OVA-PIGF and OVA-PIGF + CpG-B, measuring responses in the circulation as well as in the spleens and LNs of vaccinated mice. First, the activated CD8<sup>+</sup> T cells circulating in the blood 14 days after the first injection were measured. SIINFEKL pentamer staining was performed on blood samples of all mice, followed by flow cytometry analysis. A 1.3-fold increase in the pentamer<sup>+</sup> cells circulating in the blood was observed in the group of mice vaccinated with OVA-PIGF + CpG-B compared to free OVA + CpG-B. (Fig.1 A). However, the activation phenotype of the pentamer<sup>+</sup> cells in the OVA-PIGF + CpG-B group, determined by staining with CD44 and CD62L surface markers, was lower than for immunizations with OVA + CpG, but there were no significant differences between the two groups. Also, from the measurement of antibody titers circulating in the serum of all mice, as measured by ELISA 14 days after the prime injection (Fig. 1C), no differences were observed between the groups that included CpG-B in their vaccine formulations, although with OVA + CpG there was an order of magnitude increase in antigen-specific titers. Together, these results, from samples obtained 14 days after the first immunization, did not show a clear advantage of OVA-PIGF + CpG immunization over OVA + CpG-B.



**Figure 1: Activation of CD8<sup>+</sup> T cells after a single intradermal injection.** Mice were vaccinated intradermal with OVA, OVA + CpG-B, OVA-PIGF and OVA-PIGF + CpG-B and 14 days later blood samples were collected from the facial vein to evaluate the activation of CD8<sup>+</sup> T cells and antibody induction in circulation. **A.** Blood samples were stained with SIINFEKL pentamer and measured by flow cytometry; gate on live, CD3<sup>+</sup> CD8<sup>+</sup> cells. **B.** Evaluation of activation phenotype by flow cytometry measurements of CD44<sup>+</sup> CD62L<sup>-</sup> cells; gate on pentamer<sup>+</sup> cells. **C.** IgG OVA specific antibody titers measured by ELISA in the serum of all mice. (\*p<0.05)

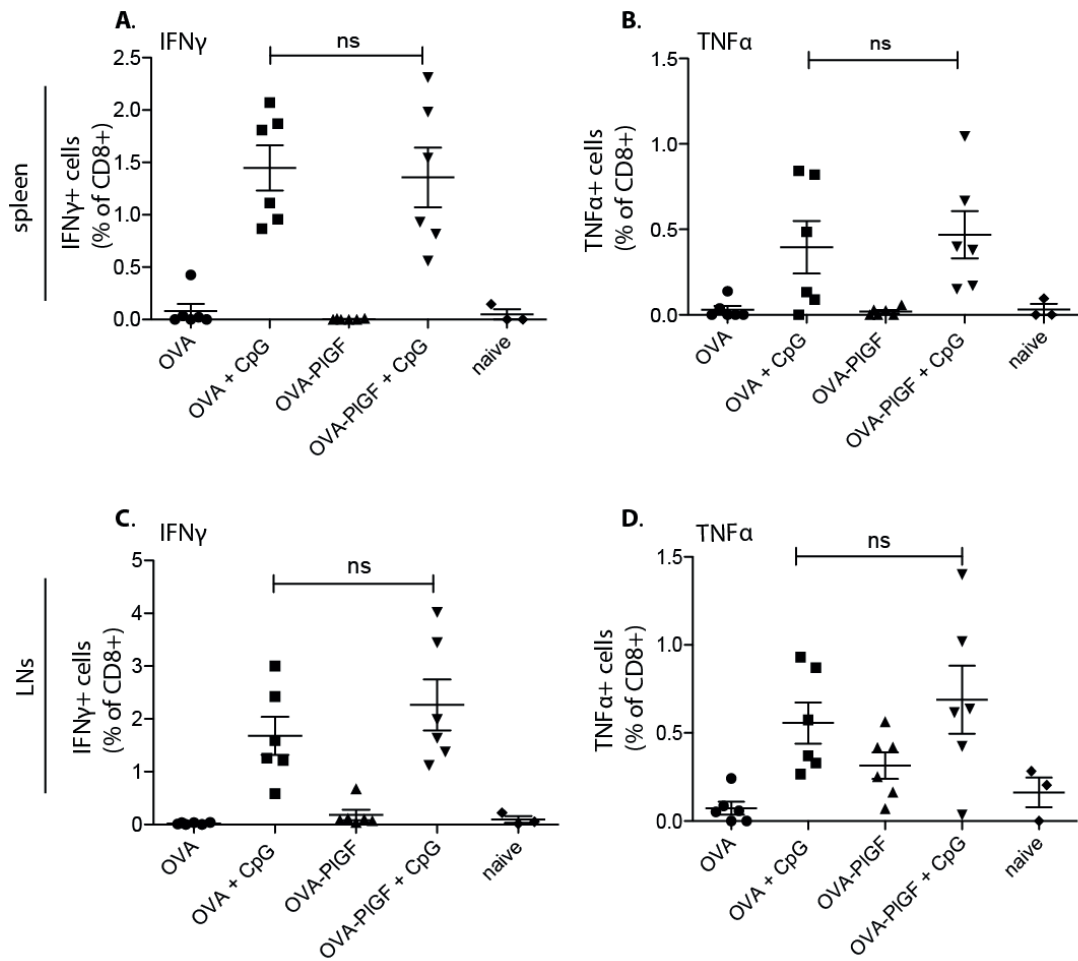
The spleen and LNs were harvested 7 days after the boost injection and the organs were processed for further analysis. Similar to the measurements made with pentamer on blood samples, the splenocytes and LN lymphocytes were stained for SIINFEKL pentamer<sup>+</sup> cells and their activation phenotype was determined by CD44 and CD62L staining. No differences were observed between the OVA + CpG-B and the OVA-PIGF + CpG-B groups in the pentamer<sup>+</sup> cells of the spleen (Fig. 2A) whereas in the LNs, the OVA-PIGF + CpG-B group showed preferred activation, although this difference was not statistically significant. The activation phenotypes in the different organs were very similar, with no significant differences observed between the different vaccination groups.



**Figure 2: OVA-PIGF + CpG-B does not activate CD8<sup>+</sup> T cells better than OVA + CpG-B.** Mice were vaccinated intradermal with OVA, OVA + CpG-B, OVA-PIGF and OVA-PIGF + CpG-B on day 0 and 14 and the spleen and LNs were collected and processed a week after the boost. Lymphocytes from spleen and LNs were stained for SIINFEKL pentamer and measured by flow cytometry on day 21. **A.** Spleen SIINFEKL pentamer<sup>+</sup> cells; gate on CD3<sup>+</sup> CD8<sup>+</sup> cells. **B.** Activation phenotype of pentamer<sup>+</sup> splenocytes measured on CD44<sup>+</sup> CD62L<sup>-</sup> cells; **C.** LN pentamer<sup>+</sup> stain and **D.** activation phenotype. \*p<0.05

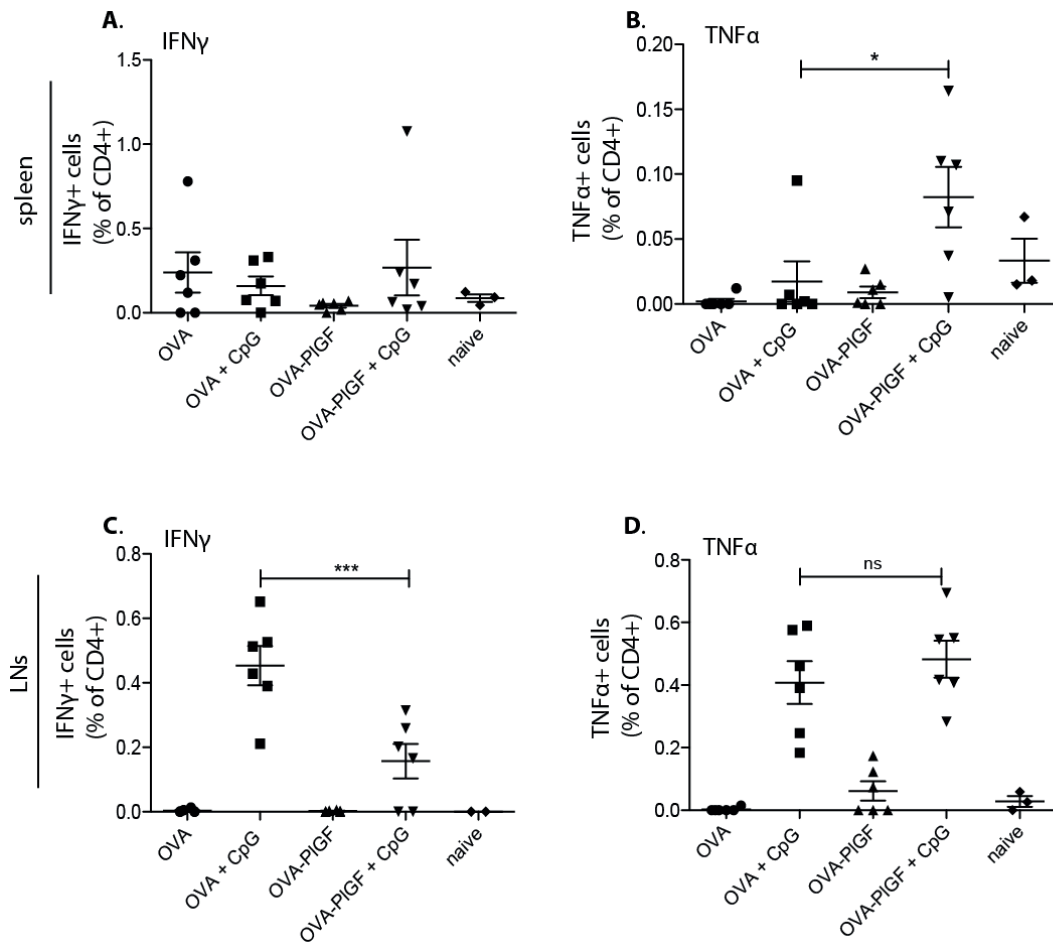
Next, the cytolytic activity of recovered CD8<sup>+</sup> T cells was evaluated. The activation of CD8<sup>+</sup> T cells in vaccination is a prerequisite for the elimination of tumor cells and virus-infected cells. The induction of cytokine secretion a week after the boost injection was measured in samples obtained from the spleens and LNs of all mice. The organs were harvested, processed and restimulated for 6 hr with the SIINFEKL peptide, and then the cells were stained for the presence of IFN $\gamma$  and TNF $\alpha$ . No significant differences were observed in the levels of cytokine production between OVA + CpG-B and OVA-PIGF + CpG-B as seen in Fig. 3, suggesting that vaccination with OVA-PIGF has no benefit over vaccination with OVA alone, for activation or cross-presentation of antigen to CD8<sup>+</sup> T cells. More specifically, identical percentages of IFN $\gamma$  (Fig. 3A) and TNF $\alpha$  (Fig. 3B) were observed in the spleens of OVA + CpG-B and OVA-PIGF + CpG-B vaccinated mice, while in the LNs of the same mice there was a trend towards increased production of both cytokines in the OVA-PIGF + CpG-B group, although not statistically significant when compared to OVA + CpG-B (Fig. 3C. and 3D).

Traditional strategies for immunization attempt to also induce activation of CD4<sup>+</sup> T cells. Activation of this subtype helps in the induction of CD8<sup>+</sup> T cell and facilitates the production of antibodies by B cells. Evaluation of the CD4<sup>+</sup> T cell activation was performed by restimulation of both spleen and LNs with OVA antigen overnight followed by staining for intracellular IFN $\gamma$  and TNF $\alpha$ . Minimal production of IFN $\gamma$  was observed in the spleen of each mouse (Fig. 4A), but the production of TNF $\alpha$  in OVA-PIGF + CpG-B samples improved 4-fold when compared to the OVA + CpG-B samples (Fig. 4B). In contrast, in the LNs, the percentage of IFN $\gamma$ -producing CD4<sup>+</sup> T cells in the OVA + CpG-B group was four times higher than the OVA-PIGF + CpG-B group (Fig. 4C), and no differences were observed in the frequencies of TNF $\alpha$ -producing CD4<sup>+</sup> T cells (Fig. 4D).

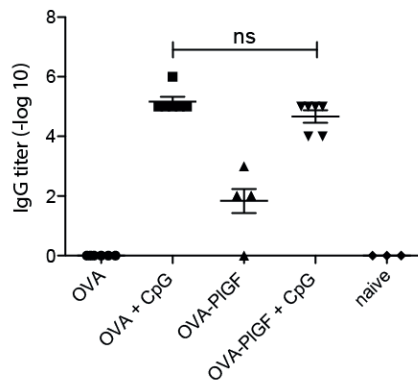


**Figure 3: OVA-PIGF mixed with CpG-B does not promote the cross-priming of CD8<sup>+</sup> T cells.** Lymphocytes from spleens and LNs were collected a week after the boost injection and evaluated for the cytolytic activity of CD8<sup>+</sup> T cells after restimulation for 6 hr with SIINFEKL peptide. Cells were labeled for intracellular expression of IFN $\gamma$  and TNF $\alpha$  and measured by flow cytometry. **A.** IFN $\gamma$ <sup>+</sup> and **B.** TNF $\alpha$ <sup>+</sup> splenocytes (gate on live, CD3<sup>+</sup>CD8<sup>+</sup> T cells). **C.** IFN $\gamma$ <sup>+</sup> and **D.** TNF $\alpha$ <sup>+</sup> CD8<sup>+</sup> T cell of LNs, as in spleen.

Finally, antibody titers were measured by ELISA in all groups at the end of the experiment. As expected, high antibody titers were measured in the groups immunized with vaccine formulations containing an adjuvant, however, there were no significant differences in titers when comparing the formulations of the OVA and OVA-PIGF antigens (Fig. 5).



**Figure 4: OVA-PIGF mixed with CpG-B does not enhance the activation of CD4<sup>+</sup> T cells.** Lymphocytes from spleens and LNs a week after the boost injection were evaluated for the activation of CD4<sup>+</sup> T cells after restimulation overnight with the OVA protein. Cells were labeled for intracellular expression of IFN $\gamma$  and TNF $\alpha$  and measured by flow cytometry. **A.** IFN $\gamma$ <sup>+</sup> and **B.** TNF $\alpha$ <sup>+</sup> secreting CD4<sup>+</sup> T cells in spleen (gate on live, CD3<sup>+</sup> CD8<sup>+</sup> T cells). **C.** IFN $\gamma$ <sup>+</sup> and **D.** TNF $\alpha$ <sup>+</sup> CD4<sup>+</sup> T cell of LNs



**Figure 5: IgG OVA specific antibody titers measured by ELISA in the serum of mice on day 21 of the experiment.**

## 4.4. Discussion

It is widely known that non-live vaccines have lower immunogenicity than live vaccines, and as such, current technologies are focused on enhancing the immune responses primed by these types of vaccines. A common approach to improve the antigen-specific immune responses in subunit vaccination, for instance, is to maintain the sustained release of the drug-protein or subunit by creating a depot effect. In this study we evaluated antigen trapping at the site of injection as a method for enhancing the immunogenicity of protein-based vaccines. The method was designed to trap antigen within the skin, at the point of injection, and prolong its presence locally, aiming for enhanced uptake by APCs. OVA was chosen as a model antigen, and it was fused to the ECM-binding domain of the PlGF-2 growth factor, namely PlGF-2<sub>123-144</sub>, which binds strongly to ECM proteins present in the skin. The immunogenicity was measured *in vivo* by vaccinating female C57BL/6 mice with OVA-PlGF and OVA, with or without the addition of the CpG-B adjuvant. Following two intradermal injections, on days 0 and 14, the humoral and cellular responses were evaluated. Contrary to the hypothesis of our design, no striking differences were observed between fused OVA-PlGF and free OVA groups when CD4<sup>+</sup> and CD8<sup>+</sup> T cell activation, and antibody production were considered.

A single intradermal injection of OVA-PlGF + CpG-B resulted in an increase in the number of CD8<sup>+</sup> T cells with antigen-specific T cell receptors compared to injection with OVA + CpG-B, based on data from pentamer staining of blood samples. However, the benefit of immunizing with OVA-PlGF observed in circulation seemed to be absent in the spleen, after the boost injection, while in the LN, a similar trend with the blood staining was observed, but this increase was no longer statistically significant. The positive results in the LNs are encouraging as these are the first organs to take up antigen, and are key for activation of the adaptive immune system. Moreover, it was expected that there would be a retention of the increased level of OVA-specific CD8<sup>+</sup> T cells, and possibly an enhancement of the response with the boost injection when OVA-PlGF was used, however, this was not observed. A potential explanation for this discrepancy is the early time chosen for evaluation of the responses. Standard protocols from our laboratory [21] and other research groups suggest that the peaks of the responses are observed 7 days after the boost injection.



However, the kinetics regarding the transport of the OVA-PIGF molecule to the APCs *in vivo* could be different from the kinetics of free OVA, as antigen trapping at the site of injection might slow trafficking to the LNs. Future studies must involve characterization of these properties for the OVA-PIGF molecule.

Ex vivo restimulation of spleen and the skin draining LNs with OVA and the SIINFEKL peptide revealed that there was similar immunogenicity between the OVA and OVA-PIGF proteins. No significant differences were observed in the levels of IFN $\gamma$  and TNF $\alpha$  cytokines produced by CD8 $^+$  T cells after vaccination with either OVA + CpG-B or OVA-PIGF + CpG-B, indicating that there may be no improvement in cross-presentation of antigen to CD8 $^+$  T cells with the platform. Furthermore, restimulation with OVA did not result in a clear outcome with regards to the activation of CD4 $^+$  T cells. In the spleen, no IFN $\gamma$  secreting cells were measured whereas the TNF $\alpha^+$  CD4 $^+$  T cells were 7-fold higher in the OVA-PIGF + CpG-B group than in the OVA + CpG-B group. In contrast, in the LNs there was a clear benefit of OVA + CpG-B in IFN $\gamma$  production, which was not seen in the TNF $\alpha^+$  CD4 $^+$  T cells. A manifestation of the mixed results in the CD4 $^+$  T cell compartment is seen by the equal IgG titers raised against the OVA antigen in both groups. Thus, in perhaps the most basic of vaccine read-outs, the OVA-PIGF variant of the wild-type OVA antigen was not beneficial.

One expected outcome of the vaccination was the rather negligible immunogenicity of the OVA-PIGF platform in the absence of CpG-B. Very little activation, mainly in the LNs, was observed in the group of mice vaccinated with OVA-PIGF only. This is in agreement with the general observation that subunit vaccines require the support of strong adjuvants in order to raise potent immune responses, unlike with live vaccines, and that the depot effect is not sufficient to activate the immune system when immunizing with only an antigen. Therefore, new technologies for subunit protein vaccination focus on simultaneous injection of antigen and adjuvant.

Considering the lack of increased efficacy of the OVA-PIGF vaccine in this study, a re-evaluation of the platform is required. With a better understanding of the release kinetics of the OVA-PIGF, it may be possible to improve the immunogenicity

of the vaccine. Combining the PIGF platform with multiple adjuvant administration or with other platforms, such as fibrin-based implanted gels [22, 23], which can stabilize the antigen and also promote its sustained release, could lead to enhancements in efficacy of the vaccine. Overall, improving the immunogenicity of subunit vaccines, and more specifically in protein based vaccines based, is very challenging, and a substantial amount of work is still required to make progress in the field.

## References

1. Bergmann-Leitner ES, Leitner WW. Adjuvants in the driver's seat: How magnitude, type, fine specificity and longevity of immune responses are driven by distinct classes of immune potentiators. *Vaccines* 2014;2(2): 252-96.
2. Awate S, Babiuk LA, Mutwiri G. Mechanisms of action of adjuvants. *Frontiers in Immunology* 2013;4.
3. Glenny AT, Pope CG, Waddington H, et al. Immunological notes xvll.-xxiv. *Journal of Pathology and Bacteriology* 1926;29(1): 31-40.
4. Mannhalter JW, Neychev HO, Zlabinger GJ, et al. Modulation of the human immune-response by the non-toxic and non-pyrogenic adjuvant aluminum hydroxide - effect on antigen uptake and antigen presentation. *Clinical and Experimental Immunology* 1985;61(1): 143-51.
5. Osebold JW. Mechanisms of action by immunological adjuvants. *Journal of the American Veterinary Medical Association* 1982;181(10): 983-7.
6. Herbert WJ. Mode of action of mineral-oil emulsion adjuvants on antibody production in mice. *Immunology* 1968;14(3): 301-&.
7. Kreuter J. Possibilities of using nanoparticles as carriers for drugs and vaccines. *Journal of Microencapsulation* 1988;5(2): 115-27.
8. Didierlaurent AM, Morel S, Lockman L, et al. As04, an aluminum salt- and tlr4 agonist-based adjuvant system, induces a transient localized innate immune response leading to enhanced adaptive immunity. *Journal of Immunology* 2009;183(10): 6186-97.
9. Petrovsky N, Aguilar JC. Vaccine adjuvants: Current state and future trends. *Immunology and Cell Biology* 2004;82(5): 488-96.
10. Lofthouse S. Immunological aspects of controlled antigen delivery. *Advanced Drug Delivery Reviews* 2002;54(6): 863-70.
11. Zhao Z, Leong KW. Controlled delivery of antigens and adjuvants in vaccine development. *Journal of Pharmaceutical Sciences* 1996;85(12): 1261-70.
12. Zhao L, Seth A, Wibowo N, et al. Nanoparticle vaccines. *Vaccine* 2014;32(3): 327-37.
13. Irvine DJ, Swartz MA, Szeto GL. Engineering synthetic vaccines using cues from natural immunity. *Nature Materials* 2013;12(11): 978-90.
14. Demento SL, Siefert AL, Bandyopadhyay A, et al. Pathogen-associated molecular patterns on biomaterials: A paradigm for engineering new vaccines. *Trends in Biotechnology* 2011;29(6): 294-306.

15. Glenn GM, Kenney RT, Hammond SA, et al. Transcutaneous immunization and immunostimulant strategies. *Immunology and Allergy Clinics of North America* 2003;23(4): 787-+.
16. Sullivan SP, Koutsonanos DG, Martin MD, et al. Dissolving polymer microneedle patches for influenza vaccination. *Nature Medicine* 2010;16(8): 915-U116.
17. Murthy N, Xu MC, Schuck S, et al. A macromolecular delivery vehicle for protein-based vaccines: Acid-degradable protein-loaded microgels. *Proceedings of the National Academy of Sciences of the United States of America* 2003;100(9): 4995-5000.
18. Gordon S, Saupe A, McBurney W, et al. Comparison of chitosan nanoparticles and chitosan hydrogels for vaccine delivery. *The Journal of pharmacy and pharmacology* 2008;60(12): 1591-600.
19. Martino MM, Briquez PS, Ranga A, et al. Heparin-binding domain of fibrin(ogen) binds growth factors and promotes tissue repair when incorporated within a synthetic matrix. *Proceedings of the National Academy of Sciences of the United States of America* 2013;110(12): 4563-8.
20. Martino MM, Briquez PS, Guc E, et al. Growth factors engineered for super-affinity to the extracellular matrix enhance tissue healing. *Science* 2014;343(6173): 885-8.
21. Nembrini C, Stano A, Dane KY, et al. Nanoparticle conjugation of antigen enhances cytotoxic t-cell responses in pulmonary vaccination. *Proceedings of the National Academy of Sciences of the United States of America* 2011;108(44): E989-E97.
22. Janmey PA, Winer JP, Weisel JW. Fibrin gels and their clinical and bioengineering applications. *Journal of the Royal Society Interface* 2009;6(30): 1-10.
23. Schense JC, Bloch J, Aebischer P, et al. Enzymatic incorporation of bioactive peptides into fibrin matrices enhances neurite extension. *Nature Biotechnology* 2000;18(4): 415-9.



## Chapter 5:

### A Cationic Micelle Complex Improves CD8<sup>+</sup> T Cell Responses in Vaccination Against Unmodified Protein Antigen

*Carrie E. Brubaker,<sup>1</sup> Vasiliki Panagiotou,<sup>1</sup> Davide Demurtas, Daniel K. Bonner, and Jeffrey A. Hubbell*

<sup>1</sup>These authors contributed equally to this work.

Manuscript submitted in ACS Biomaterials Science and Engineering

## 5.1. Abstract

Nanoscale carrier platforms promote immune responses to vaccination by facilitating delivery of vaccine components to immunologically relevant sites. The technique is particularly valuable for subunit vaccination, in which co-administration of immunostimulatory adjuvant is known to enhance immune responses to protein antigen. The fabrication of polymer-based nanoparticle vaccines commonly requires covalent attachment of vaccine components to the carrier surface. In contrast, we here describe a cationic micelle vaccination platform in which antigen and adjuvant loading is mediated by non-covalent molecular encapsulation and electrostatic complexation. Cationic micelles were generated through self-assembly of a polyarginine-conjugated diblock copolymer amphiphile, with or without encapsulation of monophosphoryl lipid A, an amphiphilic experimental vaccine adjuvant. Micelle complexes were subsequently formed by complexation of ovalbumin (OVA) and CpG-B oligodeoxynucleotide (a second experimental adjuvant) to the cationic micelles. In a 35-day study in mouse, micelle-mediated co-delivery of OVA antigen and CpG-B enhanced cellular and humoral responses to vaccination. These outcomes were highlighted in spleen and lymph node CD8<sup>+</sup> T cells, with significantly increased populations of IFN $\gamma$ <sup>+</sup>, TNF $\alpha$ <sup>+</sup>, and polyfunctional IFN $\gamma$ <sup>+</sup> TNF $\alpha$ <sup>+</sup> cells. Elevated cytokine production is a hallmark of robust cytotoxic T lymphocyte (CTL) responses sought in next-generation vaccine technologies. Increased production of OVA-specific IgG1, IgG2c, and IgG3 also confirmed micelle enhancement of humoral responses. In a subsequent 35-day study, we explored micelle-mediated vaccination against OVA antigen co-administered with MPLA and CpG-B adjuvants. A synergistic effect of adjuvant co-administration was observed in micelle-free vaccination but not in groups immunized with micelle complexes. This outcome underlines the advantage of the micelle carrier: we achieved optimal cellular and humoral responses to vaccination by use of this nanoparticle platform with a single adjuvant. In particular, enhanced CTL responses support future development of the cationic micelle platform in experimental cancer vaccines and for vaccination against reticent viral pathogens.

## 5.2. Introduction

Vaccination represents one of the most successful medical interventions against infectious pathogens. Since Edward Jenner published the first vaccination against smallpox in 1798, vaccines have been used for prevention of infectious disease and more recently, the United States Food and Drug Administration approved the first therapeutic vaccine for prostate cancer.<sup>1</sup> Vaccination strategies promote humoral immunity (antibody production for neutralization of circulating antigens) and/or cellular immunity (cytotoxic T cell responses for disease attenuation and elimination of intracellular pathogens *via* cell killing and secretion of inflammatory cytokines). Most vaccines in clinical use mediate protection through induction of neutralizing, antigen-specific antibodies. However, this humoral response is insufficient for eradication of intracellular infection or tumor-transformed cells, for which the activity of cytotoxic CD8<sup>+</sup> T lymphocytes (CTLs) is necessary to eliminate diseased cell populations. As such, recent vaccine design approaches have sought to promote cellular immunity along with induction of humoral responses.<sup>2,3</sup>

In the past, vaccines utilized live or attenuated cells or viruses to mimic natural infections, providing more potent immunogenicity compared to non-living vaccines.<sup>4</sup> However, the risk of harmful side effects associated with overt toxicity of pathogenic components has shifted interest towards methods utilizing whole proteins in subunit vaccination.<sup>5</sup> Superior safety is a significant advantage of protein-based subunit vaccines, but costly manufacturing procedures and limited immunogenicity remain challenges in current vaccine design. Improvements to subunit vaccination focus on enhancing immunogenicity by co-administration of immunostimulatory adjuvants and by carrier-mediated delivery that controls the presence and sustained release of antigen.

Adjuvants are immune potentiators that bind to pattern recognition receptors (PPRs) of antigen presenting cells (APCs) to augment immune responses to the antigen with which they are administered.<sup>6</sup> The most thoroughly characterized class of PRRs is the Toll-like receptors (TLRs), which represent an important binding target of natural and synthetic TLR agonists developed as experimental adjuvants. TLRs are expressed in a variety of immune cells including macrophages, dendritic cells (DCs), and monocytes.<sup>7</sup>

Upon adjuvant binding, activated signaling pathways downstream of the TLRs initiate secretion of proinflammatory cytokines and upregulate expression of costimulatory molecules on the APC surface.<sup>8</sup> TLRs are associated with the cell surface or intracellular compartments, based on their detection of pathogen-associated cell wall components (TLR1, 2, 4-6) or intracellular nucleotide-based molecules (TLR3, 7-9).<sup>9</sup> CpG oligodeoxynucleotide constructs are a family of experimental adjuvants frequently explored in vaccination. Presenting repeated unmethylated CpG dinucleotide motifs, these molecules are well-characterized TLR9 agonists that induce Th1 responses and elevate antibody production.<sup>10</sup> Similarly utilized is monophosphoryl lipid A (MPLA), a low-toxicity derivative of bacterial lipopolysaccharide and TLR4 agonist with potent immunostimulatory properties.<sup>11</sup>

As engineering principles are more fully adopted in the field of vaccinology,<sup>12</sup> the use of nanoparticulate platforms has evolved into a desirable and experimentally validated approach in vaccine design. The broad variety of nanoparticle preparations, their capable delivery of antigen and adjuvant, and their interactions with immunologically relevant tissues and cells has been the subject of recent reviews.<sup>13-15</sup> Significant benefits of nanoparticulate vaccine delivery are now recognized. For example, these platforms enhance delivery of protein-based subunit vaccine antigen to target immune cells, in part by protecting antigen from proteolytic degradation following administration. The platform thereby increases bioavailability, and with it, the likelihood of antigen delivery to secondary lymphoid compartments implicated in immune response to vaccination. Nanoparticle-mediated delivery also permits incorporation of multiple vaccine components in a single construct. In this biomimetic approach, the introduction of protein-based antigen and immunostimulatory adjuvant *via* nanoscale carrier closely resembles natural pathogenic infection and provokes a more robust immunological response than any of these elements presented alone.<sup>16, 17</sup> Nanoparticle vaccines capably traffic to injection site-draining lymph nodes (LN) independent of cellular uptake; previous efforts within our group have demonstrated that particles of ~20 nm diameter permit most efficient transport.<sup>18</sup> Both solid-core nanoparticles and watery-core polymersomes have subsequently been examined in our group, for antigen and/or adjuvant delivery in the context of vaccination.<sup>19-22</sup> Similarly, sub-50 nm self-assembled spherical micelles were applied for antigen delivery following covalent conjugation of ovalbumin (OVA) to the micelle surface.<sup>23</sup> The



present work expands on these studies, by defining a role for poly(ethylene glycol)-*b*-poly(propylene sulfide) (PEG-PPS) micelles as a complete vaccination platform. Through non-covalent molecular loading and charge-mediated interactions, PEG-PPS micelles act as a nanoscale carrier for two distinct adjuvants (MPLA and CpG-B) as well as model whole protein OVA antigen, without requiring the complexity of covalent attachment of the antigen to the carrier.

Here we introduce a self-contained, micelle-based nanoparticle vaccine in which neither OVA antigen nor adjuvant have been covalently modified. The cationic micelle carrier was obtained by self-assembly of a novel polymer-peptide construct defined by polyarginine-conjugated PEG-PPS, with or without MPLA encapsulation during micelle formation. Electrostatic interactions between the positively charged micelle and negatively charged OVA and CpG-B drove formation of the particulate vaccines. The performance of these nanoparticle vaccines was subsequently explored in a 35-day OVA vaccination study in mouse. We determined that the cationic micelle carrier facilitated robust, OVA-specific humoral responses desired from an adjuvanted subunit vaccine. Furthermore, cationic micelle-mediated vaccination displayed enhanced cellular responses in inflammatory cytokine-producing CD8<sup>+</sup> T cell populations derived from lymph node and spleen. Taken together, these outcomes demonstrate the ease of preparation of a self-contained, micelle-based nanoparticle vaccine, coupled with improved vaccination outcomes *via* humoral as well as cellular immune responses.

## 5.3 Materials and Methods

**Synthesis of PEG-PPS-R13 conjugate.** All reagents were from Sigma-Aldrich unless otherwise noted. Preparation of poly(ethylene glycol) (PEG)-based macroinitiator was achieved by thioacetate modification of methoxyPEG-OH (MW 2000) according to previously published methods.<sup>39, 40</sup> PEG-thioacetate initiator (300 mg, 1 equiv) was transferred to Schlenk tube under flowing argon and dissolved in air-free tetrahydrofuran (8 mL). Sodium methoxide (0.5 M solution in methanol, 1.1 equiv) was added via syringe, for macroinitiator activation during 30 min incubation. Subsequently, propylene sulfide monomer (15 equiv) was added to initiate ring-

opening polymerization of the monomer. After 1.5 hr, the reaction was terminated by addition of excess 2,2'-dipyridyl disulfide (10 equiv) solution in tetrahydrofuran. This copolymer end-capping reaction stirred overnight under ambient conditions. Excess tetrahydrofuran was removed, and the PEG-PPS block copolymer product was obtained in >85% yield following double precipitation in diethyl ether and vacuum drying. <sup>1</sup>H NMR spectroscopy was performed in CDCl<sub>3</sub> on the Bruker AVANCE (400 MHz) platform with Topspin software: δ = 1.38 (d, CH<sub>3</sub>, PPS side group); 2.63 (m, CH in PPS backbone); 2.91 (CH<sub>2</sub> in PPS backbone); 3.38 (s, OCH<sub>3</sub>); 3.6-3.7 (s, broad, PEG backbone OCH<sub>2</sub>CH<sub>2</sub>); 7.10, 7.65, 7.75, 8.46 (CH, pyridine group). The reference peak integration of PEG methoxy hydrogens was compared to peak integrations of PPS backbone hydrogens, to confirm PPS degree of polymerization = 15.

PEG-PPS (20-40 mg) was reacted for 2 hr with R13 peptide (NH<sub>2</sub>-Cys-Gly-Trp-(Arg)<sub>13</sub>, PolyPeptide Laboratories, 1.4 equiv) in DMF/trace triethylamine (0.5-1 mL). In this reaction, peptide conjugation to PEG-PPS was achieved by disulfide exchange, a by-product of which is 2-pyridinethione. Release of this molecule imparted a distinctive yellow tone to the reaction solution and confirmed efficient conjugation. The polymer-peptide conjugate was repeatedly precipitated in diethyl ether to remove 2-pyridinethione and vacuum dried. With gentle pipetting, addition of endotoxin-free water (B. Braun Medical AG, 10 mg conjugate/mL) to the dried product drove formation of cationic micelle assemblies, as confirmed by zeta potential analysis and dynamic light scattering (Zetasizer Nano ZS, Malvern Instruments) of the resulting aqueous dispersion. This dispersion was exhaustively diafiltered (10,000 MWCO) against endotoxin-free water to remove unreacted peptide. Following purification, PEG-PPS-R13 was lyophilized to obtain the final product, a viscous solid, in >70% yield.

**Preparation of the cationic micelle vaccination platform.** Self-assembly of PEG-PPS-R13 micelles was performed by solvent evaporation. PEG-PPS-R13 was dissolved in dichloromethane (1 w/v%) with gentle agitation. For preparation of MPLA-loaded assemblies, MPLA (Monophosphoryl Lipid A from *S. Minnesota* R595, InvivoGen) in 3:1 dichloromethane:methanol was added with Hamilton syringe to PEG-PPS-R13 solution. The conjugate solution was added dropwise to endotoxin-free water and allowed to stir under ambient conditions until complete evaporation of

organic solvent. The remaining aqueous phase contained formed micelles at a final concentration of 10 mg PEG-PPS-R13 per mL. MPLA-loaded micelles contained MPLA at a final concentration of 0.5 mg MPLA per mL, and their pro-inflammatory behavior was confirmed by endotoxin assay performed with InvivoGen HEK-Blue hTLR4 cell system using LPS standard. This assay confirmed no endotoxic contaminants in samples not containing MPLA. Micelles as well as complexes (described below) were characterized by dynamic light scattering for mean particle diameter and by zeta potential measurement for charge character.

Injection samples containing complexed micelles were prepared by mixing a given volume of the previously prepared micelle dispersion with sterile solutions of OVA (endograde, Hyglos, 10 mg/mL in water) and/or CpG-B (Microsynth, 3.18 mg/mL in water). Sterile normal saline was added to bring sample solutions to volume. The following final reagent concentrations were maintained across sample formulations: 2.5 mg/mL PEG-PPS-R13 conjugate, 0.5 mg/mL OVA, 0.125 mg/mL MPLA, 0.5 mg/mL CpG-B. Reagent concentrations were identical in control groups not containing micelles; these were prepared by simple mixing of antigen and adjuvant solutions. Here, MPLA was used at a concentration of 500 µg/mL (in 10 v/v % biotechnology grade dimethylsulfoxide in water). All samples were prepared under sterile conditions immediately prior to injection.

**Cryo Transmission Electron Microscopy.** 5 µL micelle sample solution was applied to electron microscopy grid (Agar Scientific) with holey carbon film. Sample grids were blotted and flash vitrified in liquid ethane using an automatic plunge freezing apparatus (Vitrobot, FEI) to control humidity (100%) and temperature (23 °C). Analysis was performed at -170 °C on a Tecnai F20 electron microscope operating at 200 kV, using the Gatan 626 cryo-specimen holder (20,000-50,000× magnification; -3 to -5 µm defocus). Digital images were recorded on in-line Eagle CCD camera.

**Animals.** Female C57BL/6J mice (8-12 weeks) were purchased from Harlan Laboratories and housed under pathogen-free conditions at the animal facility of Ecole Polytechnique Fédérale de Lausanne. All experiments were performed in accordance with Swiss law and with approval from the Cantonal Veterinary Office of Canton de Vaud, Switzerland.

**Immunizations.** Mice were immunized *via* intradermal injection at each limb hock, under isoflurane anesthesia (5% for induction and 2% for maintenance) on day 0, 14, and 28 of the studies. For the singly- and doubly-adjuvanted vaccination studies, samples groups utilizing micelle carriers are described in Table 1. Micelle-free controls included OVA + CpG-B or MPLA (singly-adjuvanted study), and uncomplexed OVA + MPLA + CpG-B and OVA alone (doubly-adjuvanted study). Injection control groups received normal saline. Mice were treated according to reagent concentrations normalized across all groups and studies; depending on sample group, mice received 100 µg PEG-PPS-R13 conjugate / 20 µg OVA / 5 µg MPLA / 20 µg CpG-B per injection. Mice were euthanized 7 days following second boost (day 35). The axillary, brachial, inguinal, and popliteal LNs and spleen were collected for *ex vivo* restimulation and staining as described below.

**Tissue and cell preparation for *ex vivo* restimulation of lymphocytes.** Splenocytes were obtained by disruption of the spleen through 70-µm cell sieve and subsequent red blood cell lysis with 0.155M NH<sub>4</sub>Cl. Lymph nodes were digested for 30 min with 2 mg/mL Collagenase D (Roche) in Iscove's Modified Dulbecco's Medium (IMDM), and passed through 70-µm cell sieve to obtain single cell suspensions. All organs were kept in Dulbecco's Modified Eagle Medium (DMEM) (Gibco) supplemented with 10% FBS and 1% penicillin/streptomycin (Invitrogen). For CD8<sup>+</sup> T cell restimulation and intracellular cytokine staining, cells were first cultured for 3 hr at 37 °C in the presence of 1 µg/mL SIINFEKL, 10<sup>4</sup> U/ml IL-2, and 0.5 µg anti-CD28 (eBioscience). Thereafter, cells were cultured an additional 3 hr following addition of 250 µg/mL brefeldin A (Sigma-Aldrich). For CD4<sup>+</sup> T cell restimulation, 10<sup>4</sup> U/ml IL-2, 0.5 µg anti-CD28 and 100 µg/mL OVA grade VI (Sigma-Aldrich) were added to the cells for 3 hr incubation, followed by incubation with 50 µg/mL brefeldin A for an additional 12 hr. Alternatively, cells were restimulated for 4 days in the presence of 100 µg/mL OVA grade VI or 1 µg/mL SIINFEKL for analysis of supernatant cytokines.

**Flow cytometry staining and ELISA.** Cells were suspended at a concentration of 10<sup>6</sup> cells per 200 µl, washed with PBS, and labeled with live/dead fixable cell viability reagent (Invitrogen). Subsequently, cells were incubated for 20 min on ice with antibodies to the T cell surface markers CD3 (1:100) and CD8 (1:200) or CD4 (1:200)

in 2% FBS in PBS (labeling buffer). For intracellular cytokine staining, cells were fixed with 2% paraformaldehyde solution, washed with 0.5% saponin (Sigma-Aldrich) in labeling buffer, and incubated with IFN $\gamma$  (1:200) or TNF $\alpha$  (1:200) antibody diluted in saponin solution for 30 min on ice. Finally, the cells were resuspended in labeling buffer for analysis. Samples were processed on CyAn ADP Analyzer (Beckman Coulter) and data were analyzed with FlowJo software (Tree Star). Antibodies against mouse CD3, CD4, CD8, IFN $\gamma$  and TNF $\alpha$  were purchased from eBioscience. Following 4-day restimulations, supernatant cytokines were quantified using Ready-SET-Go! ELISA kits (eBioscience) according to manufacturer guidelines.

**Measurement of antibody titers.** Blood was collected from the facial vein of all mice and spun at 2000  $\times$  g for 10 min. Serum was removed and stored at -20 °C prior to analysis. ELISA plates (Nunc MaxiSorp, Thermo Fisher Scientific) were coated with 10  $\mu$ g/ml OVA grade VI in PBS and incubated at 4 °C overnight. The plates were blocked with 2% bovine serum albumin (BSA) in PBS + 0.05% Tween 20 (PBS-T) for 2 hr at room temperature. The plates were washed with PBS-T and incubated for 2 hr at RT with serial serum dilutions (1:100 to 1:700) in 2% BSA in PBS-T. After sequential plate washes, plates were incubated 1 hr at RT with horseradish peroxidase-conjugated anti-IgG or -IgG subtype in 2% BSA in PBS-T, according to the following dilutions: total IgG (1:8000), IgG1 (1:8000), IgG2a (1:5000), IgG2b (1:5000), IgG2c (1:8000), and IgG3 (1:8000). All antibodies were provided by Southern Biotech. Conversion of tetramethylbenzidine substrate was detected by absorbance measurement at 450 nm.

**Data Analysis.** Graphs and statistical analyses were executed in Prism 5 (GraphPad). Statistical significance was determined by one-way ANOVA with Bonferroni post-test.

## 5.4. Results and Discussion

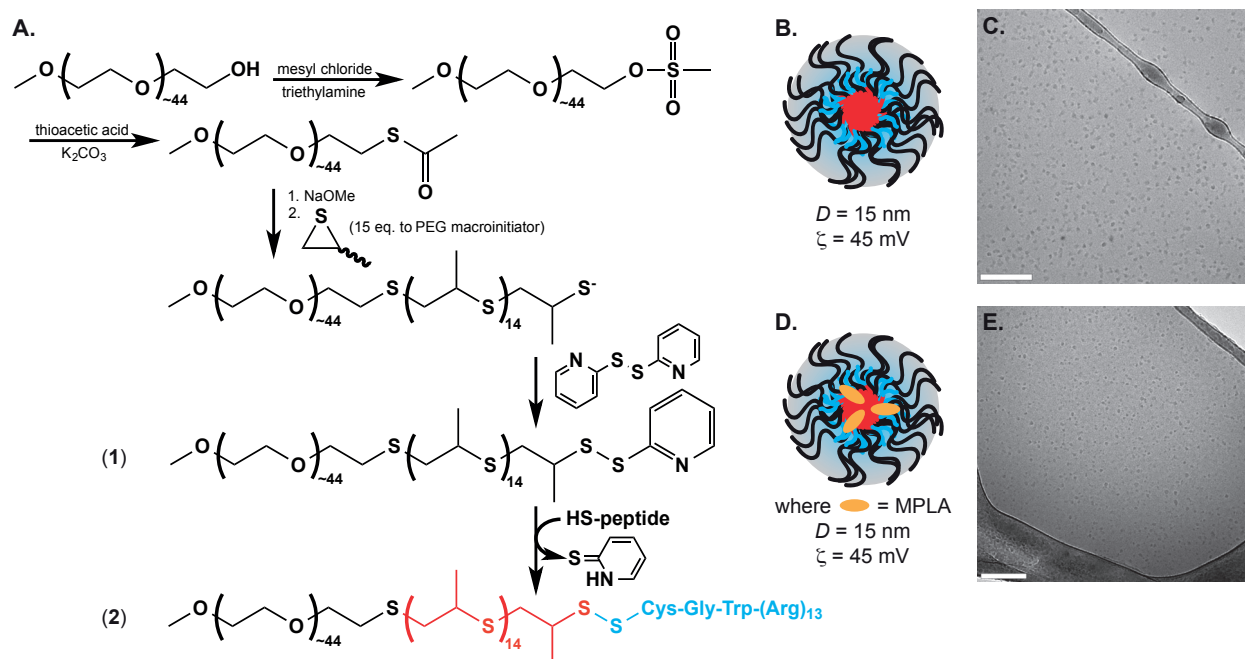
### 5.4.1. Preparation and characterization of cationic micelles and micellar aggregates.

As shown in Figure 1A, PEG-PPS diblock copolymer (**1**) was obtained by ring opening polymerization of propylene sulfide from a thioacetate-terminated poly(ethylene

glycol) macroinitiator, followed by PPS end-capping with pyridyl disulfide. Purity of the PEG-PPS diblock copolymer was verified by gel permeation chromatography (Supporting Information Figure S1). A simple disulfide exchange reaction with cysteine-containing polyarginine (degree of polymerization = 13) yielded the cationic peptide-conjugated copolymer PEG-PPS-R13 (**2**) utilized in these studies. The conjugate was insoluble in tetrahydrofuran, rendering impossible analysis by gel permeation chromatography. PEG-PPS-R13 molecular weight was assessed by MALDI mass spectrometry (Supporting Information Figure S2) and peptide conjugation to the copolymer was confirmed by FTIR spectroscopy (Supporting Figure S3). PEG-PPS-R13 self-assembly into stable micelles was mediated by water-excluding hydrophobic interactions of the PPS domain; the charged R13 peptide domain partitions into the hydrophilic PEG corona upon micelle formation (Figure 1B). Naked micelles displayed the anticipated size, charge, and topological characteristics; they are nanoscale spherical particles of significant positive charge (Figure 1B,C). Addition of MPLA to PEG-PPS-R13 during micelle formation yielded adjuvant-loaded constructs in which amphiphilic MPLA partitions between the hydrophilic corona and the hydrophobic core. Electrostatic interactions between cationic PEG-PPS-R13 and anionic MPLA promoted tighter molecular packing within the formed micelle, as confirmed by slightly decreased particle diameter (Figure 1D). As anticipated, MPLA incorporation did not interfere with self-assembly of spherical micelles (Figure 1E).


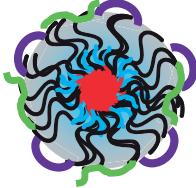

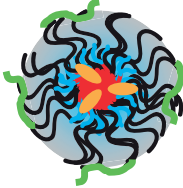
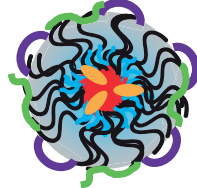



Following physical characterization of PEG-PPS-R13 micelle and MPLA-loaded PEG-PPS-R13 micelle populations, we prepared the ensemble of aggregate species designed for vaccination studies. In addition to acting as an encapsulation platform for MPLA, the cationic micelle drove electrostatic association of anionic whole protein antigen OVA and anionic CpG-B adjuvant. The assemblies were generated by simple mixing of previously prepared micelle or MPLA-loaded micelle dispersions with aqueous solutions of OVA and/or CpG-B. This highlights one of the benefits of our assembly-driven approach; once formed, the unmodified or MPLA-loaded cationic micelles represent a modular platform to which multiple vaccine components may be added, for easy, rapid, and sterile preparation of treatment samples and control groups. The basic structure, particle size, and zeta potential of the formed aggregates are presented in Table 1. Notably, the diameters of the micelle aggregates are

approximately one order of magnitude smaller than cationic PEG-polypeptide micelles examined elsewhere for OVA vaccination,<sup>24</sup> and we anticipated that this decreased size would facilitate particle trafficking. Upon association of OVA and/or CpG-B, the spherical particle increased only slightly in diameter; similarly, association of these negatively charged molecules decreased particle zeta potential. Nevertheless, charge behavior in these assemblies remained distinctly cationic. By promoting interaction with negatively charged cell surfaces, this biophysical characteristic may benefit particle uptake by APCs following administration. The ensemble of assembly species was divided for use in two *in vivo* vaccination studies, to characterize micelle performance in the context of vaccination with a single adjuvant (either MPLA or CpG-B) and vaccination with two adjuvants (both MPLA and CpG-B).



**Figure 1.** A polyarginine peptide-conjugated poly(ethylene glycol)-b-poly(propylene sulfide) (PEG-PPS) block copolymer forms cationic micelles following self-assembly. (A) Synthetic methodology for preparation of the peptide-conjugated copolymer PEG-PPS-R13. (B) Emulsion solvent evaporation promotes self-assembly of cationic PEG-PPS-R13 micelles. (C) Cryo transmission electron microscopy (cryoTEM) of PEG-PPS-R13 micelles. (D) Emulsion solvent evaporation of PEG-PPS-R13 in the presence of amphiphilic monophosphoryl lipid A (MPLA) yields MPLA-loaded micelles. (E) CryoTEM confirmed that MPLA incorporation does not interfere with formation of micelle populations. Scale bars, 200 nm.

**Table 1.** Physical characteristics of cationic micelle complexes used in vaccination

micelle + OVA	micelle + OVA + CpG-B	micelle / MPLA + OVA	micelle / MPLA + CpG-B	micelle / MPLA + OVA + CpG-B
				
where  = MPLA,  = ovalbumin (OVA), and  = CpG-B (not to scale)				
$D = 13 \text{ nm}$	$24 \text{ nm}$	$14 \text{ nm}$	$13 \text{ nm}$	$14 \text{ nm}$
$\zeta = 26 \text{ mV}$	$21 \text{ mV}$	$44 \text{ mV}$	$34 \text{ mV}$	$23 \text{ mV}$
Singly-adjuvanted study			Doubly-adjuvanted study	

#### 5.4.2. Singly-adjuvanted vaccination utilizing cationic micelles enhances cytotoxic responses in spleen- and lymph node-resident CD8<sup>+</sup> T cells.

The design of effective vaccine platforms requires that antigen reaches the secondary lymphoid organs for local presentation to lymphocytes by APCs. Induction of immune responses was evaluated in the spleen and LNs of mice vaccinated with a prime/boost/boost immunization scheme (Fig. 2A). Mice were vaccinated with cationic micelle assemblies presenting whole OVA antigen and CpG-B or MPLA (Table 1). The following groups were utilized as controls: micelle assemblies with OVA and without CpG-B, and free OVA antigen mixed with either CpG-B or MPLA. The negative (injection) control group received saline. Spleen and LNs were harvested one week after second boost and evaluated for activation within the CD8<sup>+</sup> and CD4<sup>+</sup> T cell compartments.

The cytotoxic activity of spleen- and LN-resident CD8<sup>+</sup> T cells (i.e., CTLs) was evaluated after 6 hr ex vivo SIINFEKL restimulation, as defined by intracellular staining of IFN $\gamma$ - and TNF $\alpha$ -secreting CD8<sup>+</sup> T cells. As seen in representative splenocyte flow cytometry analysis, immunization with micelle + OVA + CpG-B raised the largest population of IFN $\gamma$ <sup>+</sup> (Figure 2B, top row) and TNF $\alpha$ <sup>+</sup> (Figure 2B, bottom row) CD8<sup>+</sup> T cells. Notably, vaccination with micelle + OVA + CpG-B resulted in a population of splenic IFN $\gamma$ <sup>+</sup> CD8<sup>+</sup> T cells 3-fold larger than that derived from mice vaccinated with micelle / MPLA + OVA. This demonstrates a clear advantage of the CpG-B adjuvant compared to MPLA in the single-adjuvant study.



Furthermore, the use of micelles is necessary for enhanced induction of cytotoxic responses, as observed by minimal cytokine expression in the OVA + CpG-B and OVA + MPLA groups lacking micelle carriers. Our findings indicate that maximum stimulation of CD8<sup>+</sup> T cell cytotoxicity is achieved by micelles bearing the adsorbed OVA antigen and CpG-B. These conclusions are supported by recent vaccination studies that characterized improved CD8<sup>+</sup> T cell responses following dual delivery of polymer micelle-conjugated OVA with electrostatically complexed CpG-B.<sup>25</sup> We achieve similar results without the need for covalent conjugation of the OVA antigen.

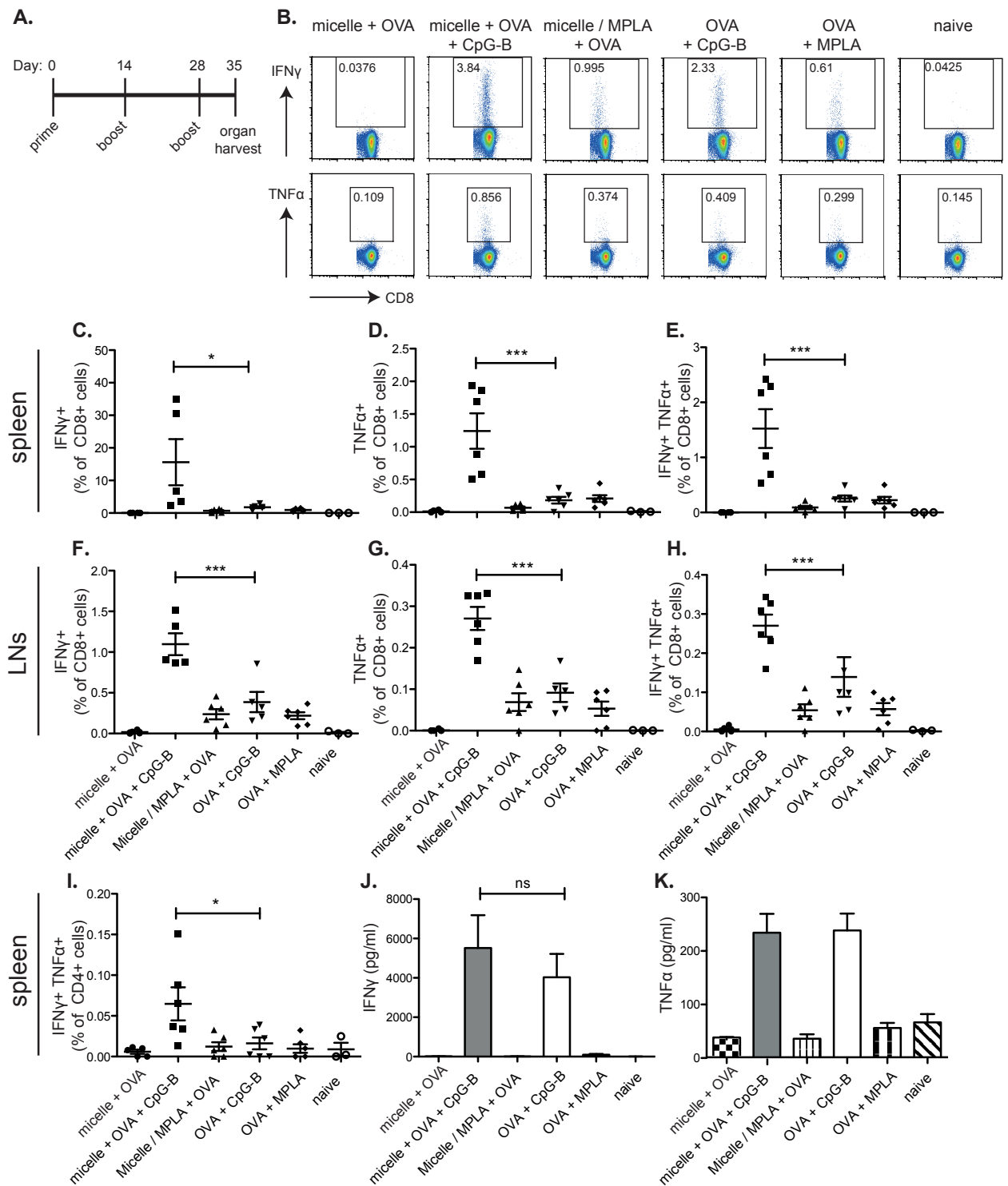
Expanding from this representative data, IFN $\gamma$  and TNF $\alpha$  secretion from spleen-resident CD8<sup>+</sup> T cells in all groups are presented in Figure 2C and 2D, respectively. Vaccination with micelle + OVA + CpG-B generated an 8-fold increase in CD8<sup>+</sup> T cell IFN $\gamma$  secretion and a 6-fold increase in CD8<sup>+</sup> T cell TNF $\alpha$  secretion, compared to the micelle-free OVA + CpG group. The remaining groups yielded negligible cytokine secretion in splenic CD8<sup>+</sup> T cells. Of particular interest in vaccine design are polyfunctional T cells, those positive for simultaneous secretion of multiple cytokines. The population of polyfunctional splenic CD8<sup>+</sup> T cells secreting both IFN $\gamma$  and TNF $\alpha$  was 6-fold greater in mice immunized with micelle + OVA + CpG-B compared with OVA + CpG-B (Figure 2E).

We similarly analyzed the profile of activated LN-resident CD8<sup>+</sup> T cells from all vaccinated mice; these data were consistent with observations from splenic populations. Compared with the micelle-free OVA + CpG-B group, vaccination with micelle + OVA + CpG-B promoted a 3-fold increase in the percentage of IFN $\gamma$ <sup>+</sup> (Figure 2F) and TNF $\alpha$ <sup>+</sup> (Figure 2G) CD8<sup>+</sup> T cells. Following trends observed in splenocyte populations, the remaining groups displayed minimal CD8<sup>+</sup> T cell cytotoxicity. Furthermore, in mice vaccinated with micelles + OVA + CpG-B, polyfunctional CD8<sup>+</sup> T cells were increased 3-fold compared to OVA + CpG-B-vaccinated mice and 5-fold compared with mice vaccinated with either micelle / MPLA + OVA or OVA + MPLA (Figure 2H).

Induction of cytotoxic CD8<sup>+</sup> T cells is particularly desirable in the context of protein-based subunit vaccination. Furthermore, CTLs play a major role in tumor eradication and clearance of pathogen-infected cells.<sup>2</sup> As a result, current vaccine design seeks to

elicit strong CD8<sup>+</sup> T cell responses for the prevention or treatment of tumor malignancies, and for elimination of cellular infection characterized by solely intracellular presentation of pathogen-derived antigen, which cannot be influenced by circulating antibodies. To be effective, these vaccines must induce activation and expansion of antigen-specific CD8<sup>+</sup> T cells, by promoting antigen loading onto MHC class I molecules and antigen cross-presentation to CD8<sup>+</sup> T cells by APCs.<sup>26</sup> In support of such desirable outcomes, our results show that the cationic micelle-based vaccine platform promotes efficient CD8<sup>+</sup> T cell cross-priming and activity. These findings underline the significant advantage of the nanoscale micelle carrier over micelle-free subunit vaccination. Indeed, in the context of cancer vaccine technologies<sup>27</sup> and vaccination against clinically challenging viral infections,<sup>28</sup> the benefits of nanoparticle carriers are already recognized.

Based on the requirement of CD4<sup>+</sup> T cell help in CD8<sup>+</sup> T cell activation and promotion of humoral responses, we evaluated the capacity of our micelle platform to activate CD4<sup>+</sup> T cells obtained from the spleen and LNs of vaccinated mice. Lymphocytes from both organs underwent overnight *ex vivo* restimulation with OVA antigen, and IFN $\gamma$  and TNF $\alpha$  cytokine secretion was determined by flow cytometry. As in CD8<sup>+</sup> T cell responses, combined IFN $\gamma$  and TNF $\alpha$  secretion in the micelles + OVA + CpG-B group was significantly higher than any other group (Figure 2I). However, the overall percentage of these double-positive cells was lower in the CD4<sup>+</sup> population (Figure 2I) versus the CD8<sup>+</sup> population (Figure 2E). In further analysis, harvested splenocytes were restimulated for 4 days with OVA, for ELISA measurement of cytokine secretion in the supernatant. Only the groups vaccinated with micelle + OVA + CpG-B and OVA + CpG-B secreted IFN $\gamma$  after restimulation, but no significant differences were measured between the two groups (Figure 2J). Similar results were observed in TNF $\alpha$  secretion (Figure 2K) and in LN restimulation (data not shown). Although present, the activation of CD4<sup>+</sup> T cells by the micelle platform is less efficient when compared to strong activation of CD8<sup>+</sup> T cells, suggesting significant cross-presentation of processed OVA antigen to CD8<sup>+</sup> T cells.



**Figure 2.** Cationic micelles electrostatically complex whole protein antigen ovalbumin (OVA) and CpG-B adjuvant to enhance cytotoxic T lymphocyte (CTL) responses in mouse spleen and lymph nodes (LNs) following singly-adjuvanted vaccination. (A) Immunization schedule; female C57BL/6 mice were immunized on day 0, 14, and 28 by intradermal injection. Spleen and LNs were harvested for processing one week after second boost. (B) The cellular cytotoxicity in all groups restimulated for 6 hrs with SIINFEKL peptide was determined by intracellular staining of IFN $\gamma$  and TNF $\alpha$  and measured by flow cytometry. Representative plots with positive gating on IFN $\gamma$  (top) or TNF $\alpha$  (bottom) populations of splenic CD8 $^+$  cells. (C, D, and E) Average cytokine secretion of splenocytes following 6 hr SIINFEKL restimulation and

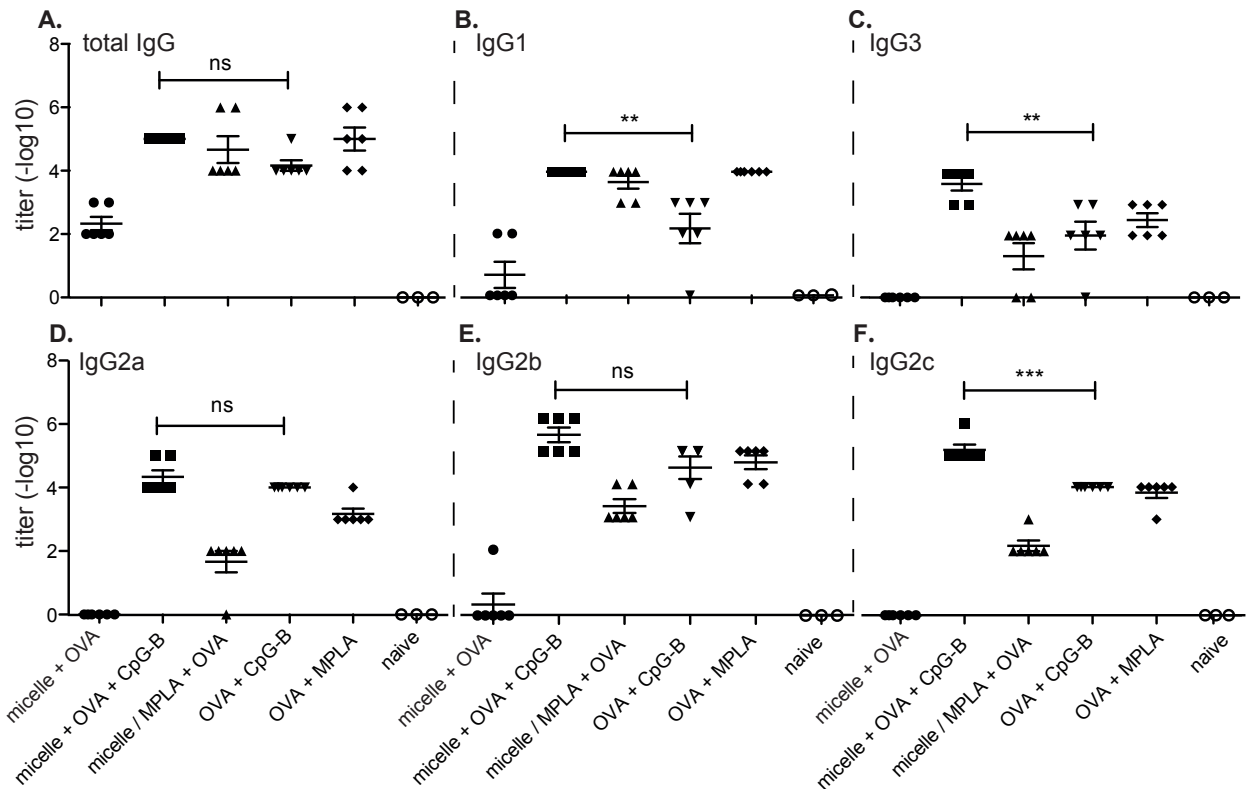
intracellular staining for (C) IFN $\gamma^+$  (D) TNF $\alpha^+$  and (E) polyfunctional IFN $\gamma^+$  TNF $\alpha^+$  cells, as determined by flow cytometry. This analysis was performed on live populations gated on CD3 $^+$  CD8 $^+$  cells. (F, G, and H) Average cytokine secretion in LN lymphocytes following 6 hr SIINFEKL restimulation. This analysis was performed on live populations gated on CD3 $^+$  CD8 $^+$  cells, with staining for (F) IFN $\gamma^+$ , (G) TNF $\alpha^+$  and (H) polyfunctional IFN $\gamma^+$  TNF $\alpha^+$  cells. (I) Splenocytes were restimulated with OVA antigen overnight and cytokine secretion was measured by flow cytometry. Polyfunctional IFN $\gamma^+$  TNF $\alpha^+$  cells were gated on live CD3 $^+$  CD4 $^+$  populations. (J and K) Splenocytes were cultured *ex vivo* with OVA antigen for 4 days and (J) IFN $\gamma$  and (K) TNF $\alpha$  secretion in supernatant was determined by ELISA. \* $p < 0.05$ , \*\*\* $p < 0.0001$ . Additional statistical relationships removed for clarity.

#### **5.4.3. Singly-adjuvanted vaccination with cationic micelles induces humoral responses.**

The protective efficacy of a vaccine for infectious disease is substantially conferred by antigen-specific antibody production. By examining IgG subclasses, we evaluated the character of OVA-specific antibody production mediated by use of micelle assemblies. At the conclusion of the experiment, analysis of antibody titers identified equivalent levels of OVA-specific total IgG in the sera of mice vaccinated with either CpG-B or MPLA adjuvant (Fig. 3A). In contrast, analysis of IgG subtype distribution revealed significantly increased IgG1 (Fig. 3B) and IgG3 (Fig. 3C) secretion in the micelle + OVA + CpG-B group, compared to free OVA + CpG-B. When comparing groups vaccinated with micelle / MPLA + OVA versus free OVA + MPLA, we observed similarly elevated IgG1 titers (Fig. 3B), while IgG3 responses were similarly limited (Fig. 3C). These findings are in agreement with proposed temporal models of antibody class switching in response to protein antigen, in which early IgG3 production is subsequently replaced by higher affinity IgG1.<sup>29, 30</sup> Both IgG3 and IgG1 are implicated in immune response to viral infection,<sup>31</sup> and together our results suggest a beneficial role of the cationic micelle platform in future viral vaccination applications.

Subtype analysis revealed robust antibody secretion in the micelle + OVA + CpG-B group in IgG2a (Fig. 3D), IgG2b (Fig. 3E) and IgG2c (Fig. 3F) subtypes. In IgG2a and IgG2b, no significant differences were observed upon comparison to titers in the micelle-free OVA + CpG-B group; however, these differences were significant in the IgG2c subtype. Vaccination with micelle / MPLA + OVA produced limited IgG2 class antibody secretion, with titers lower than the micelle-free MPLA + OVA group for all subtypes. These results indicate an advantage of the micelle + OVA + CpG-B platform

in antigen-specific antibody production, when compared to both the MPLA-presenting micelle platform and the free antigen mixed with either adjuvant. In a previous study, CpG-B incorporated into PLGA nanospheres was found to stimulate IgG1, IgG2b, and IgG3 production following vaccination against tetanus toxoid.<sup>32</sup> In the context of micelle-mediated OVA vaccination using CpG-B adjuvant, we achieved similar IgG1, IgG2b, and IgG3 expression profiles, along with enhanced IgG2c.



**Figure 3.** Post-vaccination IgG titers highlight strong humoral responses in mice injected with CpG-B. Total IgG and subtype titers in the serum of all vaccinated mice as measured by ELISA on day 35 of the experiment. (A) Total IgG titers of all mice in all groups. (B) IgG1, (C) IgG3, (D) IgG2a, (E) IgG2b, and (F) IgG2c subtypes in all groups. \*\* $p < 0.001$ , \*\*\* $p < 0.0001$ . Additional statistical relationships removed for clarity.

#### 5.4.4. Doubly-adjuvanted vaccination does not provide additive effect of the two adjuvants.

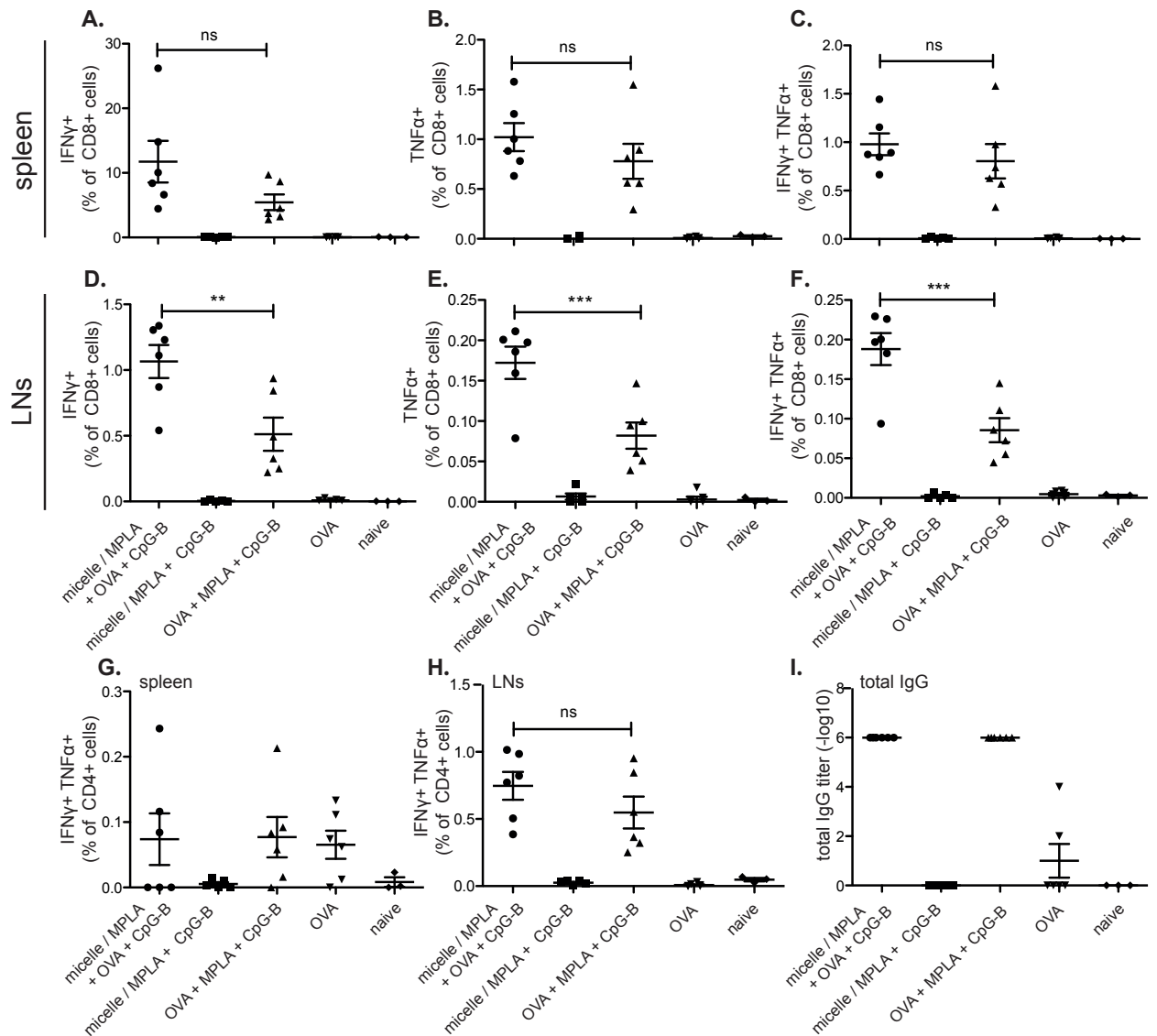
We hypothesized that vaccination with two adjuvants in combination would provide an additive effect, resulting in improved humoral and cellular responses compared to vaccination with a single adjuvant. Following the same immunization schedule, mice were vaccinated with micelle / MPLA + OVA + CpG-B or the corresponding micelle-free group, OVA + MPLA + CpG-B. Cytokine secretion from lymphocytes was

assessed following *ex vivo* restimulation with SIINFEKL or OVA. This assessment showed that use of the CpG-B- and MPLA-presenting micelle platform retains the advantage of enhanced cytotoxicity when compared to a micelle-free treatment. However, an additive effect was only observed in the micelle-free OVA + MPLA + CpG-B group, and not in the doubly-adjuvanted, OVA-presenting group utilizing the micelle carrier (Figure 4). The strong response provided by micelle-associated CpG seems to render any additional benefit due to incorporated MPLA comparatively small.

As a main readout for cytotoxic activity, we measured IFN $\gamma$  and TNF $\alpha$  cytokine secretion of CD8<sup>+</sup> T cells obtained from the spleen and LNs of vaccinated mice, following 6 hr restimulation with SIINFEKL peptide. Enhanced populations of IFN $\gamma$ <sup>+</sup> (Figure 4A) and TNF $\alpha$ <sup>+</sup> (Figure 4B) CD8<sup>+</sup> T cells were observed in the micelle / MPLA + OVA + CpG-B group, however these lacked significant improvement over the micelle-free OVA + MPLA + CpG-B group. Interestingly, cytotoxicity of the micelle-free group is improved compared with the singly-adjuvanted groups of OVA + CpG-B and OVA + MPLA described in Figure 3. This indicates additive benefit of double adjuvants only in micelle-free vaccination, and not in micelle-antigen-adjuvant aggregates. Moreover, polyfunctional IFN $\gamma$ <sup>+</sup> TNF $\alpha$ <sup>+</sup> splenic CD8<sup>+</sup> T cell populations remained higher but without significant differences compared to the OVA + MPLA + CpG-B group (Figure 4C). However, significantly enhanced cytokine production in micelle versus micelle-free doubly-adjuvanted groups was observed in lymph node-derived CD8<sup>+</sup> T cells of vaccinated mice, in which a 2-fold increase of IFN $\gamma$ <sup>+</sup> (Fig. 4D), TNF $\alpha$ <sup>+</sup> (Fig. 4E) and IFN $\gamma$ <sup>+</sup> TNF $\alpha$ <sup>+</sup> (Fig. 4F) CD8<sup>+</sup> T cells was measured between the two groups. The additive effect of two adjuvants remained absent in LNs following micelle-mediated vaccination.

Following overnight restimulation with OVA, minimal cytokine production was observed in CD4<sup>+</sup> T cells derived from spleen and LNs of vaccinated mice. The percentage of IFN $\gamma$ <sup>+</sup> TNF $\alpha$ <sup>+</sup> spleen CD4<sup>+</sup> T cells was identical between the micelle, the micelle-free and OVA-only groups, indicating inefficient activation of this cell type (Figure 4G). Higher percentages of activated CD4<sup>+</sup> T cells were measured in the LNs of mice vaccinated with micelle / MPLA + OVA + CpG-B, but the comparison with the OVA + MPLA + CpG-B group was not significant (Figure 4H). To further evaluate the systemic responses raised by micelle-mediated vaccination, we measured serum

antibody titers: equally high total IgG titers were measured in both micelle and micelle-free groups (Figure 4I), consistent with results obtained from cytokine analysis within CD4<sup>+</sup> T cell populations. The same IgG subtypes analyzed in the singly adjuvanted study were examined here; although antibody levels were high in groups immunized with CpG-B- and MPLA- adjuvanted OVA antigen, no significant differences were observed between groups immunized in the presence or absence of the micelle carrier (Supporting Information Figure S4). We conclude that adjuvant co-administration does not have an additive effect in the context of the micelle platform; as such, singly-adjuvanted micelle-antigen aggregates are sufficient to raise potent cytotoxic CD8<sup>+</sup> T cells and support induction of humoral responses. Previously, in a non-vaccination model, collaborative efforts by our group have shown that co-administration of MPLA and CpG-B in mouse increases inflammatory cytokine concentrations in bronchoalveolar lavage and blood serum.<sup>33</sup> Yet in vaccination studies elsewhere, MPLA was determined to have no additive effect when used in conjunction with alum.<sup>34</sup> Thus the role of adjuvant synergistic effect in vaccination remains poorly defined, and may depend on unaccounted factors such as variable immunization timelines or route of administration.



**Figure 4.** Cationic micelle-mediated co-administration of ovalbumin, CpG-B, and MPLA promotes cellular responses to doubly-adjuvanted vaccination against the whole protein antigen. Mice were vaccinated according to the same immunization schedule, with spleen and LNs harvested on day 35. Cells were restimulated with SIINFEKL peptide or OVA antigen. Cytokine secretion was measured by flow cytometry. (A) IFN $\gamma^+$ , (B) TNF $\alpha^+$  and (C) polyfunctional IFN $\gamma^+$  TNF $\alpha^+$  splenocytes gated on live CD3 $^+$  CD8 $^+$  cells after 6 hr SIINFEKL restimulation. (D) IFN $\gamma^+$ , (E) TNF $\alpha^+$  and (F) polyfunctional IFN $\gamma^+$  TNF $\alpha^+$  lymph node isolates, gated on live CD3 $^+$  CD8 $^+$  populations after 6 hr SIINFEKL restimulation. (G) Spleen and (H) LNs were restimulated overnight with OVA antigen and polyfunctional IFN $\gamma^+$  TNF $\alpha^+$  cells were gated on live CD3 $^+$  CD4 $^+$  populations. (I) Total IgG serum titers of all vaccinated mice on day 35 of the experiment measured by ELISA. \*\* $p < 0.01$ , \*\*\* $p < 0.0001$ . Additional statistical relationships were removed for clarity.



## 5.6. Conclusions

Here we have undertaken a simplified approach to nanoparticle vaccine formulation, utilizing molecular encapsulation and complexation to eliminate the need for covalent modification of vaccine components. Once assembled, unloaded and MPLA-loaded PEG-PPS-R13 micelles provide a modular platform for streamlined vaccine preparation. The application of PEG-PPS-R13 micelles for co-administration of OVA and CpG-B achieves meaningful vaccination outcomes through both humoral responses (enhanced production of multiple, OVA-specific IgG subtypes) and cellular responses (increased populations of cytokine-producing CTLs). Micelle-mediated delivery also eliminates the need for double adjuvants, simplifying platform preparation and reducing cost. The cationic micelle complex joins a family of nanoparticle vaccine platforms including virus-like particles,<sup>35</sup> polymer-based nanoparticles,<sup>36, 37</sup> and liposomal vesicles<sup>38</sup> characterized by notable enhancement of CD8<sup>+</sup> T cell responses. Along with the quality of humoral responses desired of a subunit vaccine, this characteristic promotes future examination of the PEG-PPS-R13 micelle carrier in cancer vaccine development and in prophylactic vaccination against viral infection.

## References

1. Cheever, M. A.; Higano, C. S. PROVENGE (Sipuleucel-T) in Prostate Cancer: The First FDA-Approved Therapeutic Cancer Vaccine. *Clin. Cancer. Res.* **2011**, *17*, 3520-3526.
2. Appay, V.; Douek, D. C.; Price, D. A. CD8<sup>+</sup> T Cell Efficacy in Vaccination and Disease. *Nat. Med.* **2008**, *14*, 623-628.
3. Nabel, G. J. Global Health Designing Tomorrow's Vaccines. *New Engl. J. Med.* **2013**, *368*, 551-560.
4. Plotkin, S. A. Vaccines: The Fourth Century. *Clin. Vaccine Immunol.* **2009**, *16*, 1709-1719.
5. Moyle, P. M.; Toth, I. Self-Adjuvanting Lipopeptide Vaccines. *Curr. Med. Chem.* **2008**, *15*, 506-516.
6. Moyle, P. M.; Toth, I. Modern Subunit Vaccines: Development, Components, and Research Opportunities. *ChemMedChem* **2013**, *8*, 360-376.

7. Takeda, K.; Kaisho, T.; Akira, S. Toll-Like Receptors. *Annu. Rev. Immunol.* **2003**, *21*, 335-376.
8. Awate, S.; Babiuk, L. A.; Mutwiri, G. Mechanisms of Action of Adjuvants. *Front. Immunol.* **2013**, *4*, 1-10.
9. Kumar, H.; Kawai, T.; Akira, S. Pathogen Recognition by the Innate Immune System. *Int. Rev. Immunol.* **2011**, *30*, 16-34.
10. Kobayashi, H.; Horner, A. A.; Takabayashi, K.; Nguyen, M. D.; Huang, E.; Cinman, N.; Raz, E. Immunostimulatory DNA Pre-Priming: A Novel Approach for Prolonged Th1-Biased Immunity. *Cell. Immunol.* **1999**, *198*, 69-75.
11. Mata-Haro, V.; Cekic, C.; Martin, M.; Chilton, P. M.; Casella, C. R.; Mitchell, T. C. The Vaccine Adjuvant Monophosphoryl Lipid A as a TRIF-Biased Agonist of TLR4. *Science* **2007**, *316*, 1628-1632.
12. Swartz, M. A.; Hirosue, S.; Hubbell, J. A. Engineering Approaches to Immunotherapy. *Sci. Transl. Med.* **2012**, *4*, 148rv149.
13. Zhao, L.; Seth, A.; Wibowo, N.; Zhao, C.-X.; Mitter, N.; Yu, C.; Middelberg, A. P. J. Nanoparticle Vaccines. *Vaccine* **2014**, *32*, 327-337.
14. Taki, A.; Smooker, P. Small Wonders - the Use of Nanoparticles for Delivering Antigen. *Vaccines* **2015**, *3*, 638-661.
15. Irvine, D. J.; Hanson, M. C.; Rakhra, K.; Tokatlian, T. Synthetic Nanoparticles for Vaccines and Immunotherapy. *Chem. Rev.* **2015**, *Article ASAP*, 10.1021/acs.chemrev.1025b00109.
16. Irvine, D. J.; Swartz, M. A.; Szeto, G. L. Engineering Synthetic Vaccines Using Cues from Natural Immunity. *Nat. Mater.* **2013**, *12*, 978-990.
17. Rosenthal, J. A.; Chen, L.; Baker, J. L.; Putnam, D.; DeLisa, M. P. Pathogen-Like Particles: Biomimetic Vaccine Carriers Engineered at the Nanoscale. *Curr. Opin. Biotechnol.* **2014**, *28*, 51-58.
18. Reddy, S. T.; van der Vlies, A. J.; Simeoni, E.; Angeli, V.; Randolph, G. J.; O'Neil, C. P.; Lee, L. K.; Swartz, M. A.; Hubbell, J. A. Exploiting Lymphatic Transport and Complement Activation in Nanoparticle Vaccines. *Nat. Biotechnol.* **2007**, *25*, 1159-1164.
19. Stano, A.; van der Vlies, A. J.; Martino, M. M.; Swartz, M. A.; Hubbell, J. A.; Simeoni, E. PPS Nanoparticles as Versatile Delivery System to Induce Systemic and Broad Mucosal Immunity after Intranasal Administration. *Vaccine* **2011**, *29*, 804-812.
20. Ballester, M.; Nembrini, C.; Dhar, N.; de Titta, A.; de Piano, C.; Pasquier, M.; Simeoni, E.; van der Vlies, A. J.; McKinney, J. D.; Hubbell, J. A.; Swartz, M. A. Nanoparticle Conjugation and Pulmonary Delivery Enhance the Protective Efficacy of Ag85B and CpG against Tuberculosis. *Vaccine* **2011**, *29*, 6959-6966.

21. Stano, A.; Scott, E. A.; Dane, K. Y.; Swartz, M. A.; Hubbell, J. A. Tunable T Cell Immunity Towards a Protein Antigen Using Polymersomes Vs. Solid-Core Nanoparticles. *Biomaterials* **2013**, *34*, 4339-4346.
22. de Titta, A.; Ballester, M.; Julier, Z.; Nembrini, C.; Jeanbart, L.; van der Vlies, A. J.; Swartz, M. A.; Hubbell, J. A. Nanoparticle Conjugation of CpG Enhances Adjuvancy for Cellular Immunity and Memory Recall at Low Dose. *Proc. Natl. Acad. Sci. U. S. A.* **2013**, *110*, 19902-19907.
23. Eby, J. K.; Dane, K. Y.; O'Neil, C. P.; Hirosue, S.; Swartz, M. A.; Hubbell, J. A. Polymer Micelles with Pyridyl Disulfide-Coupled Antigen Travel through Lymphatics and Show Enhanced Cellular Responses Following Immunization. *Acta Biomater.* **2012**, *8*, 3210-3217.
24. Luo, Z.; Li, P.; Deng, J.; Gao, N.; Zhang, Y.; Pan, H.; Liu, L.; Wang, C.; Cai, L.; Ma, Y. Cationic Polypeptide Micelle-Based Antigen Delivery System: A Simple and Robust Adjuvant to Improve Vaccine Efficacy. *J. Controlled Release* **2013**, *170*, 259-267.
25. Wilson, J. T.; Keller, S.; Manganiello, M. J.; Cheng, C.; Lee, C.-C.; Opara, C.; Convertine, A.; Stayton, P. S. pH-Responsive Nanoparticle Vaccines for Dual-Delivery of Antigens and Immunostimulatory Oligonucleotides. *ACS Nano* **2013**, *7*, 3912-3925.
26. Kurts, C.; Robinson, B. W.; Knolle, P. A. Cross-Priming in Health and Disease. *Nat. Rev. Immunol.* **2010**, *10*, 403-414.
27. Silva, J. M.; Videira, M.; Gaspar, R.; Pr eat, V.; Florindo, H. F. Immune System Targeting by Biodegradable Nanoparticles for Cancer Vaccines. *J. Controlled Release* **2013**, *168*, 179-199.
28. Sokolova, V.; Westendorf, A. M.; Buer, J.; Uberla, K.; Epple, M. The Potential of Nanoparticles for the Immunization against Viral Infections. *J. Mater. Chem. B* **2015**, *3*, 4767-4779.
29. Collins, A. M.; Jackson, K. J. A Temporal Model of Human IgE and IgG Antibody Function. *Front. Immunol.* **2013**, *4*, 235.
30. Vidarsson, G.; Dekkers, G.; Rispens, T. IgG Subclasses and Allotypes: From Structure to Effector Functions. *Front. Immunol.* **2014**, *5*.
31. Ferrante, A.; Beard, L. J.; Feldman, R. G. IgG Subclass Distribution of Antibodies to Bacterial and Viral Antigens. *Pediatr. Infect. Dis. J.* **1990**, *9*, S16-24.
32. Diwan, M.; Tafaghodi, M.; Samuel, J. Enhancement of Immune Responses by Co-Delivery of a CpG Oligodeoxynucleotide and Tetanus Toxoid in Biodegradable Nanospheres. *J. Controlled Release* **2002**, *85*, 247-262.
33. Garcia-Cordero, J. L.; Nembrini, C.; Stano, A.; Hubbell, J. A.; Maerkl, S. J. A High-Throughput Nanoimmunoassay Chip Applied to Large-Scale Vaccine Adjuvant Screening. *Integrative Biology* **2013**, *5*, 650-658.

34. Pravetoni, M.; Vervacke, J. S.; Distefano, M. D.; Tucker, A. M.; Laudenschlager, M.; Pentel, P. R. Effect of Currently Approved Carriers and Adjuvants on the Pre-Clinical Efficacy of a Conjugate Vaccine against Oxycodone in Mice and Rats. *PLoS One* **2014**, *9*, e96547.
35. Speiser, D. E.; Schwarz, K.; Baumgaertner, P.; Manolova, V.; Devedev, E.; Sterry, W.; Walden, P.; Zippelius, A.; Conzett, K. B.; Senti, G.; Voelter, V.; Cerottini, J. P.; Guggisberg, D.; Willers, J.; Geldhof, C.; Romero, P.; Kundig, T.; Knuth, A.; Dummer, R.; Trefzer, U.; Bachmann, M. F. Memory and Effector CD8 T-Cell Responses after Nanoparticle Vaccination of Melanoma Patients. *J. Immunother.* **2010**, *33*, 848-858.
36. Wang, X.; Uto, T.; Akagi, T.; Akashi, M.; Baba, M. Induction of Potent CD8+ T-Cell Responses by Novel Biodegradable Nanoparticles Carrying Human Immunodeficiency Virus Type 1 gp120. *J. Virol.* **2007**, *81*, 10009-10016.
37. Nembrini, C.; Stano, A.; Dane, K. Y.; Ballester, M.; van der Vlies, A. J.; Marsland, B. J.; Swartz, M. A.; Hubbell, J. A. Nanoparticle Conjugation of Antigen Enhances Cytotoxic T-Cell Responses in Pulmonary Vaccination. *Proc. Natl. Acad. Sci. U. S. A.* **2011**, *108*, E989–E997.
38. Moon, J. J.; Suh, H.; Bershteyn, A.; Stephan, M. T.; Liu, H.; Huang, B.; Sohail, M.; Luo, S.; Ho Um, S.; Khant, H.; Goodwin, J. T.; Ramos, J.; Chiu, W.; Irvine, D. J. Interbilayer-Crosslinked Multilamellar Vesicles as Synthetic Vaccines for Potent Humoral and Cellular Immune Responses. *Nat. Mater.* **2011**, *10*, 243-251.
39. Napoli, A.; Tirelli, N.; Kilcher, G.; Hubbell, J. A. New Synthetic Methodologies for Amphiphilic Multiblock Copolymers of Ethylene Glycol and Propylene Sulfide. *Macromolecules* **2001**, *34*, 8913-8917.
40. Velluto, D.; Demurtas, D.; Hubbell, J. A. PEG-b-PPS Diblock Copolymer Aggregates for Hydrophobic Drug Solubilization and Release: Cyclosporin A as an Example. *Mol. Pharm.* **2008**, *5*, 632-642.

## Supporting Information

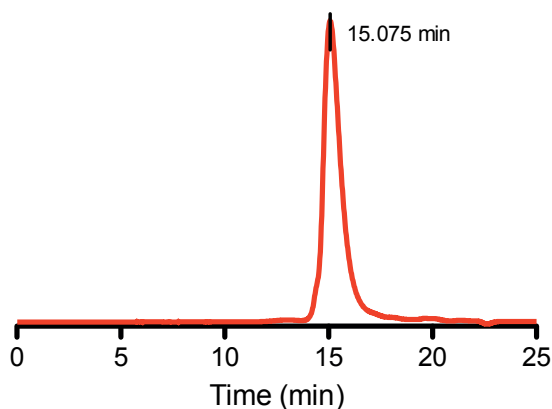


Figure S1. Gel permeation chromatography of PEG-PPS diblock copolymer, performed in tetrahydrofuran at 40°C with 1 mL/min flow rate.

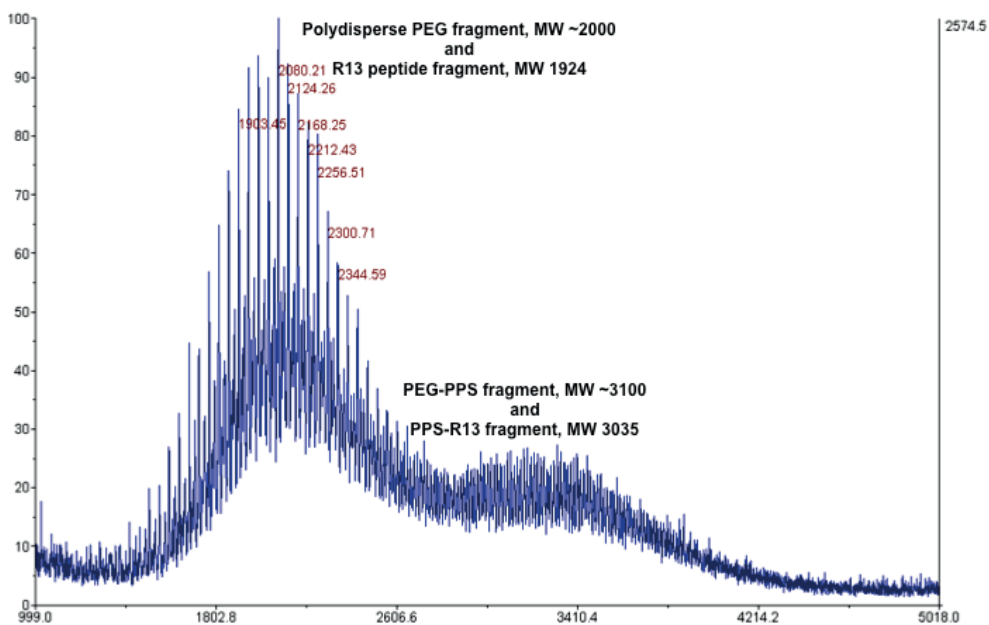


Figure S2. MALDI mass spectrometry of PEG-PPS-R13 polymer-peptide conjugate, performed in positive linear mode with CHCA matrix. Elevated laser power was necessary to induce molecular flight, resulting in fragmentation. Molecular weight of the resulting PEG-PPS-R13 fragments are indicated above.

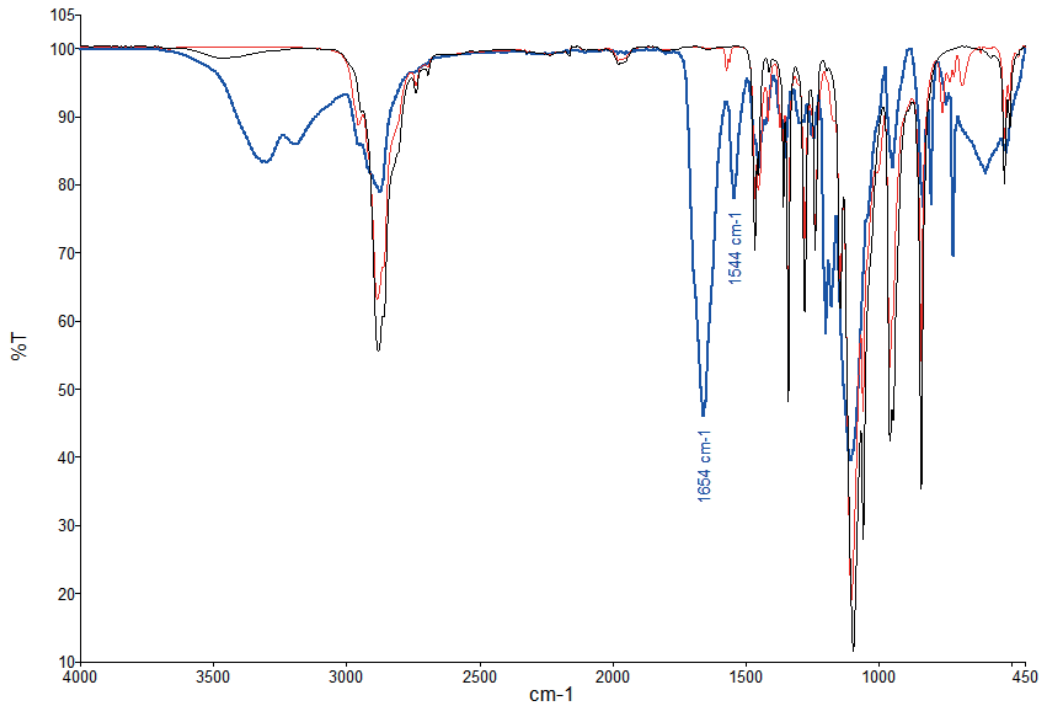


Figure S3. FTIR spectra of methoxyPEG-OH starting material (narrow black line), PEG-PPS (narrow red line), and PEG-PPS-R13 (bold blue line). The PEG-PPS-R13 spectrum shows the two characteristic amide I (1654 cm<sup>-1</sup>) and amide II (1544 cm<sup>-1</sup>) bands contributed by the R13 domain. N-H stretching vibrations in this domain also generate a broad band centered at 3300 cm<sup>-1</sup>.

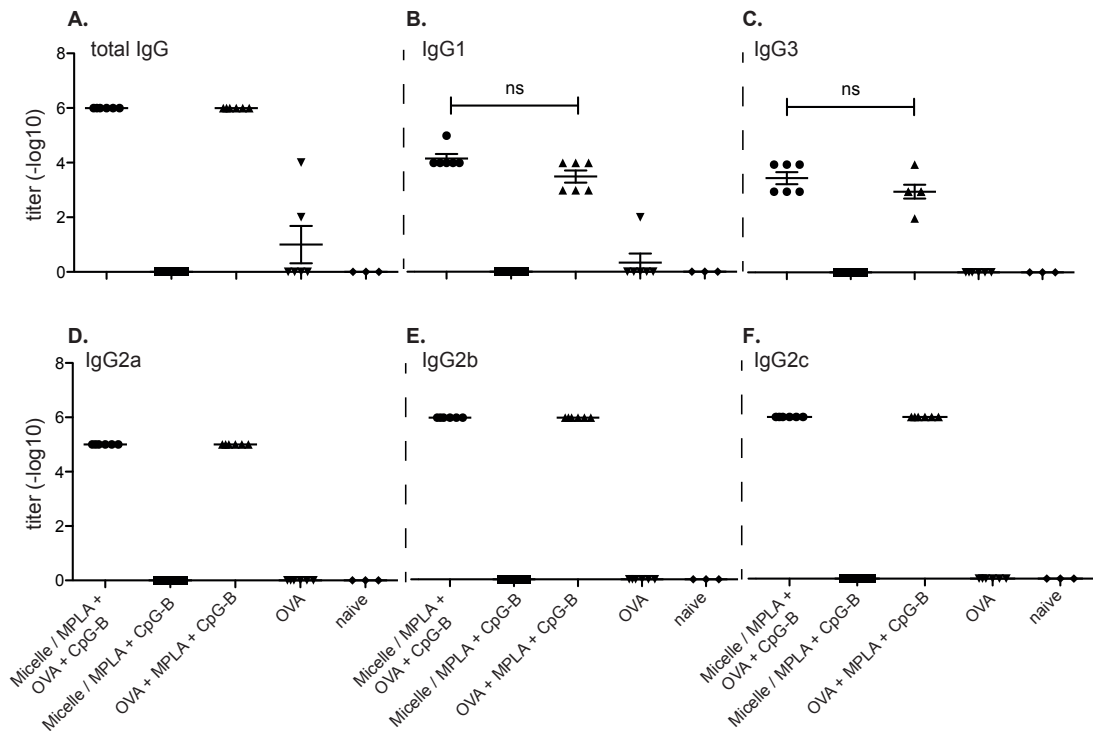


Figure S4. Post-vaccination IgG titers show no differences in subtype expression levels following micelle-mediated and micelle-free immunization in doubly-adjuvanted vaccination. Total IgG and subtype titers in serum of all vaccinated mice was measured by ELISA on day 35 of the doubly-adjuvanted experiment. (A) Total IgG titers, and titers of the (B) IgG1, (C) IgG3, (D) IgG2a, (E) IgG2b, and (F) IgG2c subtypes.

## **Chapter 6:**

### Conclusions and Future Directions

## 6.1 Conclusions

CD8<sup>+</sup> T cells are capable of recognizing and eliminating infected or transformed cells. Consequently, their activation is a primary goal of vaccine development for both infectious disease and cancer. Advances in our understanding of CD8<sup>+</sup> T cells, and in particular the cues that promote their activity, are revealing new pathways toward improved vaccine outcomes. Several studies in the past have resulted in important vaccine improvement technologies with promising results for CD8<sup>+</sup> T cell stimulation in vaccination [1-3]. However, despite these advances, effective vaccines against many pathogens, such as HIV and hepatitis C, and cancers, such as melanoma, remain significant unmet global health needs.

The generation of a robust CD8<sup>+</sup> T cell response requires the cross-priming of these cells by specialized cell types, to which the vaccine platform must efficiently deliver the antigen(s) of interest for processing and cross-presentation. Moreover, antigen delivery must occur under immunostimulatory conditions, in order to result in the activation, as opposed to tolerization, of relevant CD8<sup>+</sup> T cells [4]. The use of protein antigens in subunit vaccination poses fewer health risks than the use of live attenuated microbes. However, these antigens generally lack inherent immunogenicity and cell targeting properties. As such, effective design of subunit vaccines must incorporate additional means for efficient antigen delivery and immunostimulation. In this thesis, we have explored four different vaccine platforms for the activation of CD8<sup>+</sup> T cells and evaluated their efficacy in mouse models of liver infection and melanoma.

The first challenge was to develop a novel vaccine platform that can efficiently target the liver, cross-present the antigen to CD8<sup>+</sup> T cells and raise local antigen-specific immune responses with long-lasting memory. A tri-domain fusion protein was produced consisting of the erythrocyte-binding antibody TER119, OVA as a model antigen, and the BBOX domain of HMGB1 as an adjuvant (TER119-BBOX-OVA). TER119-BBOX-OVA co-administered with CpG-B elicited strong CTL responses intrahepatically. In particular, following a prime-boost vaccine schedule, TER119-BBOX-OVA + CpG-B resulted in a 6-fold higher level of IFN- $\gamma$  secretion in the liver of vaccinated mice compared with OVA + CpG vaccinations and in the clearance of



*Listeria* infected cells within 72 hr. More importantly, the activated CD8<sup>+</sup> T cells in the liver acquired a memory phenotype that lasted for at least 5 weeks. We hypothesized that the modular construction of this vaccine design, consisting of an erythrocyte-binding domain, an antigen of interest, and a BBOX adjuvant domain, will enable generation of recombinant vaccines for a variety of diseases of clinical relevance. For example, this vaccine may find application in malaria, where the mosquito bite infection resembles that of *Listeria* [5, 6]. Also, the direct activation of local hepatic responses against the antigen suggests that a TER119-BBOX-Ag immunization may be sufficient to deal with established liver infections, such as chronic hepatitis B, or liver carcinomas in therapeutic cancer vaccination.

A second approach for direct antigen targeting to cross-prime CD8<sup>+</sup> T cells is via delivery to a specific DC subset known to excel in cross-presentation, called CD8<sup>+</sup> DC. Cross-presenting DCs have been targeted by other groups via the XCL1 chemokine ligand that uniquely binds on their surface, as discussed earlier in Chapter 3. We improved the efficacy of the existing XCL1-targeting vaccine by introducing a novel molecule that attracted CD8<sup>+</sup> DCs at the injection site and promoted the uptake of the antigen. In particular, XCL1 was fused to a domain of PIGF-2 growth factor that binds the ECM with high affinity and was co-delivered with the XCL1-OVA fusion protein, used to activate CTLs in previous studies. The XCL1-OVA mixed with XCL1-PIGF vaccination improved by 1.5-fold the cytokine release compared to XCL1-OVA alone following a prime-boost immunization study and more importantly, significantly prolonged the survival of tumor bearing mice both in a prophylactic and a therapeutic approach. This last result is of particular interest since the main challenge with tumor vaccines is to find novel ways to vaccinate therapeutically and deal with established tumors [7]; without though underestimating the importance of prophylactic vaccination. Moreover, the results we observed in the aggressive and poorly immunogenic B16-F10 mouse tumor model further emphasize the effectiveness of this vaccine design [8].

We also examined the effect of forming a depot for antigen release as a possible inducer of T cell responses in vaccination. Slow release of an antigen has been a common approach mostly with biodegradable materials. In this thesis we attempted to create a depot effect by fusing the antigen to the PIGF-2 domain following the

hypothesis that retaining the antigen at the injection site would allow enhanced uptake by local DCs and would result in improved immunogenicity in the draining LNs. We evaluated our hypothesis by fusing OVA to PlGF-2 (OVA-PlGF) and measured the humoral and cellular responses following a regular vaccination protocol. Contrary to the hypothesis of our design, no significant benefit from binding to the ECM could be observed with OVA-PlGF vaccinations when compared to vaccinations with free OVA antigen. Possible improvement of this vaccine platform would require better understanding of the depot creation and the release kinetics of OVA-PlGF that possibly affect the peak timing of immune responses compared to free OVA.

Delivery vehicles are very commonly used for transportation of antigen to relevant immune organs. Of particular interest are nanocarriers that facilitate cross-priming and activation of CD8<sup>+</sup> T cells such as virus-like particles, polymer-based nanoparticles, and liposomes reviewed in the introduction and chapter 5. Here we explored a simplified approach to co-deliver unmodified antigen with adjuvants in a micelle-based vaccine platform. The micelle complexes were either loaded or not with encapsulated MPLA and co-administered with CpG-B and OVA in a single or double adjuvant vaccine platform. Following three consecutive intradermal injections, both humoral (enhanced production of multiple OVA-specific IgG subtypes) and cellular (increased populations of cytokine-producing CTLs) responses were observed in the group treated with micelles containing OVA and co-administered with a single CpG-B adjuvant, abolishing the need for double adjuvant administration for improved vaccination. This design achieves the highly desirable vaccination outcome of eliciting both CTL responses and neutralizing antibodies, which has been especially challenging for subunit vaccines. Furthermore, the use of unmodified antigens in this design will enable facile extension to other diseases. These characteristics promote future examination of the micelle carrier in cancer vaccine development and in prophylactic vaccination against viral infections.

Designing effective vaccine platforms is challenging and requires the collective effort of different fields in immunology and bioengineering. Improving the immunogenicity of a subunit vaccine by co-administering adjuvants and targeting the antigen to the appropriate cell type does not guarantee effective CTL responses or antibody production. One example of a commonly faced challenge in modern vaccine

design technology is related to lack of knowledge regarding the type of immune response that would result in the best long-term protection in several diseases. Moreover, searching the appropriate cell receptor for direct targeting of antigens to relevant immune cells is not always a straightforward approach. Finally, appropriate animal models that would accelerate the translation from the laboratory to the clinic are not widely available and more research needs to be focused towards this direction. We believe that the improvement of subunit vaccines will be a result of collective effort among different fields involved in vaccine design including optimal epitope and cell receptor selection [9, 10], characterization of the immunological pathways that follow a viral infection or tumor progress [11-13] and engineering of appropriate materials and molecules that will facilitate the initiation of an immune response [14-16].

## References

1. Speiser DE, Lienard D, Pittet MJ, et al. In vivo activation of melanoma-specific cd8(+) t cells by endogenous tumor antigen and peptide vaccines. A comparison to virus-specific t cells. *European Journal of Immunology* 2002;32(3): 731-41.
2. Mudd PA, Martins MA, Ericson AJ, et al. Vaccine-induced cd8(+) t cells control aids virus replication. *Nature* 2012;491(7422): 129-U52.
3. Koup RA, Douek DC. Vaccine design for cd8 t lymphocyte responses. *Cold Spring Harbor Perspectives in Medicine* 2011;1(1).
4. Chen LP, Flies DB. Molecular mechanisms of t cell co-stimulation and co-inhibition (vol 13, pg 27, 2013). *Nature Reviews Immunology* 2013;13(7).
5. Pope C, Kim SK, Marzo A, et al. Organ-specific regulation of the cd8 t cell response to listeria monocytogenes infection. (vol 166, pg 3402, 2001). *Journal of Immunology* 2001;166(9): 5840-.
6. Schmidt NW, Butler NS, Badovinac VP, et al. Extreme cd8 t cell requirements for anti-malarial liver-stage immunity following immunization with radiation attenuated sporozoites. *Plos Pathogens* 2010;6(7).
7. Speiser DE, Romero P. Molecularly defined vaccines for cancer immunotherapy, and protective t cell immunity. *Seminars in Immunology* 2010;22(3): 144-54.
8. Wang JL, Saffold S, Cao XT, et al. Eliciting t cell immunity against poorly immunogenic tumors by immunization with dendritic cell-tumor fusion vaccines. *Journal of Immunology* 1998;161(10): 5516-24.
9. Correia BE, Bates JT, Loomis RJ, et al. Proof of principle for epitope-focused vaccine design. *Nature* 2014;507(7491): 201-6.
10. Reddy ST, Georgiou G. Systems analysis of adaptive immunity by utilization of high-throughput technologies. *Current Opinion in Biotechnology* 2011;22(4): 584-9.
11. Palucka K, Banchereau J, Mellman I. Designing vaccines based on biology of human dendritic cell subsets. *Immunity* 2010;33(4): 464-78.
12. Mellman I, Coukos G, Dranoff G. Cancer immunotherapy comes of age. *Nature* 2011;480(7378): 480-9.
13. Hanahan D, Weinberg RA. Hallmarks of cancer: The next generation. *Cell* 2011;144(5): 646-74.

- 14.** Hubbell JA, Thomas SN, Swartz MA. Materials engineering for immunomodulation. *Nature* 2009;462(7272): 449-60.
- 15.** Irvine DJ, Hanson MC, Rakhra K, et al. Synthetic nanoparticles for vaccines and immunotherapy. *Chemical reviews*.
- 16.** Irvine DJ, Swartz MA, Szeto GL. Engineering synthetic vaccines using cues from natural immunity. *Nature Materials* 2013;12(11): 978-90.

# Curriculum Vitae

## VASILIKI PANAGIOTOU

[vasilikipana@gmail.com](mailto:vasilikipana@gmail.com)

(+41) 0788408942

Pre du Marche 38, 1004 Lausanne

### EDUCATION

**Ecole Polytechnic Federal Lausanne (EPFL), January 2011-November 2015** **Lausanne, Switzerland**  
Doctor of Philosophy in Biotechnology and Bioengineering.  
Laboratory of Prof. Jeffrey Hubbell. Thesis title: *Protein Engineering approaches for direct antigen targeting in CD8<sup>+</sup> T cell inducing vaccines*

**Massachusetts Institute of Technology (MIT), September 2008 - June 2010** **Cambridge, MA, USA**  
Master of Science in Chemical Engineering  
Laboratory of Prof. Christopher Love. Thesis title: *Clonal Selection and Characterization of Epigenetic Variation in Pichia Pastoris*

**Aristotle University of Thessaloniki, September 2006 - June 2008** **Thessaloniki, Greece**  
Master of Science in Applied Genetics and Biotechnology  
Laboratory of Prof. George Georgiou Thesis title: *Engineering a Humanized Catalytic Drug as a Cancer Therapeutic Agent*

**Aristotle University of Thessaloniki (AUTH), September 2001 - June 2006** **Thessaloniki, Greece**  
D.Eng., Department of Chemical Engineering.  
Laboratory of Prof. Prodromos Daoutidis. Thesis title: *Oscillation Behaviour of Dictyostelium Cells: Modelling & Robustness Analysis*

### RESEARCH EXPERIENCE

- **EPFL, Switzerland:**
  1. Independently designed 2 different vaccine platforms for effective tumor and virus killing in mice models
  2. Collaborated in the immunological characterization of a micelle based vaccine platform
  3. Search of posttranslational modifications of insulin in the islets of diabetic mice as a potential initiator mechanism in type 1 diabetes
- **MIT, USA:**  
Chemical mutagenesis of *Pichia pastoris* yeast and advanced single-cell screening looking for high secretion and top producing clones. Produced a 2.65-fold greater clone than those of the parental strain and the technology was patented by the MIT Technology Licensing Office (No14803).
- **University of Texas, Austin:**  
Use of recombinant DNA techniques to mutagenize a humanized catalytic enzyme that hydrolyzes L-Arginine in the blood and leads to death of hepatocellular carcinomas and melanomas.
- **AUTH, Greece:**  
Use of Matlab tools to predict the robustness of a Dictyostelium cell model undergoing chemotaxis. The model consisted of 7 variables and 14 kinetic parameters and the analysis was based on the bifurcation theory.

### CONTINUING EDUCATION

- **Drug Discovery, Development & Commercialization, December 2014 (online) UC, San Diego**  
Drug discovery process and tools, Target selection, Regulatory responsibilities for drug discovery, Design of clinical protocols, Market access, IP files
- **Product and Process Quality in Manufacturing, November 2014** **EPFL, Switzerland**  
Theory of quality, Market-informed quality, Quality and innovation in product and process design, Just-in-time manufacturing, Methods of inspection and quality appraisal, Quality control circles, Quality control assessment tools

## WORK EXPERIENCE

- **APIVITA Natural cosmetics, September 2010 - November 2010** **Athens, Greece**
  1. Extraction and characterization of the physical properties of plants used in cosmetics. (R&D department)
  2. Production of cosmetics and stability tests of new products. (Chemical laboratory)
- **Technical University of Harburg-Hamburg, July 2005 -August 2005)** **Hamburg, Germany**

Supercritical fluid extraction of the plant *Artemisia Annua* for the production of Artemisinin that is used as a drug in cancer.

## TECHNICAL AND IT SKILLS

- Recombinant protein production: cloning, expression and purification with affinity chromatography
- Laboratory techniques: Design of vaccine formulations, Pharmacodynamic/ pharmacokinetic measurements, flow cytometry, immunohistochemistry, microscopy imaging, protein labeling, ELISA, Western Blots, PCR, MALDI TOF
- Animal handling: all types of injections, perfusion, skin surgery, in vivo imaging, organ harvesting, islets isolation
- Cell biology: primary cells culture, different cell types isolation, MACS technology
- IT: MATLAB, flowjo, Prism graphs and analysis, statistical analysis with SPSS, excellent use of MS office

## PUBLICATIONS

1. Love, K. R., Politano, T. J., Panagiotou, V., Jiang, B., Stadheim, T. A. & Love, J. C. Systematic single-cell analysis of *Pichia pastoris* reveals secretory capacity limits productivity. PLoS One 7, e37915, doi:10.1371/journal.pone.0037915 (2012).
2. Jason R. Cantor, Vasiliki Panayiotou, Giulia Agnello, George Georgiou and Everett M. Stone. Engineering reduced-immunogenicity enzymes for amino acid depletion therapy in cancer. *Methods Enzymol.*;502:291-319 (2012)
3. Pazaitou-Panayiotou K<sup>1</sup>, Papapetrou PD, Chrisoulidou A, Konstantinidou S, Doumala E, Georgiou E, Panagiotou V, Sotiriadou E, Mavroudi E, Apostolaki-Christopoulou M. Height, whole Body Surface Area, gender, working outdoors, and sunbathing in previous summer are important determinants of serum 25-hydroxyvitamin D levels. *Exp Clin Endocrinol Diabetes*. (2012)
4. Vasiliki Panagiotiou, Kerry Routenberg Love, Bo Jiang, Terrance Stadheim, and J. Christopher Love: Generation and Screening of *Pichia pastoris* Strains with Enhanced Protein Production by Use of Microengraving. *Applied and Environmental Microbiology*, p. 3154-3156, Vol. 77, No. 9 (2011)
5. Mitsiades N, Pazaitou-Panayiotou K, Aronis KN, Moon HS, Chamberland JP, Liu X, Diakopoulos KN, Kyttaris V, Panagiotou V, Mylvaganam G, Tseleni-Balafouta S, Mantzoros CS. Circulating adiponectin is inversely associated with risk of thyroid cancer: in vivo and in vitro studies. *J Clin Endocrinol Metab*.96(12):E2023-8 (2011)
6. Kerry Routenberg Love, Vasiliki Panagiotou, Bo Jiang, Terrance Stadheim, & J. Christopher Love. Identification and selection of supersecretors in *Pichia pastoris* populations by microengraving. *Biotechnology&Bioengineering* Vol.106, Issue 2, (319–325), (2010)

## AWARDS / SCHOLARSHIPS

- 2008:** The Presidential Fellowship at MIT, USA  
**2007:** Honor award for excellence in studies, Technological Institution of Greece (TEE), Athens, Greece

## LANGUAGES

- Greek: Mother language  
English: Excellent (Proficiency in English from University of Michigan)  
German: Good (Zertifikat Deutsch als Fremdsprache from Goethe Institut)  
French: Basic

## EXTRACURRICULAR INTERESTS

Traveling and getting to know people and cultures Sports: Sailing (skipper license), running (participated in half marathon races) and swimming (1<sup>st</sup> place in freestyle in many Greek tournaments)



